California Polytechnic State University
San Luis Obispo, CA 93407

"Conservative Overset Grids for Overflow"

For The

Sonic Wave Atmospheric Propagation Project

Final Report
June 1999
NASA-Ames Cooperative Agreement NCC 2-924

Jeff T. Onufer
Russell M. Cummings
Aeronautical Engineering Department

ABSTRACT

Methods are presented that can be used to make multiple, overset grids communicate in a conservative manner. The methods are developed for use with the Chimera overset method using the PEGSUS code and the OVERFLOW solver.

NOMENCLATURE

ROMAN

a	speed of sound, $a = \sqrt{\gamma R T}$
c_p	specific heat at constant pressure
E_t	total energy
F	force
J	Jacobian of transformation
k	coefficient of thermal conductivity
k_T	coefficient of turbulent thermal conductivity
M	momentum
M_∞	freestream Mach number
$\dot{m}_{enter}$	mass flow rate entering
$\dot{m}_{exit}$	mass flow rate exiting
p	pressure
Pr	Prandtl number
Pr_T	turbulent Prandtl number
q	heat flux
Re_L	Reynolds number based on freestream conditions and reference length L, $Re_L = \dfrac{\rho_\infty V_\infty L}{\mu_\infty}$
T	temperature
t	time

u, v, w	velocity components in x, y, and z directions
W	rate of work
U, V, W	contravariant velocity components
x, y, z	cartesian coordinates

GREEK

γ	ratio of specific heats
σ	stress
τ	computational time or shear stress
ρ	air density
μ	coefficient of viscosity
μ_T	coefficient of turbulent viscosity
ξ, η, ζ	transformed coordinates

SUBSCRIPTS

a	ambient condition
L	reference length
∞	freestream condition
x, y, z	cartesian direction
v	viscous term

SUPERSCRIPT

n	time level

CHAPTER 1

Introduction

The field of Computation Fluid Dynamics (CFD), is the study of fluid flow using numerical methods to solve equations that govern the physics of these fluids. Traditional methods for understanding fluid dynamics have been the use of experimental and theoretical methods. However, since the invention of the digital computer, and more recently the high-speed digital computer, the field of CFD has grown tremendously in both its capabilities and numerical methods. Other factors that have contributed to the growth of CFD methods are relative computer costs, increased performance and availability of computers, including access to high-speed multiprocessor supercomputers all the way down to the workstations that have become a common desktop tool to the researcher [2,3].

Today, two major grid systems exist for solving complex three-dimensional flowfields [4]. The difference lies in the way the flowfield is discretized. In the first method, the flowfield is discretized into triangular-shaped elements in two dimensions, and tetrahedral elements for three-dimensional fields (Figure 1.1). This type of grid is called an "unstructured grid" since the grid points cannot be associated with grid lines. For the second method, the flowfield is discretized into quadrilateral elements in two dimensions, and hexahedral elements in three dimensions (Figure 1.2). In this method, the grids are called "structured grids" since the grid points can be associated with grid lines in an ordered manner [4].

Structured grids can be divided further into two more groups. For complex geometries, it is unrealistic to create a single grid. These geometries are usually modeled using several grids that adequately resolve specific areas on the geometry of interest. The resulting grid system is then combined using some method for communication between zones. This is where the two submethods differ. One method is the chimera grid approach, or overset method, where grids overlap each other. The second method is where grids abut against each other, and are called patched grids or blocked grids.

For the research presented here, the manner in which patched, structured grids communicate and pass information between each other will be investigated. Furthermore, this method will be incorporated into a flow-solver that was developed for overlapping grids. There are several reasons for doing so. The method in which overlapped grids communicate with each other is strictly by interpolation. The physics of the flow across the interface are not computed and thus conservation is not maintained [14]. Under certain circumstances, the method can be conservative. However, this is rarely achieved when modeling real world complex geometries. Secondly, incorporating a patched grid interface will allow users to model regions of the flowfield with the option of a conservative interface. This will allow flow discontinuities to pass across the patched interface smoothly as if the interface is transparent to the flowsolver. Lastly, it is sometimes convenient to model portions of the flowfield with a patched grid instead of overlapping grids that require a certain amount of overlapping to work correctly [14]. This also requires that portions of the overlapped grids be cut out of the geometry being modeled (Figure 1.3), which is a process that can be extremely time consuming [15].

This study will concentrate its efforts in providing a patched grid interface for the OVERFLOW flow-solver with the option of making the developed scheme fully conservative. OVERFLOW is an in-house code of NASA Ames Research Center for solving the thin layer Navier-Stokes equations with the option of using overset grids [12]. OVERFLOW requires the use of a preprocessor program called Pegsus. Pegsus provides OVERFLOW the appropriate information on how a set of overlapping grids, or zones, modeling a geometry communicate with each other [11]. Pegsus was written for overset grids and will need to be modified and new procedures implemented in order for it to handle patched grids.

The current research project was divided into two areas. The first portion of research was to investigate how to convert patched grids into overset grids. The method employed here is called volume extension and was briefly examined and determined to be too time consuming for the end user. Not only does the user have to extend the patched grids to create an adequate overlapping region, but also has to use Pegsus to create interpolation stencils and hole cuts if necessary. Although the results were somewhat promising, the volume extension program developed was determined not to work under certain circumstances due to grid topology and that an excessive amount of user input to the program was necessary.

The second portion, and the bulk of this research, was to modify and implement new methods into both Pegsus and OVERFLOW in order for these programs to handle patched grids. This was further divided into two separate development steps. The first step was to enhance Pegsus and ensure that the interpolation stencils created for patched grids were valid and would work correctly in OVERFLOW. To quickly test this new version without making any significant changes to OVERFLOW, the flow-through boundary condition was coded. This boundary condition was easily incorporated into

OVERFLOW since the method used to update boundary points for overset grids is similar to how the boundary points for patched grids with the flow-through condition will be updated. The difference lies in where the flowfield information is obtained. For overset grids, a boundary point, or a recipient point, lies within a grid cell of another grid, or a donor grid. The node values of this donor cell are used to update flowfield quantities strictly by interpolation. For the flow-through condition, the boundary point lies on a common plane or interface with the donor grid. Half the update for this recipient point will be from the grid it belongs to. The remaining half of the update will be from the donor grid using the interpolation stencils from Pegsus. The only requirement is that the update information can only come from interior node points of both the recipient and donor grids. These enhancements to Pegsus for allowing patched grids and the flow-through condition will also be useful when incorporating the conservative patched grid interfacing into OVERFLOW.

The second step for the patched grid capability will be to implement a finite difference scheme for patched interfaces into OVERFLOW. Here, one-half of the flux differencing is computed for each recipient grid. The remaining half, from the donor grid, is computed and combined using communication information from Pegsus. Although the scheme to be presented is fully conservative for patched boundaries with point-to-point matching, it does have further potential of being fully conservative for boundaries without point-to-point matching.

The test case for all three methods investigated, the volume extension, flow-through boundary condition, and the fully conservative finite difference approach, will be the ONERA M6 wing. Comparisons will be made to a single zone case as well as to experimental results.

CHAPTER 2

Governing Equations of Fluid Mechanics

The fundamental equations of fluid mechanics are based on three laws, the Conservation of Mass, Conservation of Momentum, and the Conservation of Energy laws. Applying these laws to a fluid flow results in five, coupled, non-linear, partial differential equations. The first equation is derived from the conservation of mass and is known as the continuity equation. The Momentum equations are derived from the conservation of momentum law and represent the momentum components in three orthogonal directions. The energy equation is derived from the conservation of energy, which is the First Law of Thermodynamics [1].

For a cartesian coordinate system, the continuity equation can be written in conservation-law form as (Appendix A) [1]:

$$\frac{\partial \rho}{\partial t} + \frac{\partial (\rho u)}{\partial x} + \frac{\partial (\rho v)}{\partial y} + \frac{\partial (\rho w)}{\partial z} = 0 \tag{2.1}$$

Here, u, v, and w represent the three velocity components in the x, y, and z directions respectively. Lastly, ρ is the density. The next set of equations are the momentum equations, also known as the Navier-Stokes equations. However, it is a common practice to include the continuity equation and the energy equation (defined later) as the set of equations known as the Navier-Stokes equations [2].

Written in conservation law form, the momentum equations are (Appendix B) [1]:

$$\frac{\partial(\rho u)}{\partial t}+\frac{\partial(\rho u^2+p)}{\partial x}+\frac{\partial(\rho uv)}{\partial y}+\frac{\partial(\rho uw)}{\partial z}=\frac{\partial\tau_{xx}}{\partial x}+\frac{\partial\tau_{xy}}{\partial y}+\frac{\partial\tau_{xz}}{\partial z} \tag{2.2}$$

$$\frac{\partial(\rho v)}{\partial t}+\frac{\partial(\rho uv)}{\partial x}+\frac{\partial(\rho v^2+p)}{\partial y}+\frac{\partial(\rho vw)}{\partial z}=\frac{\partial\tau_{xy}}{\partial x}+\frac{\partial\tau_{yy}}{\partial y}+\frac{\partial\tau_{yz}}{\partial z} \tag{2.3}$$

$$\frac{\partial(\rho w)}{\partial t}+\frac{\partial(\rho uw)}{\partial x}+\frac{\partial(\rho vw)}{\partial y}+\frac{\partial(\rho w^2+p)}{\partial z}=\frac{\partial\tau_{xz}}{\partial x}+\frac{\partial\tau_{yz}}{\partial y}+\frac{\partial\tau_{zz}}{\partial z} \tag{2.4}$$

Where p is the pressure and $\tau_{xx}, \tau_{yy}, \tau_{zz}, \tau_{xy}, \tau_{xz}, \tau_{yz}$ are the viscous stress tensors. They are defined by the following equations:

$$\tau_{xx} = \frac{2}{3}\mu\left(2\frac{\partial u}{\partial x}-\frac{\partial v}{\partial y}-\frac{\partial w}{\partial z}\right) \tag{2.5}$$

$$\tau_{yy} = \frac{2}{3}\mu\left(2\frac{\partial v}{\partial y}-\frac{\partial u}{\partial x}-\frac{\partial w}{\partial z}\right) \tag{2.6}$$

$$\tau_{zz} = \frac{2}{3}\mu\left(2\frac{\partial w}{\partial z}-\frac{\partial u}{\partial x}-\frac{\partial v}{\partial y}\right) \tag{2.7}$$

$$\tau_{xy} = \mu\left(\frac{\partial u}{\partial y}+\frac{\partial v}{\partial x}\right) \tag{2.8}$$

$$\tau_{xz} = \mu\left(\frac{\partial w}{\partial x}+\frac{\partial u}{\partial z}\right) \tag{2.9}$$

$$\tau_{yz} = \mu\left(\frac{\partial v}{\partial z}+\frac{\partial w}{\partial y}\right) \tag{2.10}$$

The last equation, the energy equation, is defined as follows (Appendix C) [1]:

$$\frac{\partial E_t}{\partial t} + \frac{\partial((E_t + p)u)}{\partial x} + \frac{\partial((E_t + p)v)}{\partial y} + \frac{\partial((E_t + p)w)}{\partial z} =$$
$$\frac{\partial(u\tau_{xx} + v\tau_{xy} + w\tau_{xz} - q_x)}{\partial x} + \frac{\partial(u\tau_{xy} + v\tau_{yy} + w\tau_{yz} - q_y)}{\partial y} + \qquad (2.11)$$
$$\frac{\partial(u\tau_{xz} + v\tau_{yz} + w\tau_{zz} - q_z)}{\partial z}$$

Where q_x, q_y, q_z are the heat flux terms. They are defined by the following equations:

$$q_x = -k \bullet \frac{\partial T}{\partial x} \qquad (2.12)$$

$$q_y = -k \bullet \frac{\partial T}{\partial y} \qquad (2.13)$$

$$q_z = -k \bullet \frac{\partial T}{\partial z} \qquad (2.14)$$

Where k is the coefficient of thermal conductivity, defined as:

$$k = \frac{c_p \mu}{Pr} \qquad (2.15)$$

where c_p is the specific heat at constant pressure, μ is the coefficient of viscosity. Lastly, Pr is the Prandtl numbers. The Prandtl number is a ratio of the energy dissipated by friction to the energy transported by thermal conduction. This can be seen as the ability of a fluid to diffuse momentum and energy on a molecular level.

Vectorization of Navier-Stokes Equations

Equations (2.1), (2.2), (2.3), (2.4), and (2.11) can easily be put into vector form. Rewritten, they are:

$$\frac{\partial\rho}{\partial t}+\frac{\partial(\rho u)}{\partial x}+\frac{\partial(\rho v)}{\partial y}+\frac{\partial(\rho w)}{\partial z}=0$$

$$\frac{\partial(\rho u)}{\partial t}+\frac{\partial(\rho u^2+p)}{\partial x}+\frac{\partial(\rho uv)}{\partial y}+\frac{\partial(\rho uw)}{\partial z}=\frac{\partial\tau_{xx}}{\partial x}+\frac{\partial\tau_{xy}}{\partial y}+\frac{\partial\tau_{xz}}{\partial z}$$

$$\frac{\partial(\rho v)}{\partial t}+\frac{\partial(\rho uv)}{\partial x}+\frac{\partial(\rho v^2+p)}{\partial y}+\frac{\partial(\rho vw)}{\partial z}=\frac{\partial\tau_{xy}}{\partial x}+\frac{\partial\tau_{yy}}{\partial y}+\frac{\partial\tau_{yz}}{\partial z}$$

$$\frac{\partial(\rho w)}{\partial t}+\frac{\partial(\rho uw)}{\partial x}+\frac{\partial(\rho vw)}{\partial y}+\frac{\partial(\rho w^2+p)}{\partial z}=\frac{\partial\tau_{xz}}{\partial x}+\frac{\partial\tau_{yz}}{\partial y}+\frac{\partial\tau_{zz}}{\partial z} \tag{2.16}$$

$$\frac{\partial E_t}{\partial t}+\frac{\partial((E_t+p)u)}{\partial x}+\frac{\partial((E_t+p)v)}{\partial y}+\frac{\partial((E_t+p)w)}{\partial z}=$$

$$\frac{\partial(u\tau_{xx}+v\tau_{xy}+w\tau_{xz}-q_x)}{\partial x}+\frac{\partial(u\tau_{xy}+v\tau_{yy}+w\tau_{yz}-q_y)}{\partial y}+$$

$$\frac{\partial(u\tau_{xz}+v\tau_{yz}+w\tau_{zz}-q_z)}{\partial z}$$

It follows then that the Navier-Stokes equation in conservation-law form may now be written in vector form as:

$$\frac{\partial Q}{\partial t}+\frac{\partial E}{\partial x}+\frac{\partial F}{\partial y}+\frac{\partial G}{\partial z}=\frac{\partial E_v}{\partial x}+\frac{\partial F_v}{\partial y}+\frac{\partial G_v}{\partial z} \tag{2.17}$$

Where Q, E, F, G represent the inviscid flux vectors:

$$Q = \begin{bmatrix} \rho \\ \rho u \\ \rho v \\ \rho w \\ E_t \end{bmatrix} E = \begin{bmatrix} \rho u \\ \rho u^2 + p \\ \rho uv \\ \rho uw \\ (E_t + p)u \end{bmatrix} F = \begin{bmatrix} \rho v \\ \rho uv \\ \rho v^2 + p \\ \rho vw \\ (E_t + p)v \end{bmatrix} G = \begin{bmatrix} \rho w \\ \rho uw \\ \rho vw \\ \rho w^2 + p \\ (E_t + p)w \end{bmatrix} \tag{2.18}$$

And E_v, F_v, G_v represent the viscous flux vectors:

$$E_v = \begin{bmatrix} 0 \\ \tau_{xx} \\ \tau_{xy} \\ \tau_{xz} \\ u\tau_{xx} + v\tau_{xy} + w\tau_{xz} - q_x \end{bmatrix} F_v = \begin{bmatrix} 0 \\ \tau_{xy} \\ \tau_{yy} \\ \tau_{yz} \\ u\tau_{xy} + v\tau_{yy} + w\tau_{yz} - q_y \end{bmatrix}$$

$$G_v = \begin{bmatrix} 0 \\ \tau_{xz} \\ \tau_{yz} \\ \tau_{zz} \\ u\tau_{xz} + v\tau_{yz} + w\tau_{zz} - q_z \end{bmatrix} \tag{2.19}$$

The next step will be to non-dimensionalize these equations.

Nondimensional Form Of Navier-stokes Equations

The Navier-Stokes equations are often put in nondimensional form. There are several advantages to doing so. First, characteristic parameters such as the Reynolds number, Prandtl number, and Mach number can be varied independently from each other. The second reason is that flow variables such as velocity are normalized (the resulting values are often between 0 and 1) [3]. For this analysis we will nondimensionalize the governing equations with freestream values for the flow variables and a reference length for the spatial variables. The following non-dimensionalizing variables will be used [3]:

$$
\begin{array}{lll}
x^* = \dfrac{x}{L} & u^* = \dfrac{u}{V_\infty} & \rho^* = \dfrac{\rho}{\rho_\infty} \\
y^* = \dfrac{y}{L} & v^* = \dfrac{v}{V_\infty} & p^* = \dfrac{p}{\rho_\infty V_\infty^{\;2}} \\
z^* = \dfrac{z}{L} & w^* = \dfrac{w}{V_\infty} & T^* = \dfrac{T}{T_\infty} \\
t^* = \dfrac{t}{L/V_\infty} & \mu^* = \dfrac{\mu}{\mu_\infty} & e^* = \dfrac{e}{V_\infty^{\;2}}
\end{array}
\qquad (2.20)
$$

Where the terms with asterisks are nondimensional. Applying these nondimensional variables to Equation (2.17) we get (Appendix D) [3]:

$$
\frac{\partial Q^*}{\partial t^*} + \frac{\partial E^*}{\partial x^*} + \frac{\partial F^*}{\partial y^*} + \frac{\partial G^*}{\partial z^*} = \frac{\partial E^*{}_v}{\partial x^*} + \frac{\partial F^*{}_v}{\partial y^*} + \frac{\partial G^*{}_v}{\partial z^*} \qquad (2.21)
$$

Where Q^*, E^*, F^*, G^* are:

$$Q^* = \begin{bmatrix} \rho^* \\ \rho^* u^* \\ \rho^* v^* \\ \rho^* w^* \\ E^*_t \end{bmatrix} E^* = \begin{bmatrix} \rho^* u^* \\ \rho^* u^{*2} + p^* \\ \rho^* u^* v^* \\ \rho^* u^* w^* \\ (E^*_t + p^*) v^* \end{bmatrix} F^* = \begin{bmatrix} \rho^* v^* \\ \rho^* u^* v^* \\ \rho^* v^{*2} + p^* \\ \rho^* v^* w^* \\ (E^*_t + p^*) v^* \end{bmatrix} G^* = \begin{bmatrix} \rho^* w^* \\ \rho^* u^* w^* \\ \rho^* v^* w^* \\ \rho^* w^{*2} + p^* \\ (E^*_t + p^*) w^* \end{bmatrix} \tag{2.22}$$

And E^*_v, F^*_v, G^*_v are:

$$E^*_v = \begin{bmatrix} 0 \\ \tau^*_{xx} \\ \tau^*_{xy} \\ \tau^*_{xz} \\ u^* \tau^*_{xx} + v^* \tau^*_{xy} + w^* \tau^*_{xz} - q^*_x \end{bmatrix}$$

$$F^*_v = \begin{bmatrix} 0 \\ \tau^*_{xy} \\ \tau^*_{yy} \\ \tau^*_{yz} \\ u^* \tau^*_{xy} + v^* \tau^*_{yy} + w^* \tau^*_{yz} - q^*_y \end{bmatrix} \tag{2.23}$$

$$G^*_v = \begin{bmatrix} 0 \\ \tau^*_{xz} \\ \tau^*_{yz} \\ \tau^*_{zz} \\ u^* \tau^*_{xz} + v^* \tau^*_{yz} + w^* \tau^*_{zz} - q^*_z \end{bmatrix}$$

Also:

$$E_t^* = \rho^*\left(e^* + \frac{u^{*2} + v^{*2} + w^{*2}}{2}\right) \tag{2.24}$$

The viscous stress tensors are also given by:

$$\tau^*_{xx} = \frac{2}{3}\frac{\mu^*}{Re_L}\left(2\frac{\partial u^*}{\partial x^*} - \frac{\partial v^*}{\partial y^*} - \frac{\partial w^*}{\partial z^*}\right) \tag{2.25}$$

$$\tau^*_{yy} = \frac{2}{3}\frac{\mu^*}{Re_L}\left(2\frac{\partial v^*}{\partial y^*} - \frac{\partial u^*}{\partial x^*} - \frac{\partial w^*}{\partial z^*}\right) \tag{2.26}$$

$$\tau^*_{zz} = \frac{2}{3}\frac{\mu^*}{Re_L}\left(2\frac{\partial w^*}{\partial z^*} - \frac{\partial u^*}{\partial x^*} - \frac{\partial v^*}{\partial y^*}\right) \tag{2.27}$$

$$\tau^*_{xy} = \frac{\mu^*}{Re_L}\left(\frac{\partial u^*}{\partial y^*} + \frac{\partial v^*}{\partial x^*}\right) \tag{2.28}$$

$$\tau^*_{xz} = \frac{\mu^*}{Re_L}\left(\frac{\partial w^*}{\partial x^*} + \frac{\partial u^*}{\partial z^*}\right) \tag{2.29}$$

$$\tau^*_{yz} = \frac{\mu^*}{Re_L}\left(\frac{\partial v^*}{\partial z^*} + \frac{\partial w^*}{\partial y^*}\right) \tag{2.30}$$

The heat flux terms are given by:

$$q^*_x = -\frac{\mu^*}{(\gamma - 1)M^2_\infty Re_L Pr}\frac{\partial T^*}{\partial x^*} \tag{2.31}$$

$$q^*_y = -\frac{\mu^*}{(\gamma - 1)M^2_\infty Re_L Pr}\frac{\partial T^*}{\partial y^*} \tag{2.32}$$

$$q^*_z = -\frac{\mu^*}{(\gamma - 1)M^2_\infty Re_L Pr}\frac{\partial T^*}{\partial z^*} \qquad (2.33)$$

We can now rewrite Equation (2.22) in its final form. For convenience we will drop the asterisks for the remainder of this work. The Reynolds term has been factored out from previous derivations.

$$\frac{\partial Q}{\partial t} + \frac{\partial E}{\partial x} + \frac{\partial F}{\partial y} + \frac{\partial G}{\partial z} = \frac{1}{Re_L}\left(\frac{\partial E_v}{\partial x} + \frac{\partial F_v}{\partial y} + \frac{\partial G_v}{\partial z}\right) \qquad (2.34)$$

The next step in preparation for applying a numerical scheme to the Navier-Stokes equations will be to apply a coordinate transformation to the governing equations.

Coordinate Transformation

The governing equations derived thus far have been expressed in a cartesian coordinate system (x, y, z). This system is called the physical domain. For finite difference methods, this type of coordinate system is most efficient. However, for real world geometries, such as a complete aircraft, an orthogonal coordinate system is unrealistic. These type of configurations require a nonorthogonal coordinate system. Therefore it is necessary to transform the physical domain, (x, y, z) coordinates, to a computational domain, (ξ, η, ζ) [2]. This transformation not only creates and allows an equally-spaced computational domain, but also allows the user to align one of the computational directions along a specific physical boundary such as an aircraft surface. This will help in applying boundary conditions. For this analysis, the Xi direction(ξ) is the streamwise direction, Eta(η) is the spanwise direction, and finally, Zeta(ζ) is the normal or viscous direction. Figure 2.1 illustrates the physical and computational domains. For a completely generalized transformation, consider the following transformation:

$$\xi = \xi(x, y, z) \tag{2.35}$$

$$\eta = \eta(x, y, z) \tag{2.36}$$

$$\zeta = \zeta(x, y, z) \tag{2.37}$$

$$\tau = t \tag{2.38}$$

The inverse of these equations are:

$$x = x(\xi, \eta, \zeta) \tag{2.39}$$

$$y = y(\xi, \eta, \zeta) \tag{2.40}$$

$$z = z(\xi, \eta, \zeta) \tag{2.41}$$

$$t = \tau \tag{2.42}$$

Applying the chain rule of partial differentiation, the partial derivatives of Equations (2.39) through (2.42) are:

$$\frac{\partial}{\partial x} = \frac{\partial \xi}{\partial x}\frac{\partial}{\partial \xi} + \frac{\partial \eta}{\partial x}\frac{\partial}{\partial \eta} + \frac{\partial \zeta}{\partial x}\frac{\partial}{\partial \zeta} \tag{2.43}$$

$$\frac{\partial}{\partial y} = \frac{\partial \xi}{\partial y}\frac{\partial}{\partial \xi} + \frac{\partial \eta}{\partial y}\frac{\partial}{\partial \eta} + \frac{\partial \zeta}{\partial y}\frac{\partial}{\partial \zeta} \tag{2.44}$$

$$\frac{\partial}{\partial z} = \frac{\partial \xi}{\partial z}\frac{\partial}{\partial \xi} + \frac{\partial \eta}{\partial z}\frac{\partial}{\partial \eta} + \frac{\partial \zeta}{\partial z}\frac{\partial}{\partial \zeta} \tag{2.45}$$

$$\frac{\partial}{\partial t} = \frac{\partial \xi}{\partial t}\frac{\partial}{\partial \xi} + \frac{\partial \eta}{\partial t}\frac{\partial}{\partial \eta} + \frac{\partial \zeta}{\partial t}\frac{\partial}{\partial \zeta} + \frac{\partial \tau}{\partial t}\frac{\partial}{\partial \tau} \tag{2.46}$$

The metrics in these equations are:

$$\frac{\partial \xi}{\partial x} = \xi_x, \frac{\partial \eta}{\partial x} = \eta_x, \frac{\partial \zeta}{\partial x} = \zeta_x \tag{2.47}$$

$$\frac{\partial \xi}{\partial y} = \xi_y, \frac{\partial \eta}{\partial y} = \eta_y, \frac{\partial \zeta}{\partial y} = \zeta_y \tag{2.48}$$

$$\frac{\partial \xi}{\partial z} = \xi_z, \frac{\partial \eta}{\partial z} = \eta_z, \frac{\partial \zeta}{\partial z} = \zeta_z \tag{2.49}$$

$$\frac{\partial \xi}{\partial t} = \xi_t, \frac{\partial \eta}{\partial t} = \eta_t, \frac{\partial \zeta}{\partial t} = \zeta_t, \frac{\partial \tau}{\partial t} = \tau_t = 1 \tag{2.50}$$

These metrics, in general, cannot be determined using analytical methods. Therefore, a numerical method must be used. First, consider the following differential expressions:

$$dt = t_\tau d\tau + t_\xi d\xi + t_\eta d\eta + t_\zeta d\zeta \tag{2.51}$$

$$dx = x_\tau d\tau + x_\xi d\xi + x_\eta d\eta + x_\zeta d\zeta \tag{2.52}$$

$$dy = y_\tau d\tau + y_\xi d\xi + y_\eta d\eta + y_\zeta d\zeta \tag{2.53}$$

$$dz = z_\tau d\tau + z_\xi d\xi + z_\eta d\eta + z_\zeta d\zeta \tag{2.54}$$

From Equation (2.42), time, t, is only a function of the computational domains' time, τ. Therefore the following partial derivatives must equal zero.

$$\frac{\partial t}{\partial \xi} = \frac{\partial t}{\partial \eta} = \frac{\partial t}{\partial \zeta} = 0 \tag{2.55}$$

Also using the relationship in Equation (2.42), the partial derivative of t with respect to τ must equal one. With this information and Equation (2.55), we can rewrite Equation (2.51) as:

$$dt = d\tau \tag{2.56}$$

Placing Equations (2.51), (2.52), (2.53), and (2.56) in matrix form we have:

$$\begin{bmatrix} dt \\ dx \\ dy \\ dz \end{bmatrix} = \begin{bmatrix} 1 & 0 & 0 & 0 \\ x_\tau & x_\xi & x_\eta & x_\zeta \\ y_\tau & y_\xi & y_\eta & y_\zeta \\ z_\tau & z_\xi & z_\eta & z_\zeta \end{bmatrix} \begin{bmatrix} d\tau \\ d\xi \\ d\eta \\ d\zeta \end{bmatrix} \tag{2.57}$$

Reversing the role of the independent variables, it can be shown the reverse is true with the following differential expression:

$$d\tau = dt \tag{2.58}$$

$$d\xi = \xi_t dt + \xi_x dx + \xi_y dy + \xi_z dz \tag{2.59}$$

$$dy = \eta_t d\tau + \eta_x d\xi + \eta_y d\eta + \eta_z d\zeta \tag{2.60}$$

$$dz = \zeta_t d\tau + \zeta_x d\xi + \zeta_y d\eta + \zeta_z d\zeta \tag{2.61}$$

In matrix form we have:

$$\begin{bmatrix} d\tau \\ d\xi \\ d\eta \\ d\zeta \end{bmatrix} = \begin{bmatrix} 1 & 0 & 0 & 0 \\ \xi_t & \xi_x & \xi_y & \xi_z \\ \eta_t & \eta_x & \eta_y & \eta_z \\ \zeta_t & \zeta_x & \zeta_y & \zeta_z \end{bmatrix} \begin{bmatrix} dt \\ dx \\ dy \\ dz \end{bmatrix} \tag{2.62}$$

From Equations (2.57) and (2.62), the following must be true:

$$\begin{bmatrix} 1 & 0 & 0 & 0 \\ \xi_t & \xi_x & \xi_y & \xi_z \\ \eta_t & \eta_x & \eta_y & \eta_z \\ \zeta_t & \zeta_x & \zeta_y & \zeta_z \end{bmatrix} = \begin{bmatrix} 1 & 0 & 0 & 0 \\ x_\tau & x_\xi & x_\eta & x_\zeta \\ y_\tau & y_\xi & y_\eta & y_\zeta \\ z_\tau & z_\xi & z_\eta & z_\zeta \end{bmatrix}^{-1} \tag{2.63}$$

Using a symbolic math program such as Maple V, the right-hand-side of Equation (2.63) was solved for (Appendix E) [3]. The transformation metrics can now be solved for with the following results:

$$\xi_x = J(y_\eta z_\zeta - y_\zeta z_\eta) \tag{2.64}$$

$$\xi_y = J(x_\zeta z_\eta - x_\eta z_\zeta) \tag{2.65}$$

$$\xi_z = J(x_\eta y_\zeta - x_\zeta y_\eta) \tag{2.66}$$

$$\eta_x = J(y_\zeta z_\xi - y_\xi z_\zeta) \tag{2.67}$$

$$\eta_y = J(x_\xi z_\zeta - x_\zeta z_\xi) \tag{2.68}$$

$$\eta_z = J(x_\zeta y_\xi - x_\xi y_\zeta) \tag{2.69}$$

$$\zeta_x = J(y_\xi z_\eta - y_\eta z_\xi) \tag{2.70}$$

$$\zeta_y = J(x_\eta z_\xi - x_\xi z_\eta) \tag{2.71}$$

$$\zeta_z = J(x_\xi y_\eta - x_\eta y_\xi) \tag{2.72}$$

$$\xi_t = -(x_\tau \xi_x + y_\tau \xi_y + z_\tau \xi_z) \tag{2.73}$$

$$\eta_t = -(x_\tau \eta_x + y_\tau \eta_y + z_\tau \eta_z) \tag{2.74}$$

$$\zeta_t = -(x_\tau \zeta_x + y_\tau \zeta_y + z_\tau \zeta_z) \tag{2.75}$$

Equations (2.73), (2.74), and (2.75) can be rewritten using the previous spacial metrics as:

$$\xi_t = -J[x_\tau(y_\eta z_\zeta - y_\zeta z_\eta) + y_\tau(x_\zeta z_\eta - x_\eta z_\zeta) + z_\tau(x_\eta y_\zeta - x_\zeta y_\eta)] \tag{2.76}$$

$$\eta_t = -J[x_\tau(y_\zeta z_\xi - y_\xi z_\zeta) + y_\tau(x_\xi z_\zeta - x_\zeta z_\xi) + z_\tau(x_\zeta y_\xi - x_\xi y_\zeta)] \tag{2.77}$$

$$\zeta_t = -J[x_\tau(y_\xi z_\eta - y_\eta z_\xi) + y_\tau(x_\eta z_\xi - x_\xi z_\eta) + z_\tau(x_\xi y_\eta - x_\eta y_\xi)] \tag{2.78}$$

Where the Jacobian, J, is defined as:

$$J = \frac{\partial(\xi,\eta,\zeta)}{\partial(x,y,z)} = \frac{1}{x_\xi(y_\eta z_\zeta - y_\zeta z_\eta) + (-x_\eta(y_\xi z_\zeta - y_\zeta z_\xi)) + x_\zeta(y_\xi z_\eta - y_\eta z_\xi)} \tag{2.79}$$

Applying this generalized transformation to the governing equations we get (Appendix D) [3]:

$$\frac{\partial\bar{Q}}{\partial\tau}+\frac{\partial\bar{E}}{\partial\xi}+\frac{\partial\bar{F}}{\partial\eta}+\frac{\partial\bar{G}}{\partial\zeta}=\frac{1}{Re_L}\left(\frac{\partial\overline{E_v}}{\partial\xi}+\frac{\partial\overline{F_v}}{\partial\eta}+\frac{\partial\overline{G_v}}{\partial\zeta}\right) \tag{2.80}$$

Where

$$\bar{Q} = \frac{1}{J}\begin{bmatrix}\rho\\ \rho u\\ \rho v\\ \rho w\\ E_t\end{bmatrix} \bar{E} = \frac{1}{J}\begin{bmatrix}\rho u\\ \rho uU+\xi_x p\\ \rho vU+\xi_y p\\ \rho wU+\xi_z p\\ (E_t+p)U-\xi_t p\end{bmatrix}$$
$$\bar{F} = \frac{1}{J}\begin{bmatrix}\rho V\\ \rho uV+\eta_x p\\ \rho vV+\eta_y p\\ \rho wV+\eta_z p\\ (E_t+p)V-\eta_t p\end{bmatrix} \bar{G} = \frac{1}{J}\begin{bmatrix}\rho W\\ \rho uW+\zeta_x p\\ \rho vW+\zeta_y p\\ \rho wW+\zeta_z p\\ (E_t+p)W-\zeta_t p\end{bmatrix} \tag{2.81}$$

Where U,V, and W are the contravariant velocity components defined as:

$$\begin{aligned}U &= \xi_t+\xi_x y+\xi_y v+\xi_z v\\ V &= \eta_t+\eta_x y+\eta_y v+\eta_z v\\ W &= \zeta_t+\zeta_x y+\zeta_y v+\zeta_z v\end{aligned} \tag{2.82}$$

The contravariant velocities represent the velocity components that are perpendicular to planes of constant ξ, η, ζ [3].

And the viscous flux terms $\overline{E_v}, \overline{F_v}, \overline{G_v}$ are:

$$\begin{aligned}
\overline{E_v} &= \frac{1}{J}(\xi_x E_v + \xi_y F_v + \xi_z G_v) \\
\overline{F_v} &= \frac{1}{J}(\eta_x E_v + \eta_y F_v + \eta_z G_v) \\
\overline{G_v} &= \frac{1}{J}(\zeta_x E_v + \zeta_y F_v + \zeta_z G_v)
\end{aligned} \tag{2.83}$$

Where the viscous shear stress terms are given as:

$$\tau_{xx} = \frac{2}{3}\frac{\mu}{Re_L}[2(\xi_x u_\xi + \eta_x u_\eta + \zeta_x u_\zeta) - (\xi_y v_\xi + \eta_y v_\eta + \zeta_y v_\zeta) - (\xi_z w_\xi + \eta_z w_\eta + \zeta_z w_\zeta)] \tag{2.84}$$

$$\tau_{yy} = \frac{2}{3}\frac{\mu}{Re_L}[2(\xi_y v_\xi + \eta_y v_\eta + \zeta_y v_\zeta) - (\xi_x u_\xi + \eta_x u_\eta + \zeta_x w_\zeta) - (\xi_z w_\xi + \eta_z w_\eta + \zeta_z w_\zeta)] \tag{2.85}$$

$$\tau_{zz} = \frac{2}{3}\frac{\mu}{Re_L}[2(\xi_z w_\xi + \eta_z w_\eta + \zeta_z w_\zeta) - (\xi_x u_\xi + \eta_x u_\eta + \zeta_x w_\zeta) - (\xi_y v_\xi + \eta_y v_\eta + \zeta_y v_\zeta)] \tag{2.86}$$

$$\tau_{xy} = \frac{\mu}{Re_L}(\xi_y u_\xi + \eta_y u_\eta + \zeta_y u_\zeta + \xi_x v_\xi + \eta_x v_\eta + \zeta_x v_\zeta) \tag{2.87}$$

$$\tau_{xz} = \frac{\mu}{Re_L}(\xi_z u_\xi + \eta_z u_\eta + \zeta_z u_\zeta + \xi_x w_\xi + \eta_x w_\eta + \zeta_x w_\zeta) \tag{2.88}$$

$$\tau_{yz} = \frac{\mu}{Re_L}(\xi_z v_\xi + \eta_z v_\eta + \zeta_z v_\zeta + \xi_y w_\xi + \eta_y w_\eta + \zeta_y w_\zeta) \tag{2.89}$$

Also, the heat flux terms are given by:

$$q_x = -\frac{\mu}{(\gamma - 1)M^2_{\infty}Re_L Pr}(\xi_x T_\xi + \eta_x T_\eta + \zeta_x T_\zeta) \tag{2.90}$$

$$q_y = -\frac{\mu}{(\gamma - 1)M^2_{\infty}Re_L Pr}(\xi_y T_\xi + \eta_y T_\eta + \zeta_y T_\zeta) \tag{2.91}$$

$$q_z = -\frac{\mu}{(\gamma - 1)M^2_{\infty}Re_L Pr}(\xi_z T_\xi + \eta_z T_\eta + \zeta_z T_\zeta) \tag{2.92}$$

Thin Layer Approximation

In order to adequately resolve viscous gradients due to solid surfaces, many grid points must be clustered in these regions. For flows in which separation is minimal, gradients of the stress terms normal to viscous surfaces have been found to be much larger than gradients parallel to these surfaces [10]. Therefore, it is unnecessary to construct grids with fine resolutions in directions parallel to viscous surfaces. To expand on this analysis we must include computer requirements and limitations. Since a large amount of computer time and storage is used in resolving these gradients, any valid reduction in the full Navier-Stokes equations would greatly increase the efficiency and productivity of the researcher. It has been shown that if the grid spacing parallel to viscous surfaces is too coarse, and that the full Navier-Stokes equations are being solved, the resulting solution indicates that viscous gradients in these directions have not been fully resolved [2,10]. It then only makes sense to drop the viscous terms in which partial derivatives have been take with respect to directions parallel to viscous surfaces. As mentioned before, after the governing equations have been transformed, it is a common practice to have the viscous direction to be the Zeta direction. Therefore, any of the viscous flux terms that contain partial derivatives with respect to Xi or Eta can be dropped since these terms have been shown to be much smaller than those terms that have partial derivatives with respect to Zeta. Returning to Equation (2.80), we can now drastically reduce the viscous flux terms by dropping all terms with derivatives take in respect to Xi and Eta. The resulting equation is:

$$\frac{\partial \bar{Q}}{\partial \tau} + \frac{\partial \bar{E}}{\partial \xi} + \frac{\partial \bar{F}}{\partial \eta} + \frac{\partial \bar{G}}{\partial \zeta} = \frac{1}{Re_L}\left(\frac{\partial \bar{S}}{\partial \zeta}\right) \qquad (2.93)$$

Where $\bar{s}$ is defined as (Appendix F):

$$\bar{S} = \frac{1}{J}\begin{bmatrix} 0 \\ \mu(\zeta_x^2+\zeta_y^2+\zeta_z^2)u_\zeta + \frac{1}{3}\mu\zeta_x(\zeta_x u_\zeta + \zeta_y v_\zeta + \zeta_z w_\zeta) \\ \mu(\zeta_x^2+\zeta_y^2+\zeta_z^2)v_\zeta + \frac{1}{3}\mu\zeta_y(\zeta_x u_\zeta + \zeta_y v_\zeta + \zeta_z w_\zeta) \\ \mu(\zeta_x^2+\zeta_y^2+\zeta_z^2)w_\zeta + \frac{1}{3}\mu\zeta_z(\zeta_x u_\zeta + \zeta_y v_\zeta + \zeta_z w_\zeta) \\ (\zeta_x^2+\zeta_y^2+\zeta_z^2)\left[\mu\left(\frac{\partial u^2}{\partial\zeta}+\frac{\partial v^2}{\partial\zeta}+\frac{\partial w^2}{\partial\zeta}\right)+\alpha\frac{\partial T}{\partial\zeta}\right]+\frac{1}{3}\mu\left(\zeta_x\frac{\partial u}{\partial\zeta}+\zeta_y\frac{\partial v}{\partial\zeta}+\zeta_z\frac{\partial w}{\partial\zeta}\right)(\zeta_x u+\zeta_y v+\zeta_z w) \end{bmatrix} \tag{2.94}$$

CHAPTER 3

Volume Extension

The idea behind volume extension is to extend patched grids so as to create an overlapping region between grid zones. The overlapping region is required in order for Pegsus as well as OVERFLOW to work correctly. There are several reason for investigating this approach. First, if this method of creating an overlapping region works and with little user input, it would alleviate any need to modify PEGSUS and OVERFLOW. This would be the major reason. Secondly, many researchers create patched grids for use in their own flow-solvers. Often, these researchers require validation of their results using other flow-solvers, such as OVERFLOW, that use the overset grid technology. Instead of completely remodelling the configuration, the existing patched grids could be transformed into overset grids. As will be shown, the program developed, "patched-2-overset", was not as successful as hoped.

At this point it is a good idea to explain how grids are setup and how the relationship between the physical plane and computational plane are determined. As previously discussed, the physical plane is in x, y, and z coordinates in space and the computational space is in Xi, Eta, and Zeta coordinates. These Xi, Eta, and Zeta coordinates are most often indexed using J, K, and L indices. Constant Xi planes all have the same J index. The same is true for the Eta and Zeta planes both having constant K and L indices. The indices are integers starting at one and running to however many grid points are in that specific direction. Figure 3.1 demonstrates this idea.

For the program to work successfully, the user needs to identify several features of the grid to be extended. But first, some assumptions will be made. The program assumes that the boundaries of the interface will match up perfectly with the donor side patched grid boundary. The computational indices do not necessarily have to be the same, but the physical boundaries of the interface need to match up. This assumption was made since the test case of the ONERA M6 wing had this feature. In fact, this test case was actually a single grid as shown in Figure 3.2. It was then chopped into four separate zones, thus creating twelve, mesh continuous, patched interfaces as shown in Figure 3.3. However, this assumption would rarely exist for complex geometries where patched interfaces may have several grids as donor interfaces.

The user then needs to provide information to the program in order for it to understand where in the computation space the interface exist. This includes which grid the interface exist in. Also, the J, K, and L index ranges that define where in the computational space the interface lies. As one will assume, the interface will always be either on a J=1, J=Jmax, K=1, K=Kmax, L=1, or an L=Lmax plane. The next input is tell the program where the donor side interface lies. This will requires providing the same information as previously given to the program for the recipient side interface. To help reduce user input, it was assumed that the reciprocal is true. When the donor side interface is provided, it is assumed that it will be a future recipient interface with its previous recipient interface now becoming the donor interface.

Providing both interfaces is very important, the program uses the donor grid interface boundaries as a stencil on how to extend the recipient grid. It also uses the plane of points behind the donor interface as a reference plane on how far to extend the recipient grid and how the recipient grid will conform to the donor grids outer boundaries. Figure 3.3 demonstrates this idea in two-dimensions. However, it will be shown that this may cause problems under certain circumstances. The user also has the option of how many grid points to extend the grid. The grid is extended using the donor grids interface plane and all subsequent planes behind the donor interface depending on how many planes are added. Since the recipient grid is extended using the donor grid, the user specifies a maximum stretching ratio, in returns the program alerts the user if the stretching ratio is exceeded. Since there should be little stretching across the interface, this alert should help the user in problem areas of the grid to be later refined. Table 3.1 summarizes the user required inputs as the program is executed.

The test case chosen for this research is the ONERA M6 wing as previously shown in Figure 3.3. Table 3.2 details the grid system information. For this test case, we will demonstrate the use of the extension program on one of the patched surfaces. It will be shown that all twelve interfaces will have similar results. For this demonstration, the K maximum patched surface on zone three will be extended one grid plane using the donor grid for interpolation. As Figure 3.4 shows, the K maximum interface is also on the same physical plane as another patched interface of zone three, the J minimum surface. The same is true for the donor grid, zone two. The K maximum surface of the recipient grid matches up with the K maximum surface of zone two. Also, the J minimum surface of zone three matches up with the J maximum surface of zone two. Let's now concentrate on the K maximum surface of zone three, our demonstration surface. However, all four surfaces just mentioned will in one way or another affect this surface, and will lead up to one of the setbacks of volume extension. Instead of trying to visualize this extension in the physical plane, it will be much easier to show in the computational space. Referring to Figure 3.5, the K maximum surface and the J minimum surfaces are shown. This surface will now be extended as shown in Figure 3.6. The extended plane is shown in red. This will now add one more dimensional grid point for the K direction. Disregard for now using the donor grid for the distance and placement of this extended surface. Remember that this was a single grid and was split at symmetry planes, so using the recipient grid for an extension direction and distance will have the same effect as using the donor grid. Now, lets extend the J minimum surface without extending the new K maximum plane. Figure 3.7 shows the results to this with the new J minimum plane in blue. As a result of extending the K maximum, an extra point has been added. As shown in Figure 3.7, the green dots are the result of extending the first K maximum plane and the second J minimum plane. The end result is a series of new cells at the corner of the computational grid. This is fine for the computational space since the angle alpha between the new K maximum plane and the new J minimum plane is ninety degrees. However, referring back to Figure 3.5, both the K maximum plane and J minimum plane are all on the same physical plane. This will make the angle alpha zero degrees, and as a result the new set of grid cells at the corner of the computational plane will collapse on themselves in the physical plane. An undesirable result that creates zero and negative cell volumes.

It just happens that all twelve patched surfaces in the test case have this feature. There are several options to further investigate. The other option available in this program is to use the recipient grid to extend the patched interface. That is use the plane behind the patched interface and the interface itself to linearly extrapolate a plane. As stated earlier, the four zones were created at symmetry planes and as a result, the two options created in the program will have the same effect. Another option is to extend the interface normal to the patched surface. This again will have the same effect as before with corner point B being coincident with points A and C as shown in Figure 3.7. The last option used was to go ahead with the original grid extension and force the angle alpha to be something other than zero degrees. This will force all the points beneath points A and C to spread outward from the points beneath point B. In the end this worked fine and the grids were run through Pegsus with no problems.

This test case is rare in that all the patched interfaces had this feature. For the most part, this program could handle most real world complex geometries modeled using patched grids. However, most often, a patched interface will not be an entire computational plane. Usually the patched surface will be a subset of a computational plane with boundary conditions applied to the remaining points on the surface. This will create problems later on for the user once the entire plane is extended. The extended portion of the plane that had boundary conditions will now have to be cut out during the Pegsus procedure. This may be a terribly time consuming task if for say the test case has eighty patched grids with a good portion of them needing hole cuts due to the grid extension. Also to consider, even if extending patched grids to create an overset grid system will still leave the interfaces unconservative. Due to the outcome of this investigation, and the reality of having further problems with grid extension, it was decided to continue in another direction. The results for this test case will be presented later in Chapter Six.

CHAPTER 4

Pegsus Modifications

As mentioned earlier, in order to model real world complex geometries, multiple grids must be created that model specific regions of the flow field accurately. This procedure of domain decomposition is called the chimera grid approach [11]. Since the main purpose of the flow-solver, OVERFLOW in this case, is to numerically solve the governing equations, a separate preprocessing program is required to provide information to OVERFLOW on how each grid will pass flow-field information between themselves. For OVERFLOW, the program Pegsus is used to provide grid communication information for overlapping grids. Pegsus is also used to cut holes in grids in areas that may cause interference with other grids such as overlapping solid surfaces.

The basic procedure for a researcher to apply the chimera grid approach is to first model the flow-field using multiple overlapping grids (Figure 1.3). Next, the user provides Pegsus with these separate grids and an input file that provides all necessary information on which outer boundaries on each grid will require Pegsus to compute valid stencils. A valid stencil is a when Pegsus has determined that a point lies within a donor grid cell and that the three required interpolation coefficients are between zero and one. For grids requiring hole cuts, the user specifies surfaces in one grid that will make a hole in another grid. Pegsus will then determine how to cut the hole and which fringe points on the hole will require interpolation stencils. Pegsus in returns creates a single multiple grid file containing all grids and an interpolation file [11].

For this research, the process in which Pegsus goes about searching for valid stencils and creating hole cuts will not be discussed in detail but rather how to modify Pegsus to handle patched grids. In fact, hole cutting is not required for patched grids since there are not overlapping regions.

First there is the issue of the interface itself. For grids of varying resolution or non point-matched grids, the interface is not exactly a clean smooth curve where there are no gaps or overlapping. For most cases there exist smalls gaps in some regions and small overlaps in others as demonstrated in Figure 4.1. The interface points that overlap the donor grid and those points very close to the donor grid, Pegsus will have little trouble finding valid stencils. It is difficult to determine what is a very close point in terms of a specific distance. It will vary from run to run and the grid resolutions involved in each run. One of the inputs to Pegsus is for the user to determine and supply a parameter, epsilon, that will allow Pegsus to label a stencil as valid depending on how far that point may lie outside of a donor grid cell [11]. This will result in interpolation coefficients outside the range of zero and one or that the point lies outside the donor cell by some small amount. For the points outside the domain of the donor grid, Pegsus will have trouble finding stencils. For these points to receive the appropriate interpolation coefficients, they must be projected onto the surface of the donor grid. The projection will not be permanent, it will only provide a physical coordinate to compute the interpolation coefficients. This projection requirement will be one of the modifications to Pegsus. A search routine will also be needed to find out where on the donor grid interface the projection will occur.

With both the projection and search routines added, some other features will be added to speed up the search and add functionality for the patched grid option to Pegsus. Table 4.1 summarizes these additions.

The first entry in Table 4.1 is the patched grid option. This option, specified in the input file provided by the user, enables the new search and projection subroutines. This option is only enabled if a point is labelled by Pegsus as an 'Orphan Point'. An orphan point is a point that Pegsus could not find a valid stencil for. Once a point is labelled an orphan point, the new search routine begins.

The reason for the new search routine is to find the donor grid cell that the recipient point lies within or has the possibility of being projected onto in order for interpolation coefficients to be calculated. The first step of the search is to find the closest point in the donor grid to the recipient point. This donor test point will be the starting point of the next search. The next search procedure is a clipping test. This test determines if the recipient point has the possibility of falling within a two by two cell face area of the donor grid with the donor test point just found as the center point. This is achieved by first determining the minimum and maximum x, y, and z values of all nine points that make up the two by two cell faces of the test region of the donor grid. With these minimum and maximum x, y, and z values, the clipping test is passed if any of the x, y, or z components of the recipient point lie within the minimum and maximum ranges of the donor test region. The clipping test is rather fast and reduces the number of regions in the donor grid for the next search procedure to test in. The clipping test is demonstrated in Figure 4.2. If the test fails, the search continues in a radial direction from the initial test point. Once the clipping test is passed, the next test procedure is executed.

The final search procedure is a triangle test. That is, the recipient point is projected onto the plane of the two by two cell face area using the center point as a reference point.

Even if the four cell faces are not on one distinguishable plane, the center point will be common to all four planes and is used to project the recipient point the proper distance. Once the point is projected, a triangle test is implemented. This test consist of calculating four triangular areas and making a comparison. Referring to Figure 4.3, point R, the recipient point, is projected onto the donor grid interface test region. The next step is to calculate the area of triangle abc. This will be the base area. Next using the new coordinate of point R after the projection, the areas of triangles abR, acR, and cbR are calculated. If the sum of these component areas sum up and equal to the base area, the search is over and the grid cell in the donor grid has been found. If not, the triangle test continues for this test region. If all eight possible triangle tests fail, the search continues on with the clipping test again. Once the triangle test has passed, the donor cell and projected point R are passed back to the main search of Pegsus and interpolation coefficients are calculated. To help speed up future searches of orphan points passed to the projection subroutines, the previous stencil is stored. Instead of calculating the closest point in the donor grid, the stored stencil is used as a starting point. Calculating the closest point in the donor grid is CPU intensive, avoiding having to use it drastically speeds up the search. Since orphan points tend to be confined or clustered to specific regions of the grid, storing previous stencils most often reduces calling the closest point search to only two or three times depending on grid topology.

The next option in Table 4.1 is the DGRID option. The user is responsible for providing Pegsus a set of possible donor grids. For patched grids, usually only a subset of these grids are possible donor grids for one interface and the remaining subsets are possible donor grids for the other interfaces of the recipient grid. The criteria Pegsus uses for a recipient point to even start a stencil search in a donor grid is if the points lies within the min/max box of that donor grid. However, in some cases and especially with patched grids, the recipient point may be in the min/max box of the donor grid but may not be its true donor grid. Therefore, the DGRID parameter is an option to further subset the user provided donor grid list for each of the interfaces on the recipient grid in question. This has shown to improve speed of execution in most cases. This is because once Pegsus has started its search and the point will require projection, Pegsus will continue the search over a great deal of the donor grid until it labels it an orphan point. This is costly and can be avoided if the user uses the DGRID option.

The third entry in Table 4.1 is the PROGRD option. PROGRD is a separate program to Pegsus and is used to project subsets of a recipient grid onto a reference plane of a donor grid [13]. This is primarily used in the viscous regions of grids that have varying resolution and there exist a mismatch as to were the solid surface is modeled. Referring to Figure 4.4, both the red and blue grids accurately model the cylinder. All surface points lie on the solid surface of the cylinder, however since the two grids have varying resolutions there exist a mismatch in the boundary layer of these two grids. Referring to the blue grid and line A, the point on the solid surface is actually within the boundary layer of the red grid. If these were two patched interfaces, the flow-field information being passed back and forth between the red and blue grids, in the sensitive region of the boundary layer, would be incorrect and will cause discontinuities in the flow. To fix this problem, PROGRD will project the points in line A on the blue grid onto the solid surface characterized by the red grid. The PROGRD option, if specified, will read in the resulting projected grid from PROGRD as the set of physical coordinates used to find stencils in PEGSUS. However, the original grid is used in the flow-solver since it accurately models the geometry.

The fourth entry in Table 4.1 is the METHOD option. This will tell Pegsus were to store the weights for the patched grids interface points. This will allow OVERFLOW to distinguish between the two methods used to update interface points. As mentioned earlier, the two methods used to update the interface points are the flow-through boundary condition and the cell-vertex finite volume method. Since the flow-through boundary condition only uses the first interior points behind the donor grid interface for flow-field information, it was decided to make the interpolation coefficients indicate that all the weight is on the interior plane. This will require making one of the weights zero or one. Depending on what computation plane the interface lies on, one of the weights will either be zero or one. For example if the interface is on the J maximum plane, the J weight will be zero, thus indicating no weight on the J maximum surface. Since the interface is two-dimensional, the weight being set to zero or one is in the third direction which has no effect on computing the final weights which are dependent only on the remaining two weights. The opposite is made for the cell-vertex method. One of the three interpolation coefficients will be set to zero or one indicating the remaining two weights are on the interface. For the previous example, the J weight will be set to one placing full weight on the interface. When OVERFLOW reads in the weights and the stencil, it will be able to differentiate between the two methods depending on where the weights are.

The last entry in the Table 4.1 is for the coincidence check. For the example of the ONERA M6 wing, the patched grids are mesh continuous. That is, the grid points line up, or are coincident with the donor grid interface points and vice versa. When the coincidence check is enabled Pegsus will check for coincidence with the donor side test point. This is a fairly easy task of comparing physical coordinates and is the first test in the search procedure. If the user knows that the patched grids are mesh continuous, enabling this option will speed up execution tremendously.

The modifications to Pegsus were straight forward. The bulk of the work was creating the new search and projection subroutines. The remaining options listed in Table 4.1 were consequences of debugging the program. Although the speed of the program has decreased some what as compared to the original version, the resulting number of orphan points is minimal, which is one of the goals for a patched interface.

CHAPTER 5

OVERFLOW Modifications

OVERFLOW is a three-dimensional unsteady compressible thin-layer Navier-Stokes flow-solver developed at NASA Ames Research Center. The development of OVERFLOW has been ongoing for many years and begun as a rewrite from two previous NASA codes, the ARC3D and F3D codes. OVERFLOW has several options for right-hand-side calculations [12]. These include central differencing, flux split in J (central in K, L), Liou AUSM flux split scheme, and finally the Roe upwind scheme. Left-hand-side options are the ARC3D 3-factor block tridiagonal scheme, F3D two-factor scheme, ARC3D 3-factor diagonal scheme, and also the LU-SGS algorithm. Several turbulence model options exist also. These include the Baldwin-Lomax, Spalart-Allmaras models and the $k-\varepsilon$ turbulence model. For this research, the right-hand-side calculations will be limited to central differencing and the ARC3D 3-factor diagonal scheme for the left-hand-side [13].

The first modification to OVERFLOW was to include the flow-through boundary condition. This was included since it is a simple modification to the program and was used to quickly debug problems in the modifications to Pegsus. Although the flow-through boundary condition is one solution to including the patch grid capability in OVERFLOW, it will prove to be unconservative. The goal is to include a patched grid capability with the option of further enhancing this method to be fully conservative. The flow-through boundary will not be capable of being modified to be fully conservative. The initial results were very promising, proving that the modifications made to Pegsus for patched grids were working. Also, the results of the ONERA M6 wing showed that the flow-through boundary condition worked well with very little flow-field discontinuities at the interface. This test case did not place patches near any known flow-field discontinuities such as shocks. Later test cases, with patched interfaces placed at a shock location on the top of the wing, showed that this method would not allow the shock to properly pass through the interface.

The next modification to OVERFLOW is to include a cell-vertex finite volume scheme for the interface points. This method has the further capability of being fully conservative. With the interior scheme being a finite difference method, including the cell-vertex finite volume method took careful planning and consideration to allow both methods to work together. Both right-hand-side central differencing and the left-hand-side ADI operator were implemented in several steps. This method proved to be unstable for certain test cases involving an initial garbage solution. The initial garbage solution tests to verify if the garbage input would pass through the interface cleanly and wash out the exit plane. The ONERA M6 wing test did not work at all. Severe pressure oscillations occurred immediately ahead of the leading edge of the wing. Further investigation of the cell-vertex method is needed to stabilize the scheme.

Flow-Through Boundary Condition

The flow-through boundary condition works very similar as the C-grid boundary condition [12]. The C-grid boundary condition is applied to a plane of coincident points in the region of a C-grid that folds over onto itself. Figure 5.1 demonstrates a C-grid modeling a cylinder. The wake region of the C-grid is were the C-grid boundary condition is applied. The update of the boundary points using this boundary condition requires using flow-field information from interior points on both sides of the C-mesh region. The only requirement is that the points at the boundary must be coincident with its corresponding point at the other end of the C-mesh region as demonstrated in Figure 5.2. In Figure 5.2, the C-grid boundary condition is applied to the J values of one to twenty-three. It is automatically assumed the corresponding coincident points, denoted by a negative sign, will have the same requirement. Figure 5.3 demonstrates how to update the boundary points. For the example, point thirteen is updated using the one-half the value of the first interior point behind point thirteen, point Q(13,2), plus one-half the value of the first interior point behind its corresponding coincident point, point Q(-13,2). The same will be true when updating point Q(-13), it will have the same value as its corresponding coincident point, point Q(13). All the points in the C-mesh with the boundary condition will be updated after all the interior points have been updated.

To apply this concept to a patched grid is very similar. For the C-grid boundary condition, the user specifies only one side of the range of points it is to be applied to. The corresponding coincident points are easily obtained since they are in the same grid and will also take on the boundary condition. For a patched grid, Pegsus will provide all the necessary information on how to identify the donor grid information. This will include providing a pointer and three interpolation coefficients. The pointer identifies the donor grid number and the J, K, and L index location inside that grid as to what cell will provide the donor side flow-field information. The pointer indices are the minimum index of the donor grid cell in each direction (Figure 5.4). Figure 5.4 demonstrates how to the recipient point is updated. Pegsus provides the pointer and the three weights which can be used to calculate all the weights for each of the node values for the cell. The recipient side contribution to the update is one-half of Q_1. Where Q_1 is the first interior point behind the interface. The donor side information will be one-half of the sum of several weighted Q values. As stated earlier, the weights on the interface points, weights one and four, are forced to be zero during the Pegsus process in order for OVERFLOW to distinguish the method.

The modification to OVERFLOW was straight forward. Referring to Figure 5.4, if point Q_R was an overset point, its update would take on the following formula.

$$Q_R = \{\omega_1 Q_1 + \omega_2 Q_2 + \omega_3 Q_3 + \omega_4 Q_4\} \tag{5.1}$$

The update using the overset method does not using any flow-field information from the recipient grid. For the recipient patched interface points, the donor side information has been satisfied already since weights one and four are set to zero. All that is needed is to add the recipient side Q value and divide the total update by two. Therefore, as the chimera subroutines are iterating over all the outer boundary points, the recipient side Q value is added and the total Q value is then divided by two.

To allow for both overset and patched grids was also a straight forward task to incorporate into OVERFLOW. Pegsus was further modified to insure that patched interface points will always have at least one of the interpolation coefficients set to zero or one (only two coefficients are needed, interface is two-dimensional). Then, to distinguish between the patched interface points, the overset points will always have values between zero and one. If by chance Pegsus found a stencil that had an interpolation coefficient value of zero or one, a check is made that will add or subtract a small delta value. This will have little effect on the solution but will help OVERFLOW distinguish between the two methods.

LIST OF REFERENCES

[1] Andersen, J. D., ***Fundamentals of Aerodynamics***, McGraw Hill Inc., New York, 1991.

[2] Tannehill, J. C., Anderson, D. A., and Pletcher, R. H., ***Computational Fluid Mechanics and Heat Transfer***, Taylor and Francis, Washington, 1997.

[3] Hoffmann, K. A., and Chiang, S. T., Computational Fluid Dynamics For Engineers, Engineering Education Systems, Wichita, 1993.

[4] Volpe, G., "Conservation and Transparency at Internal Boundaries of Patched Grids," AIAA Paper 93-2930, July 1993.

[5] Beam, R. M., and Warming, R. F., "An Implicit Factored Scheme for the Compressible Navier-Stokes Equations," AIAA Paper 77-645, June 1977.

[6] Mavriplis, D. J., Jameson, A., and Martinelli, L., "Multigrid Solution of the Navier-Stokes Equations on Triangular Meshes," AIAA Paper 89-0120, January 1989.

[7] Whitaker, D. L., Grossman, B., and Lohner, R., "Two-Dimensional Euler Computations on a Triangular Mesh Using an Upwind, Finite-Volume Scheme," AIAA Paper 89-0470.

[8] Pulliam, T. H., and Steger, J. L., "Implicit Finite-Difference Simulations of Three-Dimensional Compressible Flow," ***AIAA Journal***, Vol. 18, No. 2, February 1980, pp. 159-167.

[9] Ying, S., Bagonoff, D., Steger, J. L., and Schiff, L. B., "Numerical Simulation of Unsteady, Viscous, High-Angle-of-Attack Flows Using a Partially Flux-Split Algorithm," AIAA Paper 86-2179, August 1986.

[10] Baldwin, B. S., and Lomax, H., "Thin Layer Approximation and Algebraic Model for Separated Turbulent Flows," AIAA Paper 78-257, January 1978.

[11] Suhs, N. E., and Tramel, R. W., "PEGSUS 4.0 User's Manual," AEDC-TR-91-8, Calspan Corporation/AEDC Operations, June 1991.

[12] Buning, P. G., "OVERFLOW User's Manual, Version 1.7u," NASA Ames Research Center, March 1997.

[13] Chan, W. M., Buning, P. G., and Krist, S. E., "User's Guide For PROGRD," NASA Ames Research Center/MCAT Inc., August 1996.

[14] Wang, Z.J., and Yang, H.Q., "A Unified Conservative Zonal Interface Treatment For Arbitrary Patched And Overlapped Grids," AIAA Paper 94-0320.

[15] Rogers, S.E., Cao, H.V., and Su, T.Y., "Grid Generation For Complex High-Lift Configurations," AIAA Paper 98-3011.

Table 3.1: Patched-2-Overset Required Inputs

Patched-2-Overset Input Questions	Iterations
Enter the number of patched grids in system.	a=N
Enter the number of patched surfaces for grid (a).	b=1..M
Enter the J, K, and L indices for patch (b) of grid (a)	
Type of Interpolation for patch (b) of grid (a): 1=straight extrapolation follow grid lines of recipient grid. 2=straight interpolation, follow grid lines of donor grid.	1 or 2
Number of additional planes for patch (b) of grid (a).	1, 2, 3 .....
Enter the number of the donor grid.	c=N'
Enter the J, K, and L indices for donor patch (c) for grid (a) and recipient patch (b).	

Table 3.2: Four Zone ONERA M6 Wing Summary

ONERA M6 Wing: Four Zone, Mesh Continuous Grid System	
Zone One: 49x25x33 grid points	Lower downstream grid
Patched Surface	J=1,48 K=2,24 L=33,33
Patched Surface	J=1,48 K=25,25 L=2,33
Patched Surface	J=1,1 K=2,25 L=2,33
Zone Two: 73x33x49 grid points	Lower wing grid
Patched Surface	J=1,1 K=2,33 L=2,48
Patched Surface	J=73,73 K=2,33 L=2,48
Patched Surface	J=1,72 K=33,33 L=2,48
Wing Surface	J=1,73 K=2,33 L=1,1
Zone Three: 73x33x49 grid points	Upper wing grid
Patched Surface	J=1,1 K=2,33 L=2,48
Patched Surface	J=73,73 K=2,33 L=2,48

Table 3.2: Four Zone ONERA M6 Wing Summary

ONERA M6 Wing: Four Zone, Mesh Continuous Grid System	
Patched Surface	J=1,72 K=33,33 L=2,48
Wing Surface	J=1,73 K=2,33 L=1,1
Zone Four: 49x25x33 grid points	Upper downstream grid
Patched Surface	J=1,48 K=2,24 L=33,33
Patched Surface	J=1,48 K=1,1 L=2,33
Patched Surface	J=1,1 K=1,24 L=2,33

Table 4.1: Pegsus Modifications Summary

Pegsus Modifications	Description	Option
TYPE = 'Patched' or TYPE = 'Overset'	The 'Patched' option will enable the new search and projection subroutines	Required
DGRID='donor grid #'	This will further subset the donor grids. Will only search those grids specified	Optional
PROGRD = 'progrd name'	This option will read in grids that result from the program PROGRD. Stencils now will use the physical coordinates from the progrd grid for stencil searches, but retain the original grid for the flow-solver.	Optional
METHOD = 'Flow-through' or METHOD = 'Cell-vertex'	This option will determine where interpolation weights will be stored. This will help OVERFLOW distinguish between the two interface methods, the flow-through boundary condition and the cell-vertex method..	Required
COINCK = 'TRUE' or COINCK = 'FALSE'	This option will enable or disable the coincident point check option. Program execution speeds up with this option enabled for mesh continuous grids.	Optional

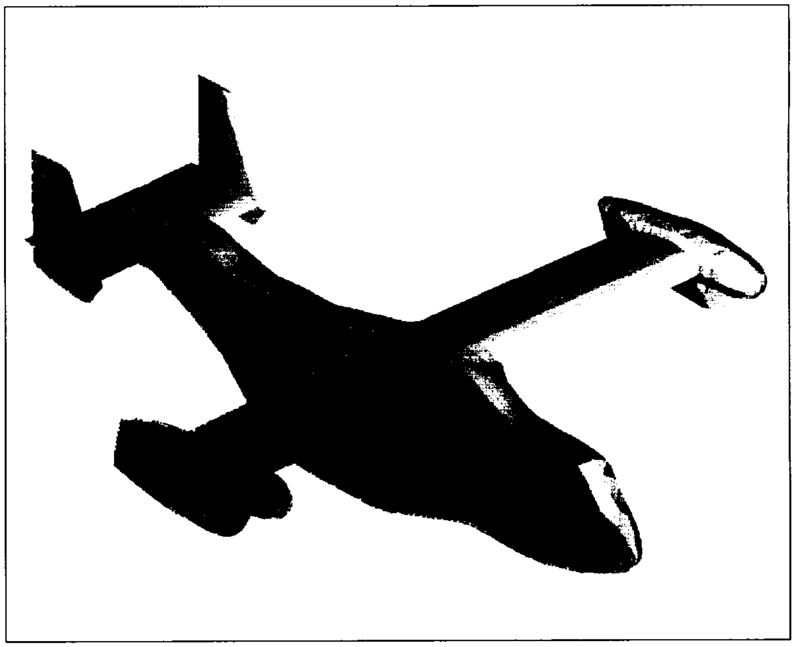

Figure 1.1 Unstructured surface grid on aircraft geometry

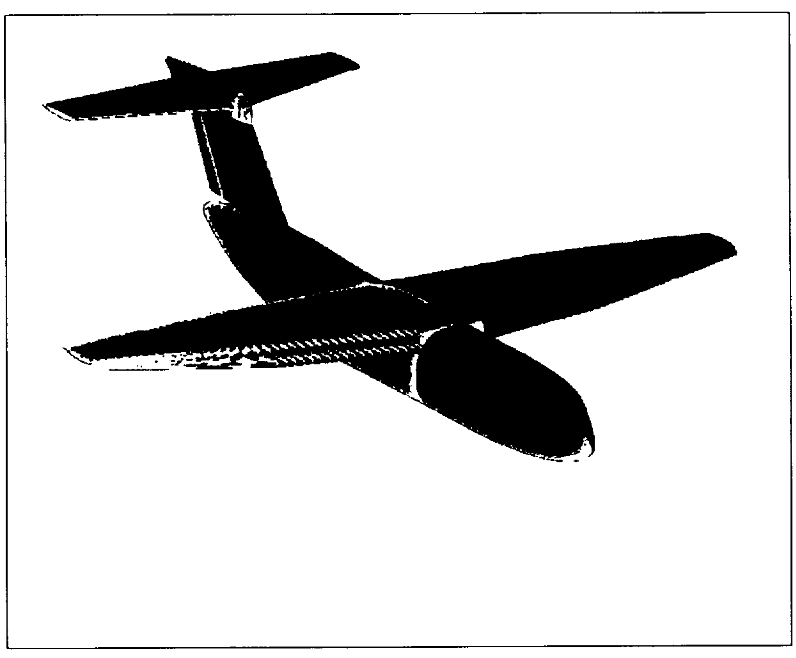

Figure 1.2 Structured surface grid on aircraft geometry

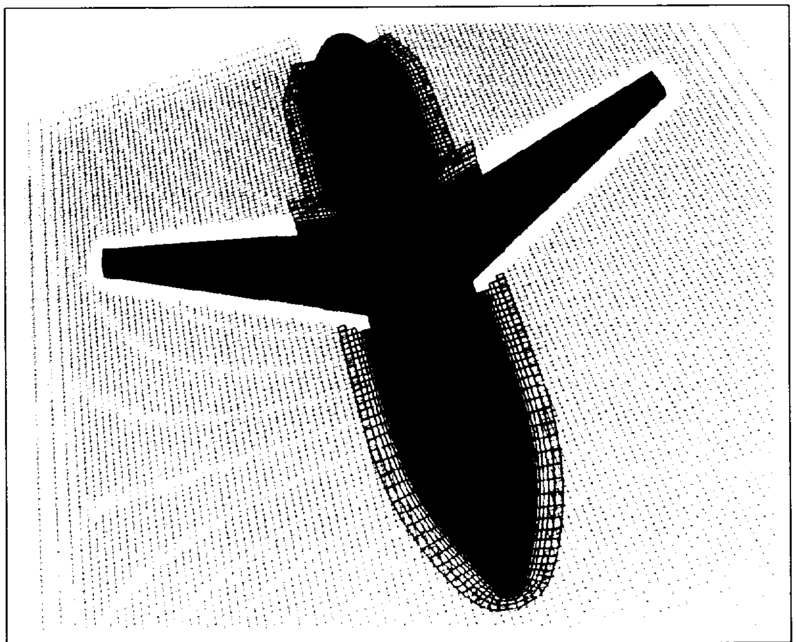

Figure 1.3 Structured overset grid, with hole cuts, of a wing-body geometry

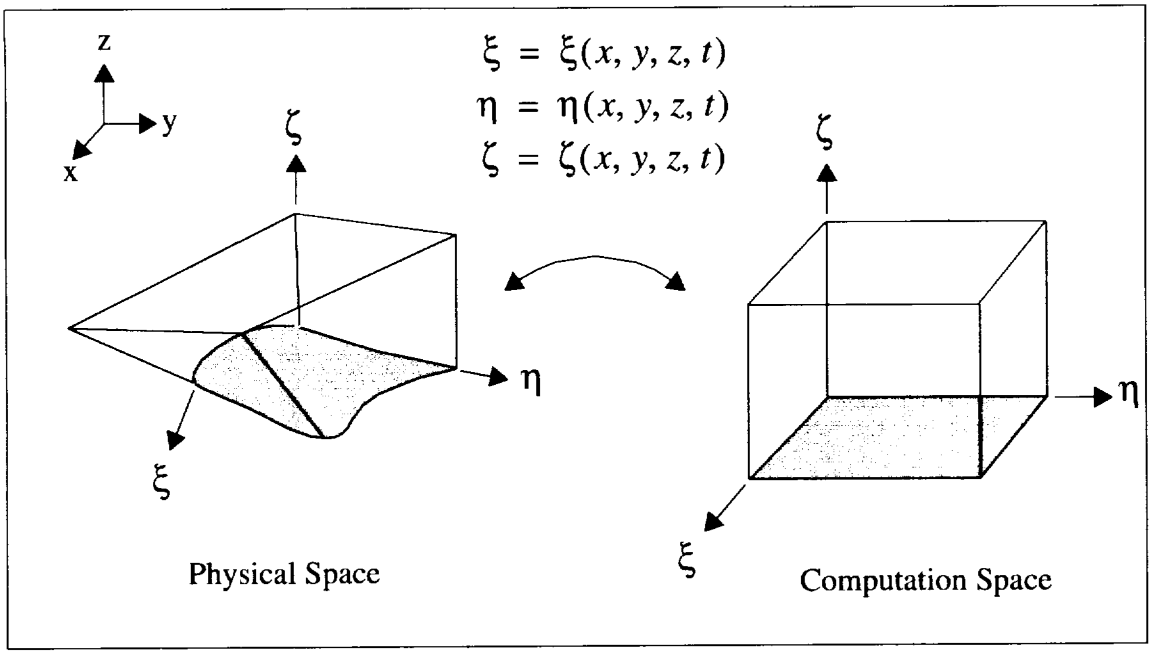

Figure 2.1 Generalized transformation between the physical and computational domains

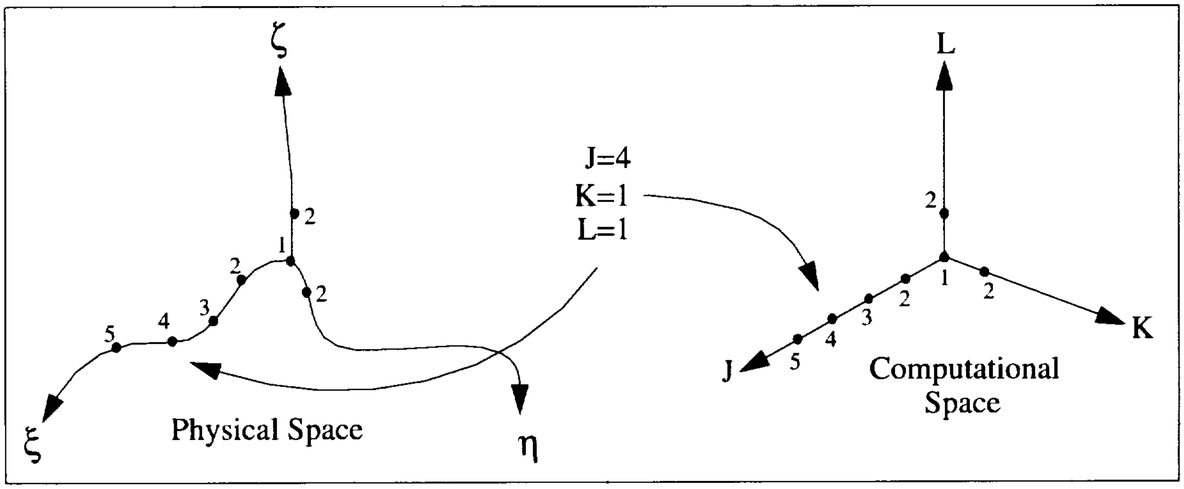

Figure 3.1 Computational space indices relative to physical space indices

Figure 3.2 ONERA M6 wing, single zone, 269x35x67 grid points

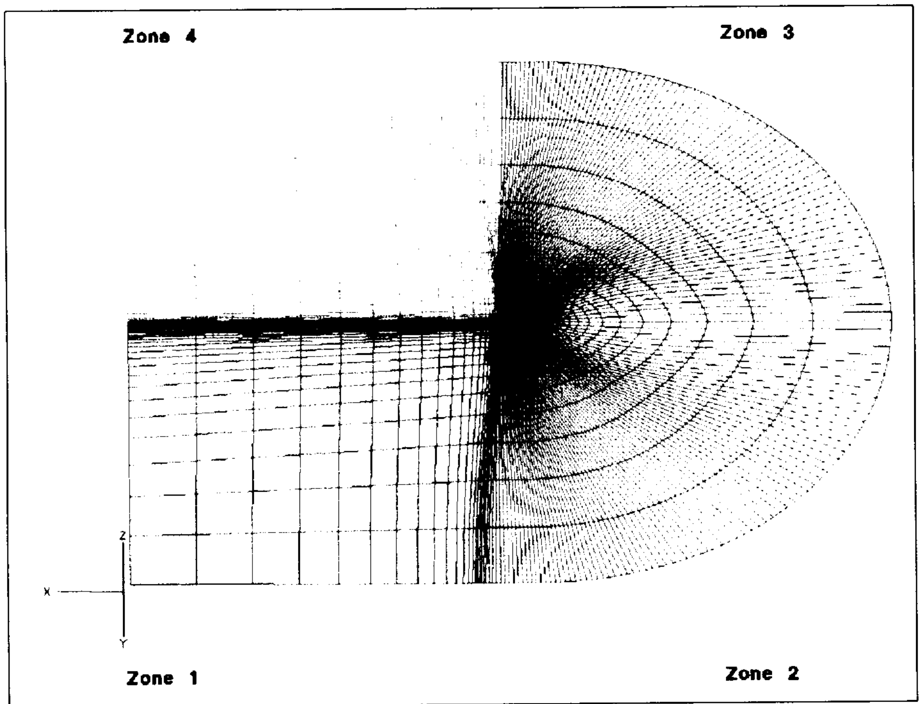

Figure 3.3 ONERA M6 wing, four zone patched grid system

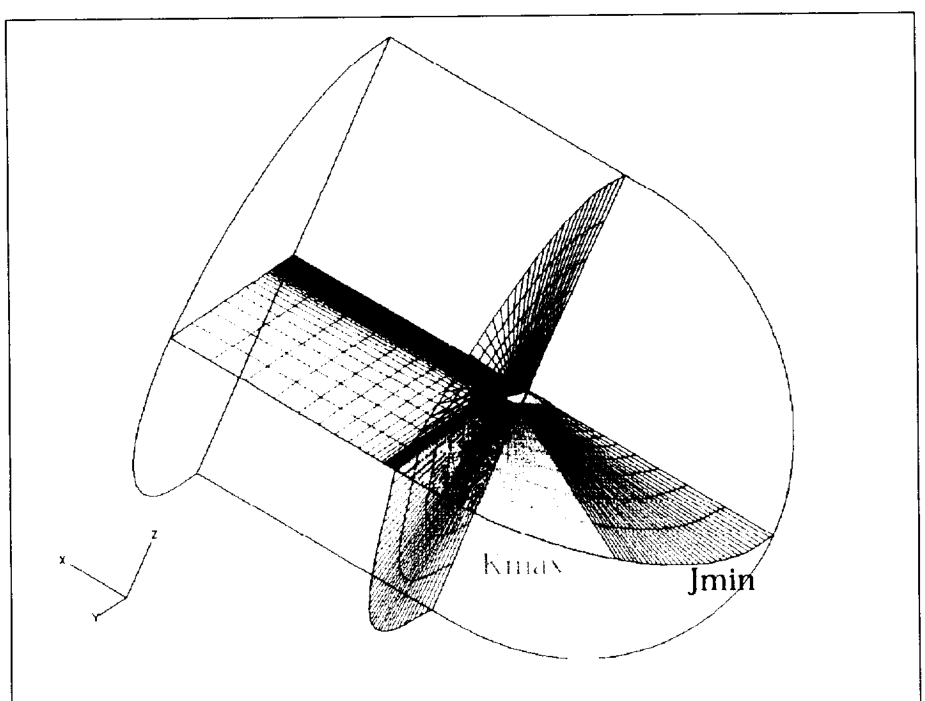

Figure 3.4 ONERA M6 wing, twelve patched interfaces

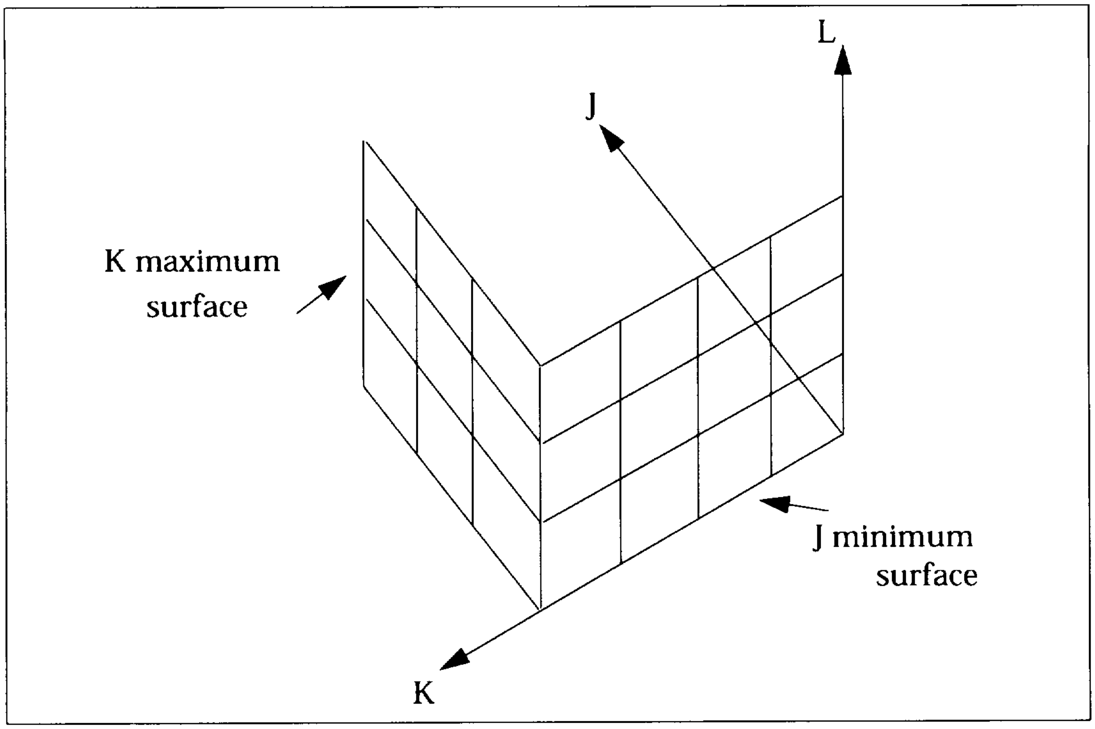

Figure 3.5 Zone three, patched interface at the K maximum surface and the J minimum surface

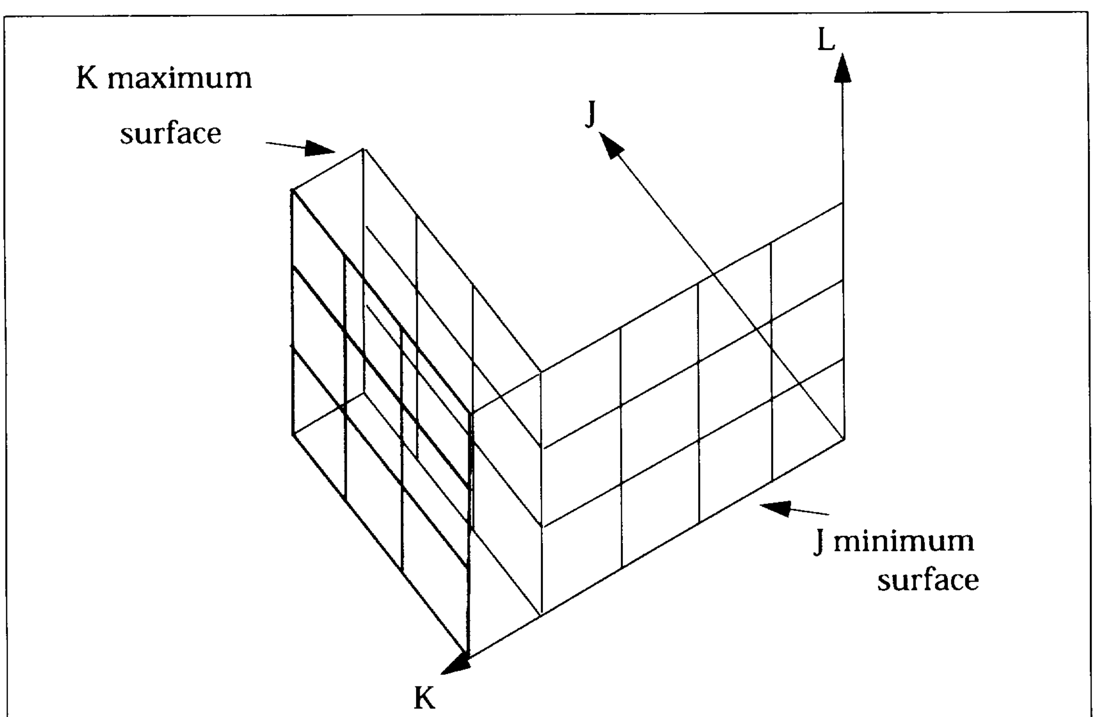

Figure 3.6 Zone three, extending the K maximum surface

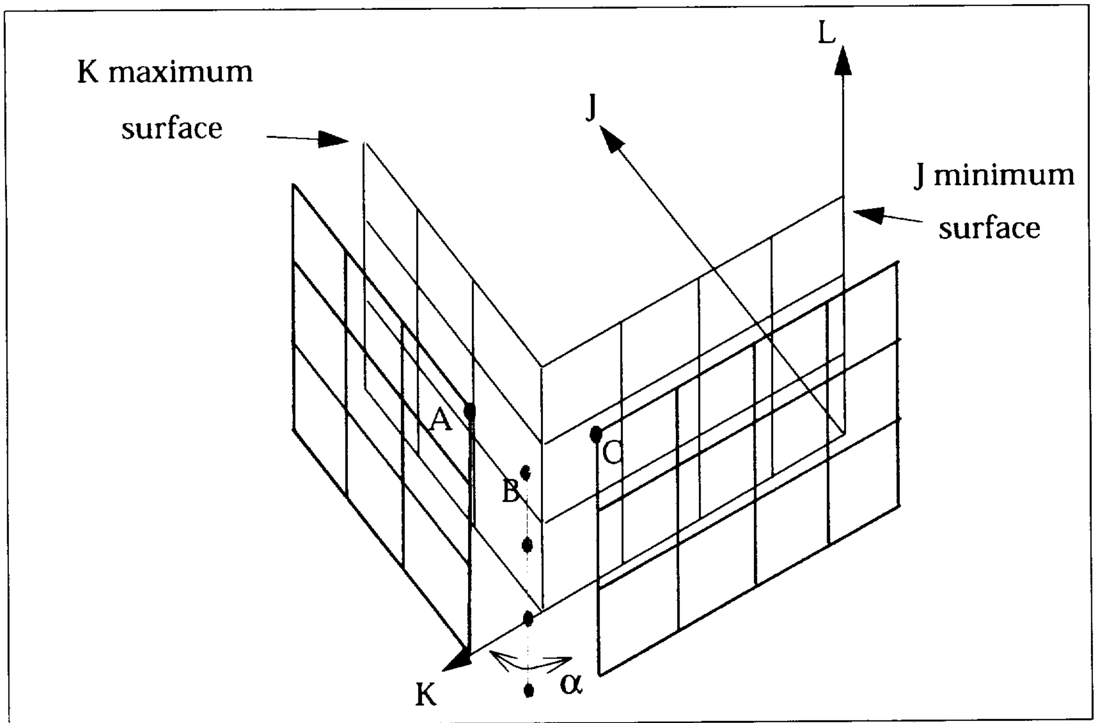

Figure 3.7 Zone three, extension of K maximum surface and J minimum surface

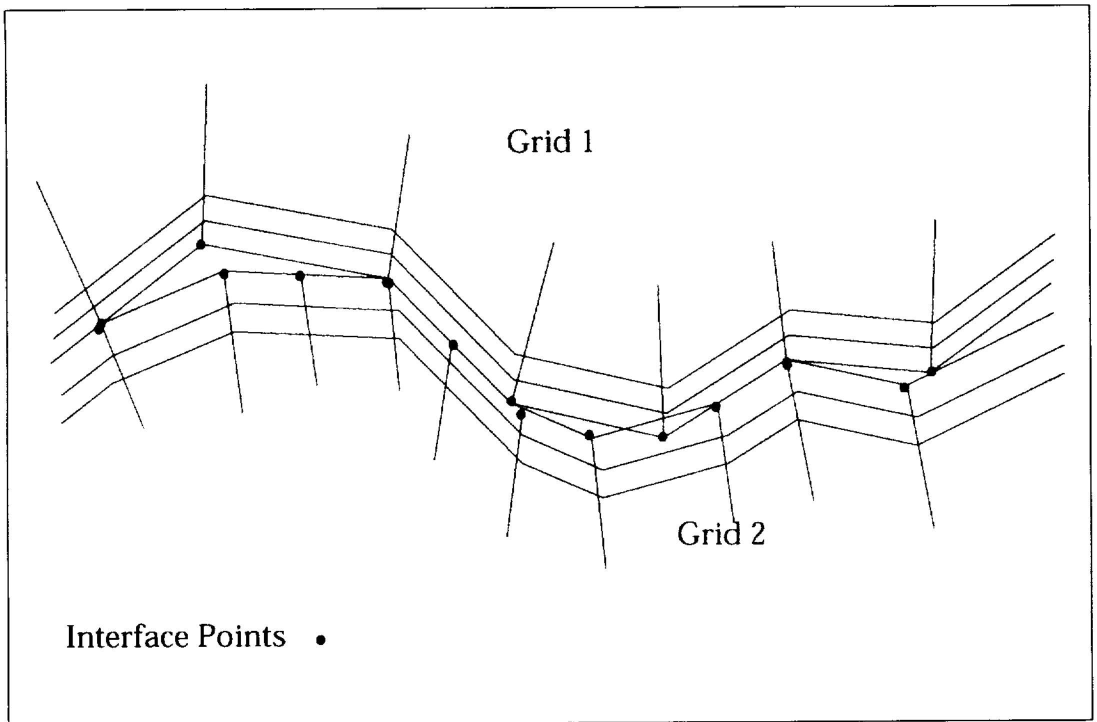

Figure 4.1 Patched grid interface characteristics

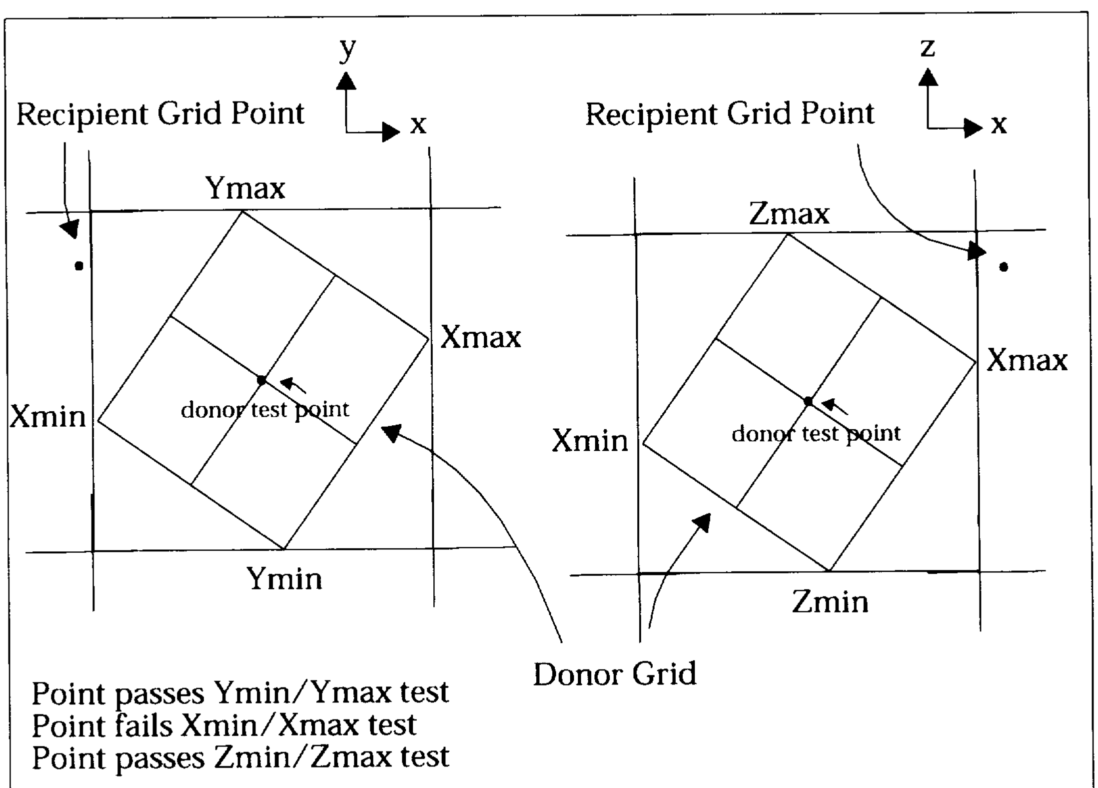

Figure 4.2 Clipping test example

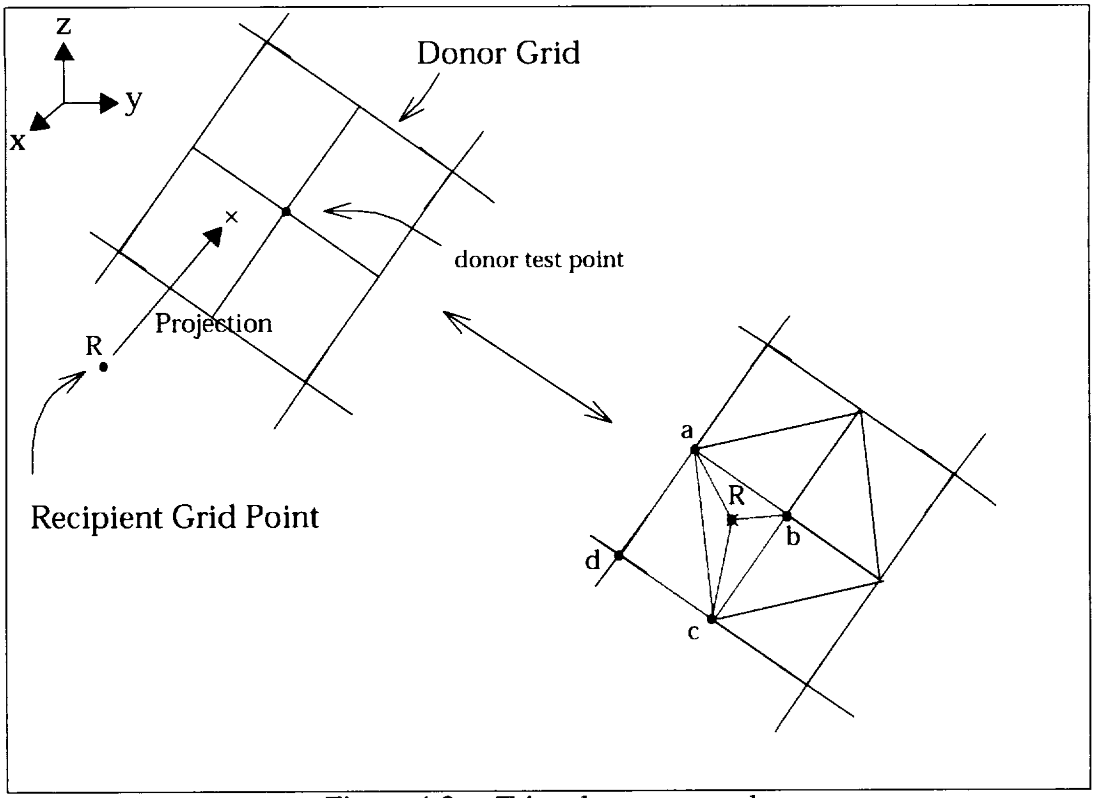

Figure 4.3 Triangle test example

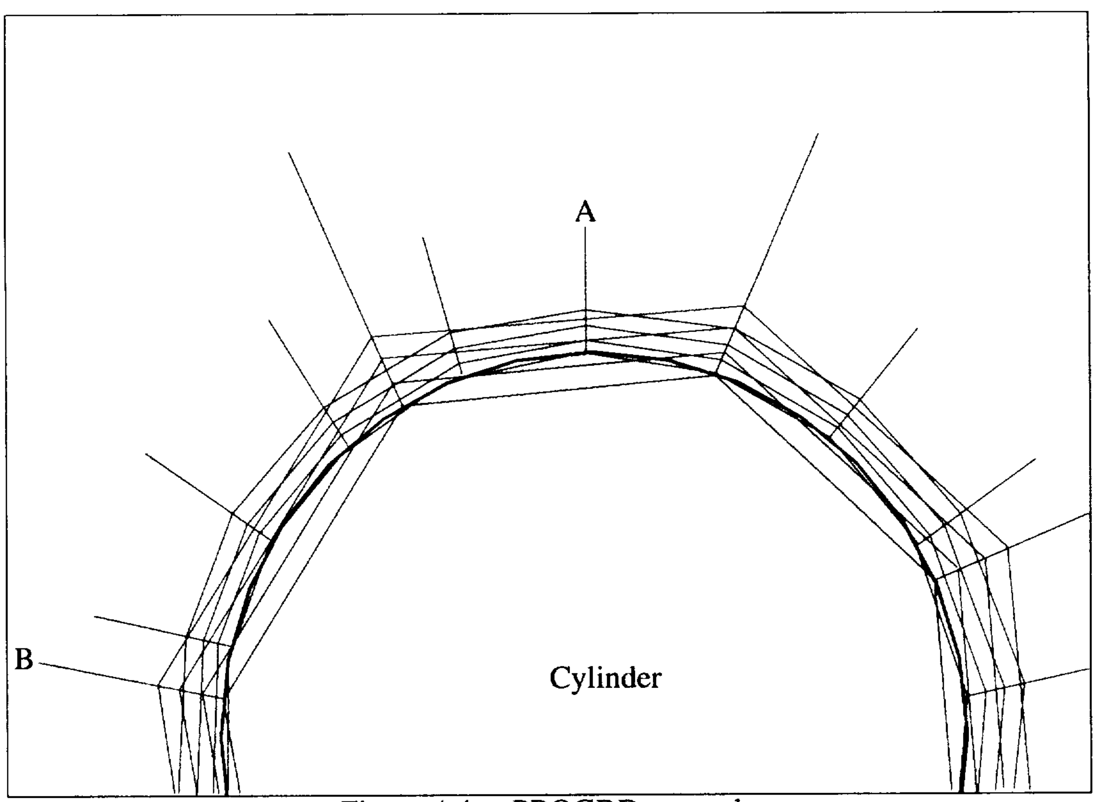

Figure 4.4 PROGRD example

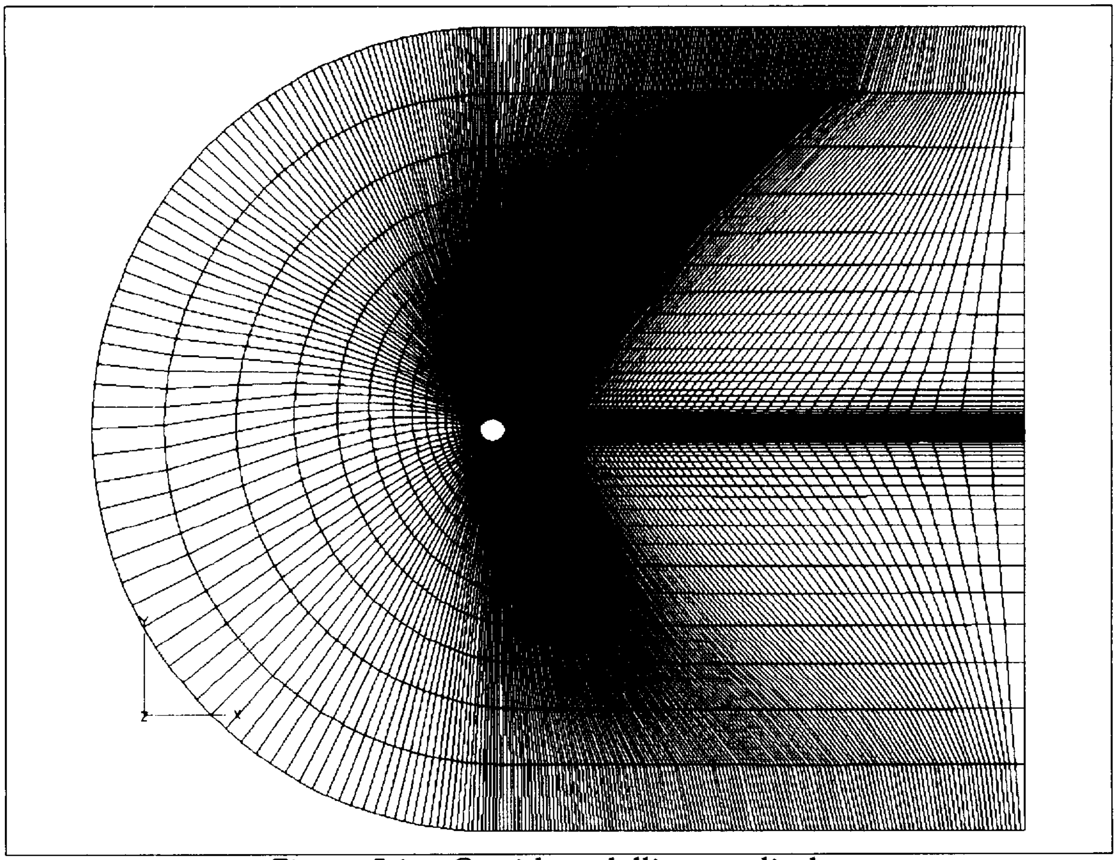

Figure 5.1 C-grid modelling a cylinder

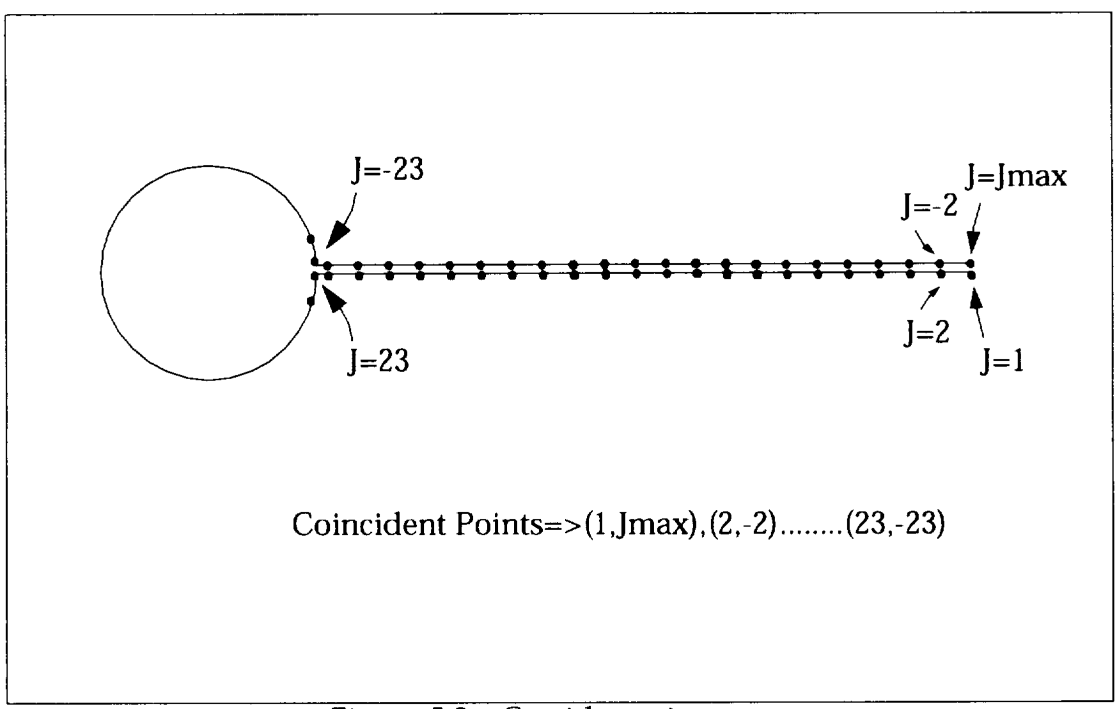

Figure 5.2 C-grid requirements

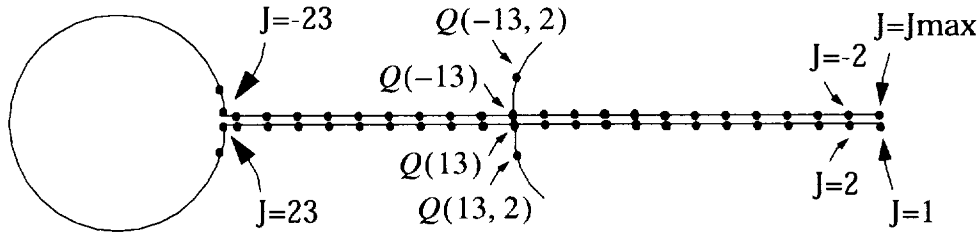

$$Q(13) = \frac{1}{2}\{Q(13, 2) + Q(-13, 2)\}$$

$$Q(-13) = Q(13)$$

Coincident Points=>(1,Jmax),(2,-2)........(23,-23)

Figure 5.3 C-grid boudary condition formula

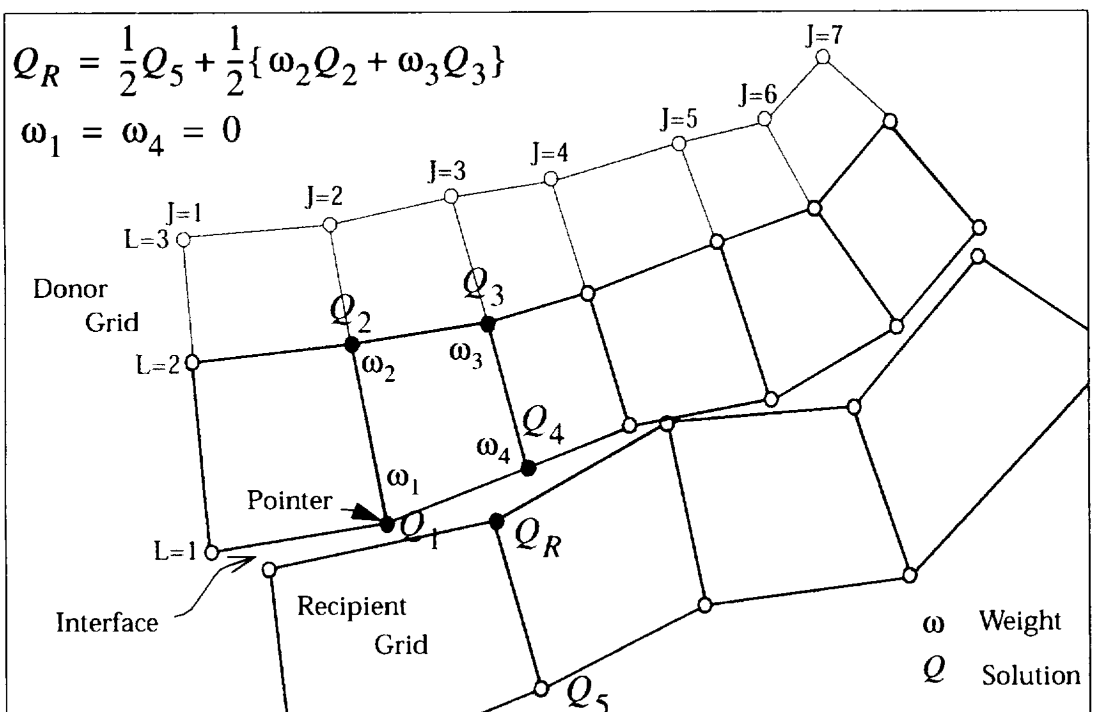

Figure 5. 4 Patched grid interface with flow-through condition

APPENDIX A

Derivation of the Continuity Equation

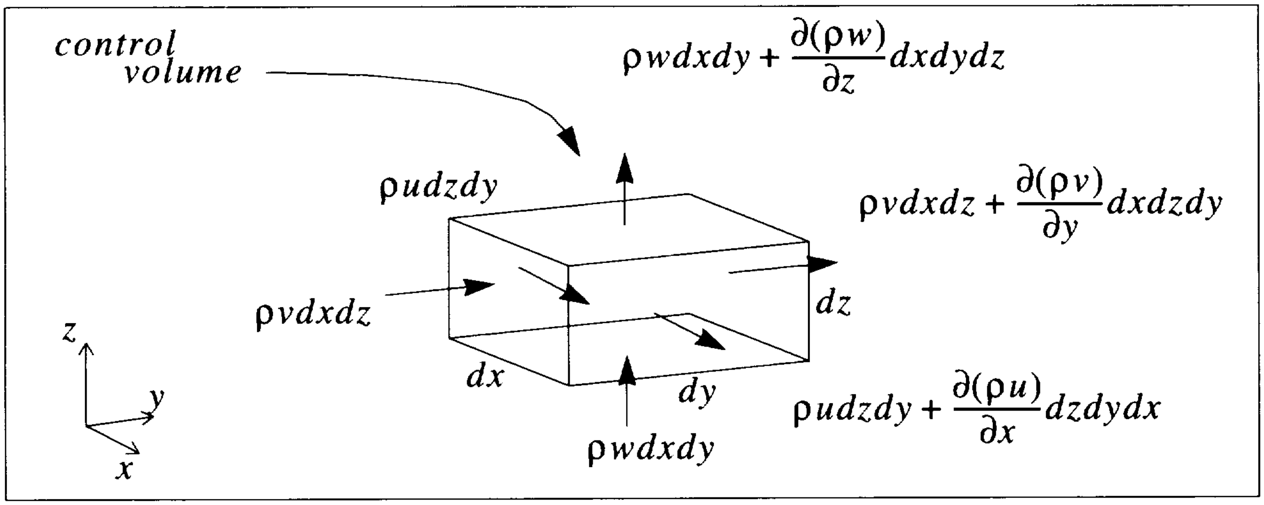

Figure A.1 Differential fluid element with mass flow rate quantities prescribed for each of the elements six faces

The Conservation of Mass law basically states that mass cannot be created nor destroyed. We can demonstrate this by creating a control volume of arbitrary size in three dimensions as illustrated above in Figure A.1. Then using the conservation of mass law, we can say that the rate of change of mass within the control volume must be equal to the net rate of inflow of mass, or in equation form we have:

$$\frac{\partial m}{\partial t} = \dot{m}_{enter} - \dot{m}_{exiting} \tag{A.1}$$

Substituting the mass flow rates for each direction, as illustrated in Figure A.1, we then have:

$$\begin{aligned}
&\left[(\rho u dzdy)_{enter} - \left(\rho u dydz + \frac{\partial(\rho u)}{\partial x} dydzdx\right)_{exit}\right]_{xdirection} + \\
&\left[(\rho v dxdz)_{enter} - \left(\rho v dxdz + \frac{\partial(\rho v)}{\partial y} dxdzdy\right)_{exit}\right]_{ydirection} + \\
&\left[(\rho w dxdy)_{enter} - \left(\rho w dxdy + \frac{\partial(\rho w)}{\partial z} dxdydz\right)_{exit}\right]_{zdirection} = \\
&\frac{\partial(\rho) dxdydz_{volumemass}}{\partial t}
\end{aligned} \tag{A.2}$$

Further reducing we have:

$$\begin{aligned}
&-\left[\frac{\partial(\rho u)}{\partial x} dxdydz\right]_{xdirection} - \left[\frac{\partial(\rho v)}{\partial xy} dxdydz\right]_{ydirection} - \\
&\left[\frac{\partial(\rho w)}{\partial z} dxdydz\right]_{zdirection} = \left[\frac{\partial(\rho)}{\partial t} dxdydz\right]_{volumemass}
\end{aligned} \tag{A.3}$$

Finally, with further reduction we get equation (2.1):

$$\frac{\partial \rho}{\partial t} + \frac{\partial(\rho u)}{\partial x} + \frac{\partial(\rho v)}{\partial y} + \frac{\partial(\rho w)}{\partial z} = 0 \tag{A.4}$$

APPENDIX B

Derivation of the Momentum Equations

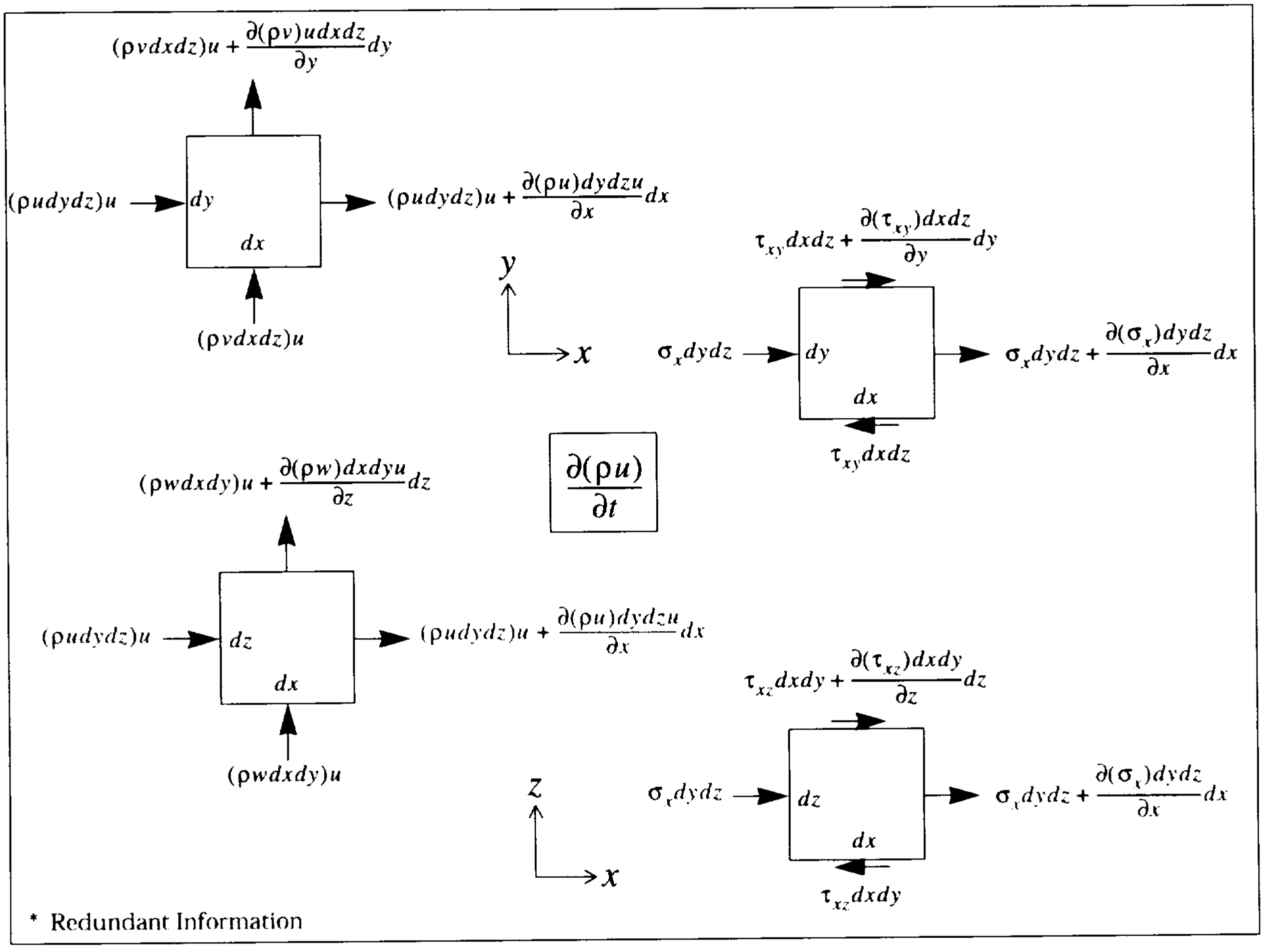

Figure B.1 Differential fluid elements with force quantities prescribed for the x direction only

The Conservation of Momentum law, otherwise known as Newton's Second Law, will now be applied to a fluid element. Newton's Second Law states that the rate of change of momentum plus the net inflow of momentum within a control volume is equal to the net force on the control volume. For this derivation, we will only consider the x-direction. A similar analysis can easily be applied to the y and z directions. We will also only consider laminar flow.

Therefore, the momentum equation for the x-direction can be written as:

$$\left[(M)_{out} + (M)_{in} + \frac{\partial(M)_{cv}}{\partial t}\right]_x = [\sum F]_x \tag{B.1}$$

Further expansion of the right hand side leads to the following:

$$\left[(M)_{out} - (M)_{in} + \frac{\partial(M)_{cv}}{\partial t}\right]_x = [\sum F_{surface} + \sum F_{pressure} + \sum F_{body}]_x \tag{B.2}$$

For our analysis, we will neglect any body forces which include terms such as forces due to gravity. It then follows after substituting the values shown in Figure B.1, the momentum equation applied to a fluid particle is:

$$\begin{aligned}
&\left[(\rho v dxdz)u + \frac{\partial(\rho v)dxdzu}{\partial y}dy + (\rho w dxdy)u + \frac{\partial(\rho w)dxdyu}{\partial z}dz + \right.\\
&\left.(\rho u dydz)u + \frac{\partial(\rho u)dydzu}{\partial x}\Delta x\right] - [(\rho u dydz)u + (\rho v dxdz)u + (\rho w dxdy)u] + \\
&\frac{\partial(\rho u)}{\partial t} = \left[\sigma_x dydz + \frac{\partial(\sigma_x)dydz}{\partial x}dx + \tau_{xy}dxdz + \frac{\partial(\tau_{xy})dxdz}{\partial y}dy + \right.\\
&\left.\tau_{xz}dxdy + \frac{\partial(\tau_{xz})dxdy}{\partial z}dz\right] - [\sigma_x dydz + \tau_{xy}dxdz + \tau_{xz}dxdy]
\end{aligned} \tag{B.3}$$

Further reducing we have:

$$\begin{aligned}
&\frac{\partial(\rho u)dydzu}{\partial x}dx + \frac{\partial(\rho v)dxdzu}{\partial y}dy + \frac{\partial(\rho w)dxdyu}{\partial z}dz + \frac{\partial(\rho u)}{\partial t} = \\
&\frac{\partial(\sigma_x)dydz}{\partial x}dx + \frac{\partial(\tau_{xy})dxdz}{\partial y}dy + \frac{\partial(\tau_{xz})dxdy}{\partial z}dz
\end{aligned} \tag{B.4}$$

We can further reduce the previous equation and rearrange it to get:

$$\frac{\partial(\rho u)}{\partial t} + \frac{\partial(\rho u^2)}{\partial x} + \frac{\partial(\rho uw)}{\partial z} + \frac{\partial(\rho uv)}{\partial y} = \frac{\partial\sigma_x}{\partial x} + \frac{\partial\tau_{xy}}{\partial y} + \frac{\partial\tau_{xz}}{\partial z} \tag{B.5}$$

With the following relationship we can rearrange equation (B.5):

$$\sigma_x = -p + \tau_{xx} \tag{B.6}$$

With this last relationship, we can now show that equation B.5 is the same as equation (2.2):

$$\frac{\partial(\rho u)}{\partial t}+\frac{\partial(\rho u^2+p)}{\partial x}+\frac{\partial(\rho uv)}{\partial y}+\frac{\partial(\rho uw)}{\partial z}=\frac{\partial\tau_{xx}}{\partial x}+\frac{\partial\tau_{xy}}{\partial y}+\frac{\partial\tau_{xz}}{\partial z} \qquad \text{(B.7)}$$

Furthermore, it can be similarly shown that for the y and z directions, the following two equations exist respectively:

$$\frac{\partial(\rho v)}{\partial t}+\frac{\partial(\rho uv)}{\partial x}+\frac{\partial(\rho v^2+p)}{\partial y}+\frac{\partial(\rho vw)}{\partial z}=\frac{\partial\tau_{xy}}{\partial x}+\frac{\partial\tau_{yy}}{\partial y}+\frac{\partial\tau_{yz}}{\partial z} \qquad \text{(B.8)}$$

$$\frac{\partial(\rho w)}{\partial t}+\frac{\partial(\rho uw)}{\partial x}+\frac{\partial(\rho vw)}{\partial y}+\frac{\partial(\rho w^2+p)}{\partial z}=\frac{\partial\tau_{xz}}{\partial x}+\frac{\partial\tau_{yz}}{\partial y}+\frac{\partial\tau_{zz}}{\partial z} \qquad \text{(B.9)}$$

APPENDIX C

Derivation of the Energy Equation

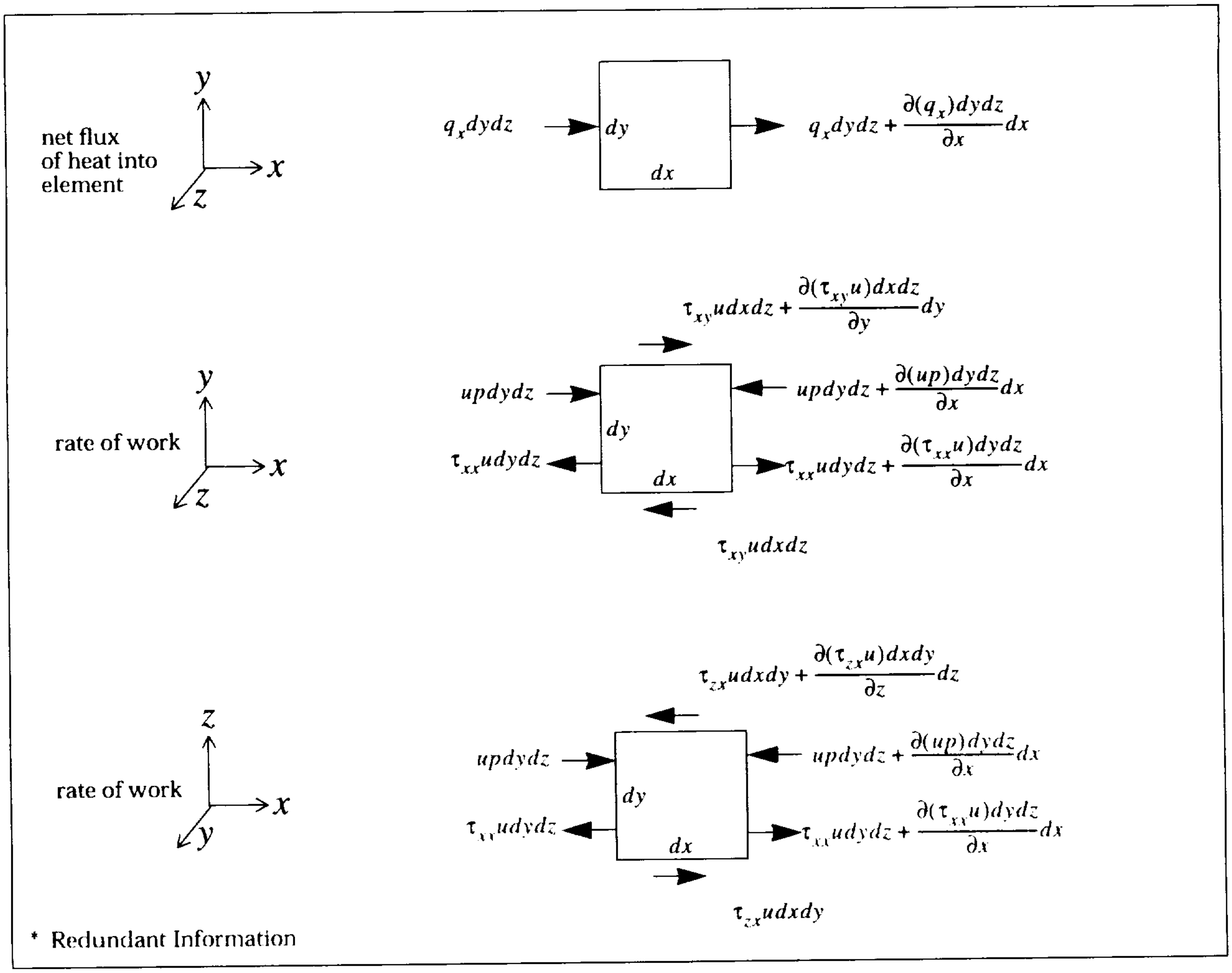

Figure C.1 Differential fluid elements with energy quantities prescribed for the x direction only

The Energy Equation is derived from the first law of thermodynamics. Applying this law to a fluid element as shown above in Figure C.1,, the law states that the rate of change of energy inside the differential element is equal the net flux of heat into the element plus the rate of work done on element due to pressure and stress forces on the element surface.

In equation form this is simply:

$$\frac{DE_t}{Dt} = q_{net} - W \tag{C.1}$$

Where E_t is the total energy, q is the rate of volumetric heat addition into the element and finally, W is the rate of work done on the element. As with prior derivations, body forces such as those resulting from gravity will be neglected. Beginning with the left-hand-side of equation (C.1), the rate of change of energy within the fluid element is the substantial derivative of the total Energy, E_t. Expanding this term out we get the following:

$$\frac{DE_t}{Dt} = \frac{\partial E_t}{\partial t} + \frac{\partial(E_t u)}{\partial x} + \frac{\partial(E_t v)}{\partial y} + \frac{\partial(E_t w)}{\partial z} \tag{C.2}$$

We will now move onto the first term on the right-hand-side of equation (C.1). This term represents the net flux of heat into the element. Referring to Figure C.1, we will add the appropriate terms to this element. For our discussion, the figure represent only the x-direction. A similar analysis can be done for the y and z directions. The net flux is then written as:

$$[q]_{net} = q_x dydz - \left(q_x dydz + \frac{\partial(q_x)dydz}{\partial x}dx\right) \tag{C.3}$$

Further reducing:

$$[q]_{net} = -\frac{\partial q_x}{\partial x} \tag{C.4}$$

Adding in the y and z directions we finally get:

$$[q]_{net} = -\frac{\partial q_x}{\partial x} - \frac{\partial q_y}{\partial y} - \frac{\partial q_z}{\partial z} \tag{C.5}$$

The last term on the right-hand-side of equation (C.1) is the rate of work done on the differential element. Again, referring to Figure C.1, we will again make the appropriate substitutions. This term can be written as:

$$\begin{aligned} W = & \left[updydz - \left(updydz + \frac{\partial(up)dydz}{\partial x}dx\right)\right] + \\ & \left[\left(\tau_{xx}udydz + \frac{\partial(\tau_{xx}u)dydz}{\partial x}dx\right) - \tau_{xx}udydz\right] + \\ & \left[\left(\tau_{xy}udxdz + \frac{\partial(\tau_{xy}u)dxdz}{\partial y}dy\right) - \tau_{xy}udxdz\right] + \\ & \left[\left(\tau_{zx}udxdy + \frac{\partial(\tau_{zx}u)dxdy}{\partial z}dz\right) - \tau_{zx}udxdy\right] \end{aligned} \tag{C.6}$$

Making further reductions in the above equation we get:

$$W = -\frac{\partial(up)}{\partial x} + \frac{\partial(\tau_{xx}u)}{\partial x} + \frac{\partial(\tau_{xy}u)}{\partial y} + \frac{\partial(\tau_{zx}u)}{\partial z} \tag{C.7}$$

We will now add the y and z direction components to the above equation. The final form of the rate of work term is:

$$\begin{aligned} W = & -\frac{\partial(up)}{\partial x} + \frac{\partial(\tau_{xx}u)}{\partial x} + \frac{\partial(\tau_{xy}u)}{\partial y} + \frac{\partial(\tau_{xz}u)}{\partial z} \\ & -\frac{\partial(vp)}{\partial y} + \frac{\partial(\tau_{xy}v)}{\partial x} + \frac{\partial(\tau_{yy}v)}{\partial y} + \frac{\partial(\tau_{yz}v)}{\partial z} - \\ & \frac{\partial(wp)}{\partial z} + \frac{\partial(\tau_{xz}w)}{\partial x} + \frac{\partial(\tau_{yz}w)}{\partial y} + \frac{\partial(\tau_{zz}w)}{\partial z} \end{aligned} \tag{C.8}$$

We will now finally substitute equations (C.2), (C.5), (C.8) into equation (C.1) and get:

$$\begin{aligned}
\frac{\partial E_t}{\partial t} + \frac{\partial(E_t u)}{\partial x} + \frac{\partial(E_t v)}{\partial y} + \frac{\partial(E_t w)}{\partial y} &= -\frac{\partial q_x}{\partial x} - \frac{\partial q_y}{\partial y} - \frac{\partial q_z}{\partial z} - \\
&\frac{\partial(up)}{\partial x} + \frac{\partial(\tau_{xx} u)}{\partial x} + \frac{\partial(\tau_{xy} u)}{\partial y} + \frac{\partial(\tau_{xz} u)}{\partial z} \\
&- \frac{\partial(vp)}{\partial y} + \frac{\partial(\tau_{xy} v)}{\partial x} + \frac{\partial(\tau_{yy} v)}{\partial y} + \frac{\partial(\tau_{yz} v)}{\partial z} - \\
&\frac{\partial(wp)}{\partial z} + \frac{\partial(\tau_{xz} w)}{\partial x} + \frac{\partial(\tau_{yz} w)}{\partial y} + \frac{\partial(\tau_{zz} w)}{\partial z}
\end{aligned} \tag{C.9}$$

Rearranging this equation, we can now be shown that equations (2.11) and (C.10) are the same:

$$\begin{aligned}
&\frac{\partial E_t}{\partial t} + \frac{\partial((E_t + p)u)}{\partial x} + \frac{\partial((E_t + p)v)}{\partial y} + \frac{\partial((E_t + p)w)}{\partial z} = \\
&\frac{\partial(u\tau_{xx} + v\tau_{xy} + w\tau_{xz} - q_x)}{\partial x} + \frac{\partial(u\tau_{xy} + v\tau_{yy} + w\tau_{yz} - q_y)}{\partial y} + \\
&\frac{\partial(u\tau_{xz} + v\tau_{yz} + w\tau_{zz} - q_z)}{\partial z}
\end{aligned} \tag{C.10}$$

APPENDIX D

Nondimensional Form of the Navier-Stokes Equations

We will begin our analysis by first rewriting the governing equations. The following are the continuity, momentum, and energy equations respectively from appendices A, B, and C:

$$\frac{\partial\rho}{\partial t}+\frac{\partial(\rho u)}{\partial x}+\frac{\partial(\rho v)}{\partial y}+\frac{\partial(\rho w)}{\partial z}=0 \tag{D.1}$$

$$\frac{\partial(\rho u)}{\partial t}+\frac{\partial(\rho u^2+p)}{\partial x}+\frac{\partial(\rho uv)}{\partial y}+\frac{\partial(\rho uw)}{\partial z}=\frac{\partial\tau_{xx}}{\partial x}+\frac{\partial\tau_{xy}}{\partial y}+\frac{\partial\tau_{xz}}{\partial z} \tag{D.2}$$

$$\frac{\partial(\rho v)}{\partial t}+\frac{\partial(\rho uv)}{\partial x}+\frac{\partial(\rho v^2+p)}{\partial y}+\frac{\partial(\rho vw)}{\partial z}=\frac{\partial\tau_{xy}}{\partial x}+\frac{\partial\tau_{yy}}{\partial y}+\frac{\partial\tau_{yz}}{\partial z} \tag{D.3}$$

$$\frac{\partial(\rho w)}{\partial t}+\frac{\partial(\rho uw)}{\partial x}+\frac{\partial(\rho vw)}{\partial y}+\frac{\partial(\rho w^2+p)}{\partial z}=\frac{\partial\tau_{xz}}{\partial x}+\frac{\partial\tau_{yz}}{\partial y}+\frac{\partial\tau_{zz}}{\partial z} \tag{D.4}$$

$$\frac{\partial E_t}{\partial t}+\frac{\partial((E_t+p)u)}{\partial x}+\frac{\partial((E_t+p)v)}{\partial y}+\frac{\partial((E_t+p)w)}{\partial z}=$$

$$\frac{\partial(u\tau_{xx}+v\tau_{xy}+w\tau_{xz}-q_x)}{\partial x}+\frac{\partial(u\tau_{xy}+v\tau_{yy}+w\tau_{yz}-q_y)}{\partial y}+ \tag{D.5}$$

$$\frac{\partial(u\tau_{xz}+v\tau_{yz}+w\tau_{zz}-q_z)}{\partial z}$$

We will now nondimensionalize these equations one at a time.

The nondimensional variables will be the same as those in equation (2.21). They are:

$$x^* = \frac{x}{L} \qquad u^* = \frac{u}{V_\infty} \qquad \rho^* = \frac{\rho}{\rho_\infty}$$
$$y^* = \frac{y}{L} \qquad v^* = \frac{v}{V_\infty} \qquad p^* = \frac{p}{\rho_\infty V_\infty^{\ 2}}$$
$$z^* = \frac{z}{L} \qquad w^* = \frac{w}{V_\infty} \qquad T^* = \frac{T}{T_\infty} \tag{D.6}$$
$$t^* = \frac{t}{L/V_\infty} \qquad \mu^* = \frac{\mu}{\mu_\infty} \qquad e^* = \frac{e}{V_\infty^{\ 2}}$$

The asterisk terms are nondimensional. They can be rewritten to solve for the dimensional variables.

$$x = x^*L \qquad u = u^*V_\infty \qquad \rho = \rho^*\rho_\infty$$
$$y = y^*L \qquad v = v^*V_\infty \qquad p = p^*V^2{}_\infty\rho_\infty$$
$$z = z^*L \qquad w = w^*V_\infty \qquad T = T^*T_\infty \tag{D.7}$$
$$t = t^*(L/V_\infty) \qquad \mu = \mu^*\mu_\infty \qquad e = e^*V^2{}_\infty$$

Substituting the appropriate values from equation (D.6) into equation (D.1) we have:

$$\frac{\partial(\rho^*\rho_\infty)}{\partial(t^*(L/V_\infty))} + \frac{\partial(\rho^*\rho_\infty u^* V_\infty)}{\partial(x^*L)} + \frac{\partial(\rho^*\rho_\infty v^* V_\infty)}{\partial(y^*L)} + \frac{\partial(\rho^*\rho_\infty w^* V_\infty)}{\partial(z^*L)} = 0 \tag{D.8}$$

The left -hand-side of equation (D.8) can be factored further.

$$\frac{\rho_\infty V_\infty}{L}\left(\frac{\partial(\rho^*)}{\partial t^*} + \frac{\partial(\rho^* u^*)}{\partial x^*} + \frac{\partial(\rho^* v^*)}{\partial y^*} + \frac{\partial(\rho^* w^*)}{\partial z^*}\right) = 0 \tag{D.9}$$

With further reduction, the resulting equation is:

$$\frac{\partial(\rho^*)}{\partial t^*} + \frac{\partial(\rho^* u^*)}{\partial x^*} + \frac{\partial(\rho^* v^*)}{\partial y^*} + \frac{\partial(\rho^* w^*)}{\partial z^*} = 0 \tag{D.10}$$

Next, we will nondimensionalize the x direction of the momentum equations. Again, we will substitute the appropriate values from equations (D.7). We will first begin with the left-hand-side of equation (D.2):

$$\begin{aligned}&\frac{\partial(\rho^*\rho_\infty u^* V_\infty)}{\partial(t^*(L/V_\infty))} + \frac{\partial(\rho^*\rho_\infty u^{*2} V^2_\infty + p^* V_\infty{}^2 \rho_\infty)}{\partial(x^* L)} + \\ &\frac{\partial(\rho_\infty u^* V_\infty v^* V_\infty)}{\partial(y^* L)} + \frac{\partial(\rho_\infty u^* V_\infty w^* V_\infty)}{\partial(z^* L)} = LHS\end{aligned} \tag{D.11}$$

With further factorization, we get:

$$\left(\frac{\rho_\infty V_\infty{}^2}{L}\right)\left(\frac{\partial(\rho^* u^*)}{\partial t^*} + \frac{\partial(\rho^* u^{*2} + p^*)}{\partial x^*} + \frac{\partial(u^* v^*)}{\partial y^*} + \frac{\partial(u^* w^*)}{\partial z^*}\right) = LHS \tag{D.12}$$

Next, we will do the right-hand-side of equation (D.2). It follows then:

$$RHS = \frac{\partial\tau^*{}_{xx}}{\partial(x^* L)} + \frac{\partial\tau^*{}_{xy}}{\partial(y^* L)} + \frac{\partial\tau^*{}_{xz}}{\partial(z^* L)} \tag{D.13}$$

With further factorization, we get:

$$RHS = \left(\frac{1}{L}\right)\left(\frac{\partial\tau^*{}_{xx}}{\partial x^*} + \frac{\partial\tau^*{}_{xy}}{\partial y^*} + \frac{\partial\tau^*{}_{xz}}{\partial z^*}\right) \tag{D.14}$$

The nondimensional viscous stress tensors follow as:

$$\tau^*{}_{xx} = \frac{2}{3}\mu^*\mu_\infty\left(2\frac{\partial(u^* V_\infty)}{\partial(x^* L)} - \frac{\partial(v^* V_\infty)}{\partial(y^* L)} - \frac{\partial(w^* V_\infty)}{\partial(z^* L)}\right) \tag{D.15}$$

With further factorization, we get:

$$\tau^*{}_{xx} = \left(\frac{\mu_\infty V_\infty}{L}\right)\frac{2}{3}\mu^*\left(2\frac{\partial u^*}{\partial x^*} - \frac{\partial v^*}{\partial y^*} - \frac{\partial w^*}{\partial z^*}\right) \tag{D.16}$$

Also,

$$\tau^*_{xy} = \mu^*\mu_\infty\left(\frac{\partial(u^*V_\infty)}{\partial(y^*L)} + \frac{\partial(v^*V_\infty)}{\partial(x^*L)}\right) \tag{D.17}$$

With further factorization, we get:

$$\tau^*_{xy} = \left(\frac{\mu_\infty V_\infty}{L}\right)\mu^*\left(\frac{\partial u^*}{\partial y^*} + \frac{\partial v^*}{\partial x^*}\right) \tag{D.18}$$

Also,

$$\tau^*_{xz} = \mu^*\mu_\infty\left(\frac{\partial(w^*V_\infty)}{\partial(x^*L)} + \frac{\partial(u^*V_\infty)}{\partial(z^*L)}\right) \tag{D.19}$$

With further factorization, we get:

$$\tau^*_{xz} = \left(\frac{\mu_\infty V_\infty}{L}\right)\mu^*\left(\frac{\partial w^*}{\partial x^*} + \frac{\partial u^*}{\partial z^*}\right) \tag{D.20}$$

Substituting equations (D.16), (D.18), and (D.20) into equation (D.14) we get:

$$RHS = \left(\frac{1}{L}\right)\left(\frac{\mu_\infty V_\infty}{L}\right)\left(\frac{\partial\tau^*_{xx}}{\partial x^*} + \frac{\partial\tau^*_{xy}}{\partial y^*} + \frac{\partial\tau^*_{xz}}{\partial z^*}\right) \tag{D.21}$$

If we divide both sides by $\frac{\rho_\infty V_\infty{}^2}{L}$ we get:

$$\left(\frac{\partial(\rho^*u^*)}{\partial t^*} + \frac{\partial(\rho^*u^{*2} + p^*)}{\partial x^*} + \frac{\partial(u^*v^*)}{\partial y^*} + \frac{\partial(u^*w^*)}{\partial z^*}\right) = LHS \tag{D.22}$$

$$RHS = \left(\frac{L}{\rho_\infty V_\infty{}^2}\right)\left(\frac{1}{L}\right)\left(\frac{\mu_\infty V_\infty}{L}\right)\left(\frac{\partial\tau^*_{xx}}{\partial x^*} + \frac{\partial\tau^*_{xy}}{\partial y^*} + \frac{\partial\tau^*_{xz}}{\partial z^*}\right) \tag{D.23}$$

With further reduction and defining the Reynolds number as:

$$RE_L = \frac{\rho_\infty V_\infty L}{\mu_\infty} \tag{D.24}$$

The x direction momentum equation follows as:

$$\frac{\partial(\rho^* u^*)}{\partial t^*} + \frac{\partial(\rho^* u^{*2} + p^*)}{\partial x^*} + \frac{\partial(u^* v^*)}{\partial y^*} + \frac{\partial(u^* w^*)}{\partial z^*} = \left(\frac{1}{RE_L}\right)\left(\frac{\partial \tau^*_{xx}}{\partial x^*} + \frac{\partial \tau^*_{xy}}{\partial y^*} + \frac{\partial \tau^*_{xz}}{\partial z^*}\right) \tag{D.25}$$

With a similar analysis, it can be shown that the y and z directions respectively are:

$$\frac{\partial(\rho^* v^*)}{\partial t^*} + \frac{\partial(\rho^* uv)}{\partial x^*} + \frac{\partial(\rho^* v^{*2} + p^*)}{\partial y^*} + \frac{\partial(v^* w^*)}{\partial z^*} = \left(\frac{1}{RE_L}\right)\left(\frac{\partial \tau^*_{xy}}{\partial x^*} + \frac{\partial \tau^*_{yy}}{\partial y^*} + \frac{\partial \tau^*_{yz}}{\partial z^*}\right) \tag{D.26}$$

$$\frac{\partial(\rho^* w^*)}{\partial t^*} + \frac{\partial(u^* w^*)}{\partial x^*} + \frac{\partial(v^* w^*)}{\partial y^*} + \frac{\partial(\rho^* w^{*2} + p^*)}{\partial z^*} = \left(\frac{1}{RE_L}\right)\left(\frac{\partial \tau^*_{xz}}{\partial x^*} + \frac{\partial \tau^*_{yz}}{\partial y^*} + \frac{\partial \tau^*_{zz}}{\partial z^*}\right) \tag{D.27}$$

Lastly, we will non dimensionalize the energy equation. Again, we will substitute the appropriate terms from the list of equations in (D.6).

$$\frac{\partial E^*_t}{\partial(t^*(L/V_\infty))} + \frac{\partial((E^*_t + p^*\rho_\infty V^2_\infty)u^* V_\infty)}{\partial(x^* L)} +$$

$$\frac{\partial((E^*_t + p^*\rho_\infty V^2_\infty)v^* V_\infty)}{\partial(y^* L)} + \frac{\partial((E^*_t + p^*\rho_\infty V^2_\infty)w^* V_\infty)}{\partial(z^* L)} =$$

$$\frac{\partial(u^* V_\infty \tau^*_{xx} + v^* V_\infty \tau^*_{xy} + w^* V_\infty \tau^*_{xz} - q^*_x)}{\partial(x^* L)} + \tag{D.28}$$

$$\frac{\partial(u^* V_\infty \tau^*_{xy} + v^* V_\infty \tau^*_{yy} + w^* V_\infty \tau^*_{yz} - q^*_y)}{\partial(y^* L)} +$$

$$\frac{\partial(u^* V_\infty \tau^*_{xz} + v^* V_\infty \tau^*_{yz} + w^* V_\infty \tau^*_{zz} - q^*_z)}{\partial(z^* L)}$$

Where

$$E_t = \rho\left(e + \frac{u^2 + v^2 + w^2}{2}\right) \tag{D.29}$$

Or in nondimensional form:

$$E^*_t = \rho^*\rho_\infty\left(e^* V^2_\infty + \frac{u^{*2} V^2_\infty + v^{*2} V^2_\infty + w^{*2} V^2_\infty}{2}\right) \tag{D.30}$$

Reducing, we get:

$$E^*_t = (\rho_\infty V^2_\infty)\rho^*\left(e^* + \frac{u^{*2} + v^{*2} + w^{*2}}{2}\right) \qquad \text{(D.31)}$$

Also, from previous derivations, the nondimensional viscous stress tensors follow as:

$$\tau^*_{xx} = \left(\frac{\mu_\infty V_\infty}{L}\right)\frac{2}{3}\mu^*\left(2\frac{\partial u^*}{\partial x^*} - \frac{\partial v^*}{\partial y^*} - \frac{\partial w^*}{\partial z^*}\right) \qquad \text{(D.32)}$$

$$\tau^*_{yy} = \left(\frac{\mu_\infty V_\infty}{L}\right)\frac{2}{3}\mu^*\left(2\frac{\partial v^*}{\partial y^*} - \frac{\partial u^*}{\partial x^*} - \frac{\partial w^*}{\partial z^*}\right) \qquad \text{(D.33)}$$

$$\tau^*_{zz} = \left(\frac{\mu_\infty V_\infty}{L}\right)\frac{2}{3}\mu^*\left(2\frac{\partial w^*}{\partial z^*} - \frac{\partial u^*}{\partial x^*} - \frac{\partial v^*}{\partial y^*}\right) \qquad \text{(D.34)}$$

$$\tau^*_{xy} = \left(\frac{\mu_\infty V_\infty}{L}\right)\mu^*\left(\frac{\partial u^*}{\partial y^*} + \frac{\partial v^*}{\partial x^*}\right) \qquad \text{(D.35)}$$

$$\tau^*_{xz} = \left(\frac{\mu_\infty V_\infty}{L}\right)\mu^*\left(\frac{\partial w^*}{\partial x^*} + \frac{\partial u^*}{\partial z^*}\right) \qquad \text{(D.36)}$$

$$\tau^*_{yz} = \left(\frac{\mu_\infty V_\infty}{L}\right)\mu^*\left(\frac{\partial v^*}{\partial z^*} + \frac{\partial w^*}{\partial y^*}\right) \qquad \text{(D.37)}$$

Lastly, the heat flux term in the x direction is given by:

$$q_x = -k\frac{\partial T}{\partial x} = -\frac{\gamma\mu R}{(\gamma - 1)Pr}\frac{\partial T}{\partial x} \qquad \text{(D.38)}$$

In nondimensional form we get:

$$q^*{}_x = -\frac{\gamma\mu^*\mu_\infty R}{(\gamma-1)Pr}\frac{\partial(T^*T_\infty)}{\partial(x^*L)} \tag{D.39}$$

Rearranging we get:

$$q^*{}_x = -\frac{1}{L}\frac{\mu_\infty}{Pr}\frac{\gamma RT_\infty}{(\gamma-1)}\mu^*\frac{\partial T^*}{\partial x^*} \tag{D.40}$$

It then follows the heat flux terms for the y and z directions are:

$$q^*{}_y = -\frac{1}{L}\frac{\mu_\infty}{Pr}\frac{\gamma RT_\infty}{(\gamma-1)}\mu^*\frac{\partial T^*}{\partial y^*} \tag{D.41}$$

$$q^*{}_z = -\frac{1}{L}\frac{\mu_\infty}{Pr}\frac{\gamma RT_\infty}{(\gamma-1)}\mu^*\frac{\partial T^*}{\partial z^*} \tag{D.42}$$

Next, we will substitute equations (D.31-D38) and equations (D.40-D.42) into equation (D.28).

With some factoring, this results in:

$$\left(\frac{\rho_\infty V^3_\infty}{L}\right)\frac{\partial E^*_t}{\partial t^*} + \left(\frac{\rho_\infty V^3_\infty}{L}\right)\frac{\partial((E^*_t + p^*)u^*)}{\partial x^*} +$$

$$\left(\frac{\rho_\infty V^3_\infty}{L}\right)\frac{\partial((E^*_t + p^*)v^*)}{\partial y^*} + \left(\frac{\rho_\infty V^3_\infty}{L}\right)\frac{\partial((E^*_t + p^*)w^*)}{\partial z^*} =$$

$$\left(\frac{\mu_\infty V^2_\infty}{L^2}\right)\frac{\partial(u^*\tau^*_{xx} + v^*\tau^*_{xy} + w^*\tau^*_{xz})}{\partial x^*} - \frac{\partial q^*_x}{\partial x^*} + \tag{D.43}$$

$$\left(\frac{\mu_\infty V^2_\infty}{L^2}\right)\frac{\partial(u^*\tau^*_{xy} + v^*\tau^*_{yy} + w^*\tau^*_{yz})}{\partial y^*} - \frac{\partial q^*_y}{\partial y^*} +$$

$$\left(\frac{\mu_\infty V^2_\infty}{L^2}\right)\frac{\partial(u^*\tau^*_{xz} + v^*\tau^*_{yz} + w^*\tau^*_{zz})}{\partial z^*} - \frac{\partial q^*_z}{\partial z^*}$$

If we divide both sides by $\frac{\rho_\infty V^3_\infty}{L}$ and using the definition of the Reynolds number, equation (D.43) becomes:

$$\frac{\partial E^*_t}{\partial t^*}+\frac{\partial((E^*_t+p^*)u^*)}{\partial x^*}+\frac{\partial((E^*_t+p^*)v^*)}{\partial y^*}+\frac{\partial((E^*_t+p^*)w^*)}{\partial z^*}=$$

$$\left(\frac{1}{RE_L}\right)\frac{\partial(u^*\tau^*_{xx}+v^*\tau^*_{xy}+w^*\tau^*_{xz}-q^*_x)}{\partial x^*}+$$

$$\left(\frac{1}{RE_L}\right)\frac{\partial(u^*\tau^*_{xy}+v^*\tau^*_{yy}+w^*\tau^*_{yz}-q_y^*)}{\partial y^*}+ \tag{D.44}$$

$$\left(\frac{1}{RE_L}\right)\frac{\partial(u^*\tau^*_{xz}+v^*\tau^*_{yz}+w^*\tau^*_{zz}-q_z^*)}{\partial z^*}$$

Where the heat flux terms are defined as:

$$q^*_x = -\frac{\mu^*}{RE_L M_\infty^{\ 2}(\gamma-1)Pr}\frac{\partial T^*}{\partial x^*} \tag{D.45}$$

$$q^*_y = -\frac{\mu^*}{RE_L M_\infty^{\ 2}(\gamma-1)Pr}\frac{\partial T^*}{\partial y^*} \tag{D.46}$$

$$q^*_z = -\frac{\mu^*}{RE_L M_\infty^{\ 2}(\gamma-1)Pr}\frac{\partial T^*}{\partial z^*} \tag{D.47}$$

From equations (D.9), (D.24-D.26), and (D.42), we can place these in equation in vector form. The resulting expression is the same as equation (2.35).

$$\frac{\partial Q^*}{\partial t^*}+\frac{\partial E^*}{\partial x^*}+\frac{\partial F^*}{\partial y^*}+\frac{\partial G^*}{\partial z^*}=\frac{1}{Re_L}\left(\frac{\partial E^*_v}{\partial x^*}+\frac{\partial F^*_v}{\partial y^*}+\frac{\partial G^*_v}{\partial z^*}\right) \tag{D.48}$$

Where Q^*, E^*, F^*, G^* are:

$$Q^* = \begin{bmatrix} \rho^* \\ \rho^* u^* \\ \rho^* v^* \\ \rho^* w^* \\ E^*_t \end{bmatrix} E^* = \begin{bmatrix} \rho^* u^* \\ \rho^* u^{*2} + p^* \\ \rho^* u^* v^* \\ \rho^* u^* w^* \\ (E^*_t + p^*) v^* \end{bmatrix} F^* = \begin{bmatrix} \rho^* v^* \\ \rho^* u^* v^* \\ \rho^* v^{*2} + p^* \\ \rho^* v^* w^* \\ (E^*_t + p^*) v^* \end{bmatrix} G^* = \begin{bmatrix} \rho^* w^* \\ \rho^* u^* w^* \\ \rho^* v^* w^* \\ \rho^* w^{*2} + p^* \\ (E^*_t + p^*) w^* \end{bmatrix} \tag{D.49}$$

And E^*_v, F^*_v, G^*_v are:

$$E^*_v = \begin{bmatrix} 0 \\ \tau^*_{xx} \\ \tau^*_{xy} \\ \tau^*_{xz} \\ u^*\tau^*_{xx} + v^*\tau^*_{xy} + w^*\tau^*_{xz} - q^*_x \end{bmatrix}$$

$$F^*_v = \begin{bmatrix} 0 \\ \tau^*_{xy} \\ \tau^*_{yy} \\ \tau^*_{yz} \\ u^*\tau^*_{xy} + v^*\tau^*_{yy} + w^*\tau^*_{yz} - q^*_y \end{bmatrix} \tag{D.50}$$

$$G^*_v = \begin{bmatrix} 0 \\ \tau^*_{xz} \\ \tau^*_{yz} \\ \tau^*_{zz} \\ u^*\tau^*_{xz} + v^*\tau^*_{yz} + w^*\tau^*_{zz} - q^*_z \end{bmatrix}$$

APPENDIX E

Transformation of the Navier-Stokes Equations

First we will begin by solving equation (2.64). Repeated for convenience:

$$\begin{bmatrix} 1 & 0 & 0 & 0 \\ \xi_t & \xi_x & \xi_y & \xi_z \\ \eta_t & \eta_x & \eta_y & \eta_z \\ \zeta_t & \zeta_x & \zeta_y & \zeta_z \end{bmatrix} = \begin{bmatrix} 1 & 0 & 0 & 0 \\ x_\tau & x_\xi & x_\eta & x_\zeta \\ y_\tau & y_\xi & y_\eta & y_\zeta \\ z_\tau & z_\xi & z_\eta & z_\zeta \end{bmatrix}^{-1} \tag{E.1}$$

In order to solve for each matrix element on the left-hand-side, it will be necessary to take the inverse of the right-hand-side matrix. To expedite this calculation, a symbolic math program, Maple V was used. Figure E.1 is the output from this Maple V session.

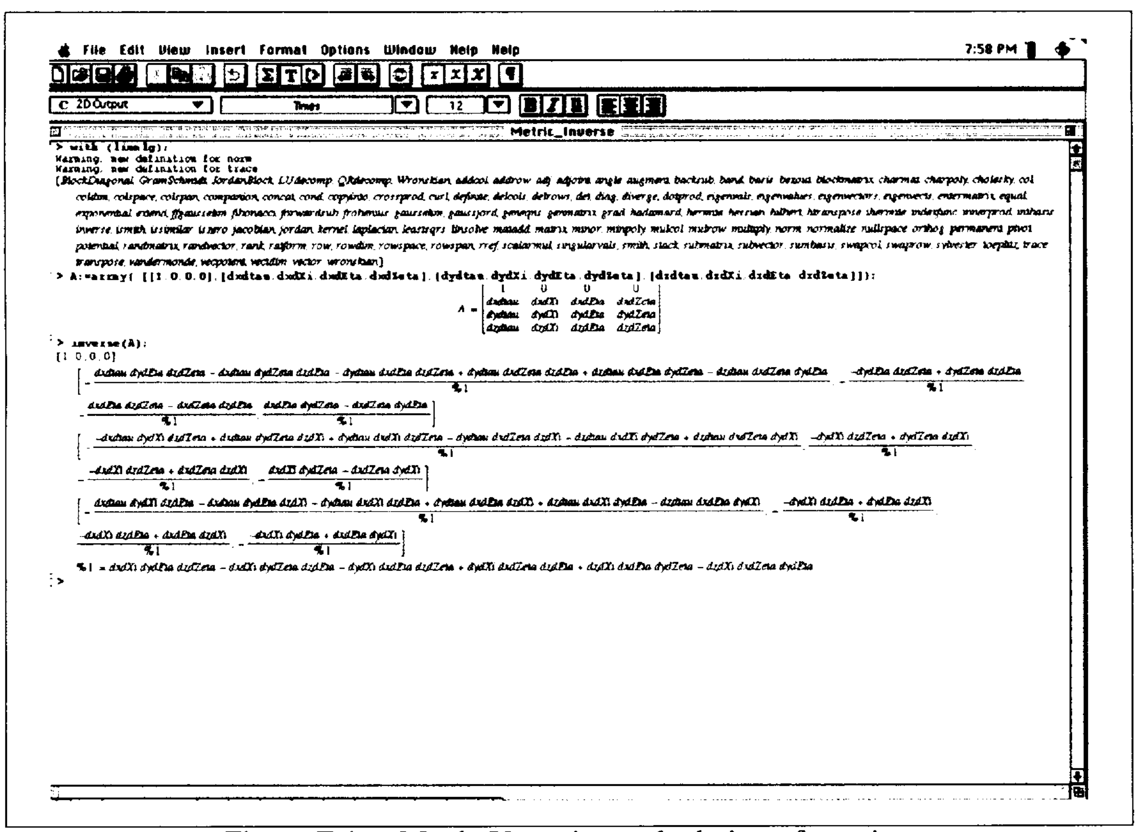

Figure E.1 Maple V session, calculation of metrics.

With the following generalized transformation, the governing equations will be transformed.

$$x = x(\xi, \eta, \zeta) \tag{E.2}$$

$$y = y(\xi, \eta, \zeta) \tag{E.3}$$

$$z = z(\xi, \eta, \zeta) \tag{E.4}$$

$$t = \tau \tag{E.5}$$

Using the chain rule of partial differentiation on these expressions, the following derivatives result:

$$\frac{\partial}{\partial x} = \frac{\partial \xi}{\partial x}\frac{\partial}{\partial \xi} + \frac{\partial \eta}{\partial x}\frac{\partial}{\partial \eta} + \frac{\partial \zeta}{\partial x}\frac{\partial}{\partial \zeta} \tag{E.6}$$

$$\frac{\partial}{\partial y} = \frac{\partial \xi}{\partial y}\frac{\partial}{\partial \xi} + \frac{\partial \eta}{\partial y}\frac{\partial}{\partial \eta} + \frac{\partial \zeta}{\partial y}\frac{\partial}{\partial \zeta} \tag{E.7}$$

$$\frac{\partial}{\partial z} = \frac{\partial \xi}{\partial z}\frac{\partial}{\partial \xi} + \frac{\partial \eta}{\partial z}\frac{\partial}{\partial \eta} + \frac{\partial \zeta}{\partial z}\frac{\partial}{\partial \zeta} \tag{E.8}$$

$$\frac{\partial}{\partial t} = \frac{\partial \xi}{\partial t}\frac{\partial}{\partial \xi} + \frac{\partial \eta}{\partial t}\frac{\partial}{\partial \eta} + \frac{\partial \zeta}{\partial t}\frac{\partial}{\partial \zeta} + \frac{\partial}{\partial \tau} \tag{E.9}$$

These derivatives will then have to be applied to the governing equations. For this analysis, we will apply the derivatives separately to each of the nondimensional elements of equation (2.35). The continuity equation written in non dimensional form is:

$$\frac{\partial \rho}{\partial t} + \frac{\partial(\rho u)}{\partial x} + \frac{\partial(\rho v)}{\partial y} + \frac{\partial(\rho w)}{\partial z} = 0 \tag{E.10}$$

Applying the transformation derivatives we have:

$$
\begin{aligned}
&\frac{\partial\xi}{\partial t}\frac{\partial\rho}{\partial\xi}+\frac{\partial\eta}{\partial t}\frac{\partial\rho}{\partial\eta}+\frac{\partial\zeta}{\partial t}\frac{\partial\rho}{\partial\zeta}+\frac{\partial\rho}{\partial\tau}+\\
&\frac{\partial\xi}{\partial x}\frac{\partial(\rho u)}{\partial\xi}+\frac{\partial\eta}{\partial x}\frac{\partial(\rho u)}{\partial\eta}+\frac{\partial\zeta}{\partial x}\frac{\partial(\rho u)}{\partial\zeta}+\\
&\frac{\partial\xi}{\partial y}\frac{\partial(\rho v)}{\partial\xi}+\frac{\partial\eta}{\partial y}\frac{\partial(\rho v)}{\partial\eta}+\frac{\partial\zeta}{\partial y}\frac{\partial(\rho v)}{\partial\zeta}+\\
&\frac{\partial\xi}{\partial z}\frac{\partial(\rho w)}{\partial\xi}+\frac{\partial\eta}{\partial z}\frac{\partial(\rho w)}{\partial\eta}+\frac{\partial\zeta}{\partial z}\frac{\partial(\rho w)}{\partial\zeta}=0
\end{aligned}
\tag{E.11}
$$

Rearranging and reducing:

$$
\begin{aligned}
&\xi_t\frac{\partial\rho}{\partial\xi}+\eta_t\frac{\partial\rho}{\partial\eta}+\zeta_t\frac{\partial\rho}{\partial\zeta}+\frac{\partial\rho}{\partial\tau}+\\
&\xi_x\frac{\partial(\rho u)}{\partial\xi}+\eta_x\frac{\partial(\rho u)}{\partial\eta}+\zeta_x\frac{\partial(\rho u)}{\partial\zeta}+\\
&\xi_y\frac{\partial(\rho v)}{\partial\xi}+\eta_y\frac{\partial(\rho v)}{\partial\eta}+\zeta_y\frac{\partial(\rho v)}{\partial\zeta}+\\
&\xi_z\frac{\partial(\rho w)}{\partial\xi}+\eta_z\frac{\partial(\rho w)}{\partial\eta}+\zeta_z\frac{\partial(\rho w)}{\partial\zeta}=0
\end{aligned}
\tag{E.12}
$$

$$
\begin{aligned}
&\frac{\partial\rho}{\partial\tau}+\\
&\xi_t\frac{\partial\rho}{\partial\xi}+\xi_x\frac{\partial(\rho u)}{\partial\xi}+\xi_y\frac{\partial(\rho v)}{\partial\xi}+\xi_z\frac{\partial(\rho w)}{\partial\xi}+\\
&\eta_t\frac{\partial\rho}{\partial\eta}+\eta_x\frac{\partial(\rho u)}{\partial\eta}+\eta_y\frac{\partial(\rho v)}{\partial\eta}+\eta_z\frac{\partial(\rho w)}{\partial\eta}+\\
&\zeta_t\frac{\partial\rho}{\partial\zeta}+\zeta_x\frac{\partial(\rho u)}{\partial\zeta}+\zeta_y\frac{\partial(\rho v)}{\partial\zeta}+\zeta_z\frac{\partial(\rho w)}{\partial\zeta}=0
\end{aligned}
\tag{E.13}
$$

$$
\begin{aligned}
&\frac{\partial\rho}{\partial\tau}+\\
&\frac{\partial[\rho(\xi_t+\xi_x u+\xi_y v+\xi_z w)]}{\partial\xi}+\\
&\frac{\partial[\rho(\eta_t+\eta_x u+\eta_y v+\eta_z w)]}{\partial\eta}+\\
&\frac{\partial[\rho(\zeta_t+\zeta_x u+\zeta_y v+\zeta_z w)]}{\partial\zeta}=0
\end{aligned}
\tag{E.14}
$$

As mentioned in chapter two, the quantities in parenthesis of equation (E.14) are the contravariant velocities. Restated, they are:

$$\begin{aligned} U &= \xi_t + \xi_x y + \xi_y v + \xi_z v \\ V &= \eta_t + \eta_x y + \eta_y v + \eta_z v \\ W &= \zeta_t + \zeta_x y + \zeta_y v + \zeta_z v \end{aligned} \tag{E.15}$$

Rewriting equation (E.14):

$$\frac{\partial \rho}{\partial \tau} + \frac{\partial(\rho U)}{\partial \xi} + \frac{\partial(\rho V)}{\partial \eta} + \frac{\partial(\rho W)}{\partial \zeta} = 0 \tag{E.16}$$

Next, we will transform the x direction momentum equation. In non-dimensional form, the x component of the momentum equation is:

$$\frac{\partial(\rho u)}{\partial t} + \frac{\partial(\rho u^2 + p)}{\partial x} + \frac{\partial(\rho u v)}{\partial y} + \frac{\partial(\rho u w)}{\partial z} = \frac{1}{Re_L}\left(\frac{\partial \tau_{xx}}{\partial x} + \frac{\partial \tau_{xy}}{\partial y} + \frac{\partial \tau_{xz}}{\partial z}\right) \tag{E.17}$$

Applying the transformation derivatives to equation (E.17):

$$\begin{aligned} &\frac{\partial \xi}{\partial t}\frac{\partial(\rho u)}{\partial \xi} + \frac{\partial \eta}{\partial t}\frac{\partial(\rho u)}{\partial \eta} + \frac{\partial \zeta}{\partial t}\frac{\partial(\rho u)}{\partial \zeta} + \frac{\partial(\rho u)}{\partial \tau} + \\ &\frac{\partial \xi}{\partial x}\frac{\partial(\rho u^2 + p)}{\partial \xi} + \frac{\partial \eta}{\partial x}\frac{\partial(\rho u^2 + p)}{\partial \eta} + \frac{\partial \zeta}{\partial x}\frac{\partial(\rho u^2 + p)}{\partial \zeta} + \\ &\frac{\partial \xi}{\partial y}\frac{\partial(\rho u v)}{\partial \xi} + \frac{\partial \eta}{\partial y}\frac{\partial(\rho u v)}{\partial \eta} + \frac{\partial \zeta}{\partial y}\frac{\partial(\rho u v)}{\partial \zeta} + \\ &\frac{\partial \xi}{\partial z}\frac{\partial(\rho u w)}{\partial \xi} + \frac{\partial \eta}{\partial z}\frac{\partial(\rho u w)}{\partial \eta} + \frac{\partial \zeta}{\partial z}\frac{\partial(\rho u w)}{\partial \zeta} = \\ &\frac{1}{Re_L}\left(\frac{\partial \xi}{\partial x}\frac{\partial \tau_{xx}}{\partial \xi} + \frac{\partial \eta}{\partial x}\frac{\partial \tau_{xx}}{\partial \eta} + \frac{\partial \zeta}{\partial x}\frac{\partial \tau_{xx}}{\partial \zeta}\right) + \\ &\frac{1}{Re_L}\left(\frac{\partial \xi}{\partial y}\frac{\partial \tau_{xy}}{\partial \xi} + \frac{\partial \eta}{\partial y}\frac{\partial \tau_{xy}}{\partial \eta} + \frac{\partial \zeta}{\partial y}\frac{\partial \tau_{xy}}{\partial \zeta}\right) + \\ &\frac{1}{Re_L}\left(\frac{\partial \xi}{\partial z}\frac{\partial \tau_{xz}}{\partial \xi} + \frac{\partial \eta}{\partial z}\frac{\partial \tau_{xz}}{\partial \eta} + \frac{\partial \zeta}{\partial z}\frac{\partial \tau_{xz}}{\partial \zeta}\right) \end{aligned} \tag{E.18}$$

Rearranging and reducing:

$$
\begin{aligned}
&\xi_t \frac{\partial(\rho u)}{\partial \xi} + \eta_t \frac{\partial(\rho u)}{\partial \eta} + \zeta_t \frac{\partial(\rho u)}{\partial \zeta} + \frac{\partial(\rho u)}{\partial \tau} + \\
&\xi_x \frac{\partial(\rho u^2 + p)}{\partial \xi} + \eta_x \frac{\partial(\rho u^2 + p)}{\partial \eta} + \zeta_x \frac{\partial(\rho u^2 + p)}{\partial \zeta} + \\
&\xi_y \frac{\partial(\rho u v)}{\partial \xi} + \eta_y \frac{\partial(\rho u v)}{\partial \eta} + \zeta_y \frac{\partial(\rho u v)}{\partial \zeta} + \\
&\xi_z \frac{\partial(\rho u w)}{\partial \xi} + \eta_z \frac{\partial(\rho u w)}{\partial \eta} + \zeta_z \frac{\partial(\rho u w)}{\partial \zeta} = \\
&\frac{1}{Re_L}\left(\xi_x \frac{\partial \tau_{xx}}{\partial \xi} + \eta_x \frac{\partial \tau_{xx}}{\partial \eta} + \zeta_x \frac{\partial \tau_{xx}}{\partial \zeta}\right) + \\
&\frac{1}{Re_L}\left(\xi_y \frac{\partial \tau_{xy}}{\partial \xi} + \eta_y \frac{\partial \tau_{xy}}{\partial \eta} + \zeta_y \frac{\partial \tau_{xy}}{\partial \zeta}\right) + \\
&\frac{1}{Re_L}\left(\xi_z \frac{\partial \tau_{xz}}{\partial \xi} + \eta_z \frac{\partial \tau_{xz}}{\partial \eta} + \zeta_z \frac{\partial \tau_{xz}}{\partial \zeta}\right)
\end{aligned}
\tag{E.19}
$$

Further

$$
\begin{aligned}
&\frac{\partial(\rho u)}{\partial \tau} + \\
&\xi_t \frac{\partial(\rho u)}{\partial \xi} + \xi_x \frac{\partial(\rho u^2 + p)}{\partial \xi} + \xi_y \frac{\partial(\rho u v)}{\partial \xi} + \xi_z \frac{\partial(\rho u w)}{\partial \xi} + \\
&\eta_t \frac{\partial(\rho u)}{\partial \eta} + \eta_x \frac{\partial(\rho u^2 + p)}{\partial \eta} + \eta_y \frac{\partial(\rho u v)}{\partial \eta} + \eta_z \frac{\partial(\rho u w)}{\partial \eta} + \\
&\zeta_t \frac{\partial(\rho u)}{\partial \zeta} + \zeta_x \frac{\partial(\rho u^2 + p)}{\partial \zeta} + \zeta_y \frac{\partial(\rho u v)}{\partial \zeta} + \zeta_z \frac{\partial(\rho u w)}{\partial \zeta} = \\
&\frac{1}{Re_L}\left(\xi_x \frac{\partial \tau_{xx}}{\partial \xi} + \xi_y \frac{\partial \tau_{xy}}{\partial \xi} + \xi_z \frac{\partial \tau_{xz}}{\partial \xi}\right) + \\
&\frac{1}{Re_L}\left(\eta_x \frac{\partial \tau_{xx}}{\partial \eta} + \eta_y \frac{\partial \tau_{xy}}{\partial \eta} + \eta_z \frac{\partial \tau_{xz}}{\partial \eta}\right) + \\
&\frac{1}{Re_L}\left(\zeta_x \frac{\partial \tau_{xx}}{\partial \zeta} + \zeta_y \frac{\partial \tau_{xy}}{\partial \zeta} + \zeta_z \frac{\partial \tau_{xz}}{\partial \zeta}\right)
\end{aligned}
\tag{E.20}
$$

Also

$$
\begin{aligned}
&\frac{\partial(\rho u)}{\partial\tau} + \\
&\frac{\partial[\rho u(\xi_t + \xi_x u + \xi_y v + \xi_z w) + \xi_x p]}{\partial\xi} + \\
&\frac{\partial[\rho u(\eta_t + \eta_x u + \eta_y v + \eta_z w) + \eta_x p]}{\partial\eta} + \\
&\frac{\partial[\rho u(\zeta_t + \zeta_x u + \zeta_y v + \zeta_z w) + \zeta_x p]}{\partial\zeta} = \\
&\frac{1}{Re_L}\frac{\partial(\xi_x\tau_{xx} + \xi_y\tau_{xy} + \xi_z\tau_{xz})}{\partial\xi} + \\
&\frac{1}{Re_L}\frac{\partial(\eta_x\tau_{xx} + \eta_y\tau_{xy} + \eta_z\tau_{xz})}{\partial\xi} + \\
&\frac{1}{Re_L}\frac{\partial(\zeta_x\tau_{xx} + \zeta_y\tau_{xy} + \zeta_z\tau_{xz})}{\partial\zeta}
\end{aligned}
\tag{E.21}
$$

Once again, the contravariant velocities can be reduced:

$$
\begin{aligned}
&\frac{\partial(\rho u)}{\partial\tau} + \frac{\partial(\rho u U + \xi_x p)}{\partial\xi} + \frac{\partial(\rho u V + \eta_x p)}{\partial\eta} + \frac{\partial(\rho u W + \zeta_x p)}{\partial\zeta} = \\
&\frac{1}{Re_L}\frac{\partial(\xi_x\tau_{xx} + \xi_y\tau_{xy} + \xi_z\tau_{xz})}{\partial\xi} + \\
&\frac{1}{Re_L}\frac{\partial(\eta_x\tau_{xx} + \eta_y\tau_{xy} + \eta_z\tau_{xz})}{\partial\xi} + \\
&\frac{1}{Re_L}\frac{\partial(\zeta_x\tau_{xx} + \zeta_y\tau_{xy} + \zeta_z\tau_{xz})}{\partial\zeta}
\end{aligned}
\tag{E.22}
$$

Also, the viscous stress tensors are given by:

$$\tau_{xx} = \frac{2}{3}\mu\left(2\frac{\partial u}{\partial x} - \frac{\partial v}{\partial y} - \frac{\partial w}{\partial z}\right) \tag{E.23}$$

$$\tau_{yy} = \frac{2}{3}\mu\left(2\frac{\partial v}{\partial y} - \frac{\partial u}{\partial x} - \frac{\partial w}{\partial z}\right) \tag{E.24}$$

$$\tau_{zz} = \frac{2}{3}\mu\left(2\frac{\partial w}{\partial z} - \frac{\partial u}{\partial x} - \frac{\partial v}{\partial y}\right) \tag{E.25}$$

$$\tau_{xy} = \mu\left(\frac{\partial u}{\partial y} + \frac{\partial v}{\partial x}\right) \tag{E.26}$$

$$\tau_{xz} = \mu\left(\frac{\partial w}{\partial x} + \frac{\partial u}{\partial z}\right) \tag{E.27}$$

$$\tau_{yz} = \mu\left(\frac{\partial v}{\partial z} + \frac{\partial w}{\partial y}\right) \tag{E.28}$$

These terms will also have to be transformed. Applying the transformation derivatives to equation (E.23), we get:

$$\begin{aligned}\tau_{xx} = {} & \frac{2}{3}\mu\left(2\frac{\partial\xi}{\partial x}\frac{\partial u}{\partial\xi} + 2\frac{\partial\eta}{\partial x}\frac{\partial u}{\partial\eta} + 2\frac{\partial\zeta}{\partial x}\frac{\partial u}{\partial\zeta}\right) - \\ & \frac{2}{3}\mu\left(\frac{\partial\xi}{\partial y}\frac{\partial v}{\partial\xi} + \frac{\partial\eta}{\partial y}\frac{\partial v}{\partial\eta} + \frac{\partial\zeta}{\partial y}\frac{\partial v}{\partial\zeta}\right) - \\ & \frac{2}{3}\mu\left(\frac{\partial\xi}{\partial z}\frac{\partial w}{\partial\xi} + \frac{\partial\eta}{\partial z}\frac{\partial w}{\partial\eta} + \frac{\partial\zeta}{\partial z}\frac{\partial w}{\partial\zeta}\right)\end{aligned} \tag{E.29}$$

Rearranging:

$$\begin{aligned}\tau_{xx} = {} & \frac{2}{3}\mu\left(2\xi_x\frac{\partial u}{\partial\xi} - \xi_y\frac{\partial v}{\partial\xi} - \xi_z\frac{\partial w}{\partial\xi}\right) + \\ & \frac{2}{3}\mu\left(2\eta_x\frac{\partial u}{\partial\eta} - \eta_y\frac{\partial v}{\partial\eta} - \eta_z\frac{\partial w}{\partial\eta}\right) + \\ & \frac{2}{3}\mu\left(2\zeta_x\frac{\partial u}{\partial\zeta} - \zeta_y\frac{\partial v}{\partial\zeta} - \zeta_z\frac{\partial w}{\partial\zeta}\right)\end{aligned} \tag{E.30}$$

Transforming equation (E.24):

$$\tau_{yy} = \frac{2}{3}\mu\left(2\frac{\partial\xi}{\partial y}\frac{\partial v}{\partial\xi} + 2\frac{\partial\eta}{\partial y}\frac{\partial v}{\partial\eta} + 2\frac{\partial\zeta}{\partial y}\frac{\partial v}{\partial\zeta}\right) - \frac{2}{3}\mu\left(\frac{\partial\xi}{\partial x}\frac{\partial u}{\partial\xi} + \frac{\partial\eta}{\partial x}\frac{\partial u}{\partial\eta} + \frac{\partial\zeta}{\partial x}\frac{\partial u}{\partial\zeta}\right) - \frac{2}{3}\mu\left(\frac{\partial\xi}{\partial z}\frac{\partial w}{\partial\xi} + \frac{\partial\eta}{\partial z}\frac{\partial w}{\partial\eta} + \frac{\partial\zeta}{\partial z}\frac{\partial w}{\partial\zeta}\right) \tag{E.31}$$

Rearranging:

$$\tau_{yy} = \frac{2}{3}\mu\left(2\xi_y\frac{\partial v}{\partial\xi} - \xi_x\frac{\partial u}{\partial\xi} - \xi_z\frac{\partial w}{\partial\xi}\right) + \frac{2}{3}\mu\left(2\eta_y\frac{\partial v}{\partial\eta} - \eta_x\frac{\partial u}{\partial\eta} - \eta_z\frac{\partial w}{\partial\eta}\right) + \frac{2}{3}\mu\left(2\zeta_y\frac{\partial v}{\partial\zeta} - \zeta_x\frac{\partial u}{\partial\zeta} - \zeta_z\frac{\partial w}{\partial\zeta}\right) \tag{E.32}$$

Transforming equation (E.25):

$$\tau_{zz} = \frac{2}{3}\mu\left(2\frac{\partial\xi}{\partial z}\frac{\partial w}{\partial\xi} + 2\frac{\partial\eta}{\partial z}\frac{\partial w}{\partial\eta} + 2\frac{\partial\zeta}{\partial z}\frac{\partial w}{\partial\zeta}\right) - \frac{2}{3}\mu\left(\frac{\partial\xi}{\partial x}\frac{\partial u}{\partial\xi} + \frac{\partial\eta}{\partial x}\frac{\partial u}{\partial\eta} + \frac{\partial\zeta}{\partial x}\frac{\partial u}{\partial\zeta}\right) - \frac{2}{3}\mu\left(\frac{\partial\xi}{\partial y}\frac{\partial v}{\partial\xi} + \frac{\partial\eta}{\partial y}\frac{\partial v}{\partial\eta} + \frac{\partial\zeta}{\partial y}\frac{\partial v}{\partial\zeta}\right) \tag{E.33}$$

Rearranging:

$$\tau_{zz} = \frac{2}{3}\mu\left(2\xi_z\frac{\partial w}{\partial\xi} - \xi_x\frac{\partial u}{\partial\xi} - \xi_y\frac{\partial v}{\partial\xi}\right) + \frac{2}{3}\mu\left(2\eta_z\frac{\partial w}{\partial\eta} - \eta_x\frac{\partial u}{\partial\eta} - \eta_y\frac{\partial v}{\partial\eta}\right) + \frac{2}{3}\mu\left(2\zeta_z\frac{\partial w}{\partial\zeta} - \zeta_x\frac{\partial u}{\partial\zeta} - \zeta_y\frac{\partial v}{\partial\zeta}\right) \tag{E.34}$$

Transforming equation (E.26):

$$\tau_{xy} = \mu\left(\frac{\partial\xi}{\partial y}\frac{\partial u}{\partial\xi} + \frac{\partial\eta}{\partial y}\frac{\partial u}{\partial\eta} + \frac{\partial\zeta}{\partial y}\frac{\partial u}{\partial\zeta}\right) + \mu\left(\frac{\partial\xi}{\partial x}\frac{\partial v}{\partial\xi} + \frac{\partial\eta}{\partial x}\frac{\partial v}{\partial\eta} + \frac{\partial\zeta}{\partial x}\frac{\partial v}{\partial\zeta}\right) \tag{E.35}$$

Rearranging:

$$\tau_{xy} = \mu\left(\xi_y\frac{\partial u}{\partial\xi} + \eta_y\frac{\partial u}{\partial\eta} + \zeta_y\frac{\partial u}{\partial\zeta} + \xi_x\frac{\partial v}{\partial\xi} + \eta_x\frac{\partial v}{\partial\eta} + \zeta_x\frac{\partial v}{\partial\zeta}\right) \tag{E.36}$$

Transforming equation (E.27):

$$\tau_{xz} = \mu\left(\frac{\partial\xi}{\partial x}\frac{\partial w}{\partial\xi} + \frac{\partial\eta}{\partial x}\frac{\partial w}{\partial\eta} + \frac{\partial\zeta}{\partial x}\frac{\partial w}{\partial\zeta}\right) + \mu\left(\frac{\partial\xi}{\partial z}\frac{\partial u}{\partial\xi} + \frac{\partial\eta}{\partial z}\frac{\partial u}{\partial\eta} + \frac{\partial\zeta}{\partial z}\frac{\partial u}{\partial\zeta}\right) \tag{E.37}$$

Rearranging:

$$\tau_{xz} = \mu\left(\xi_x\frac{\partial w}{\partial\xi} + \eta_x\frac{\partial w}{\partial\eta} + \zeta_x\frac{\partial w}{\partial\zeta} + \xi_z\frac{\partial u}{\partial\xi} + \eta_z\frac{\partial u}{\partial\eta} + \zeta_z\frac{\partial u}{\partial\zeta}\right) \tag{E.38}$$

Transforming equation (E.2):

$$\tau_{yz} = \mu\left(\frac{\partial\xi}{\partial z}\frac{\partial v}{\partial\xi} + \frac{\partial\eta}{\partial z}\frac{\partial v}{\partial\eta} + \frac{\partial\zeta}{\partial z}\frac{\partial v}{\partial\zeta}\right) + \mu\left(\frac{\partial\xi}{\partial y}\frac{\partial w}{\partial\xi} + \frac{\partial\eta}{\partial y}\frac{\partial w}{\partial\eta} + \frac{\partial\zeta}{\partial y}\frac{\partial w}{\partial\zeta}\right) \tag{E.39}$$

Rearranging:

$$\tau_{yz} = \mu\left(\xi_z\frac{\partial v}{\partial\xi} + \eta_z\frac{\partial v}{\partial\eta} + \zeta_z\frac{\partial v}{\partial\zeta} + \xi_y\frac{\partial w}{\partial\xi} + \eta_y\frac{\partial w}{\partial\eta} + \zeta_y\frac{\partial w}{\partial\zeta}\right) \tag{E.40}$$

A similar analysis can be done for the y and z component momentum equations.

The transformations for these equations are respectively:

$$\frac{\partial(\rho v)}{\partial\tau}+\frac{\partial(\rho vU+\xi_y p)}{\partial\xi}+\frac{\partial(\rho vV+\eta_y p)}{\partial\eta}+\frac{\partial(\rho vW+\zeta_y p)}{\partial\zeta}=$$
$$\frac{1}{Re_L}\frac{\partial(\xi_x\tau_{xy}+\xi_y\tau_{yy}+\xi_z\tau_{yz})}{\partial\xi}+$$
$$\frac{1}{Re_L}\frac{\partial(\eta_x\tau_{xy}+\eta_y\tau_{yy}+\eta_z\tau_{yz})}{\partial\xi}+ \tag{E.41}$$
$$\frac{1}{Re_L}\frac{\partial(\zeta_x\tau_{xy}+\zeta_y\tau_{yy}+\zeta_z\tau_{yz})}{\partial\zeta}$$

$$\frac{\partial(\rho w)}{\partial\tau}+\frac{\partial(\rho wU+\xi_z p)}{\partial\xi}+\frac{\partial(\rho wV+\eta_z p)}{\partial\eta}+\frac{\partial(\rho wW+\zeta_z p)}{\partial\zeta}=$$
$$\frac{1}{Re_L}\frac{\partial(\xi_x\tau_{xz}+\xi_y\tau_{yz}+\xi_z\tau_{zz})}{\partial\xi}+$$
$$\frac{1}{Re_L}\frac{\partial(\eta_x\tau_{xz}+\eta_y\tau_{yz}+\eta_z\tau_{zz})}{\partial\xi}+ \tag{E.42}$$
$$\frac{1}{Re_L}\frac{\partial(\zeta_x\tau_{xz}+\zeta_y\tau_{yz}+\zeta_z\tau_{zz})}{\partial\zeta}$$

The last equation is the energy equation. Restating the energy equation we have:

$$\frac{\partial E_t}{\partial t}+\frac{\partial((E_t+p)u)}{\partial x}+\frac{\partial((E_t+p)v)}{\partial y}+\frac{\partial((E_t+p)w)}{\partial z}=$$

$$\frac{1}{Re_L}\frac{\partial(u\tau_{xx}+v\tau_{xy}+w\tau_{xz}-q_x)}{\partial x}+\frac{1}{Re_L}\frac{\partial(u\tau_{xy}+v\tau_{yy}+w\tau_{yz}-q_y)}{\partial y}+ \tag{E.43}$$

$$\frac{1}{Re_L}\frac{\partial(u\tau_{xz}+v\tau_{yz}+w\tau_{zz}-q_z)}{\partial z}$$

Beginning first with the left-hand-side of equation (E.43), the transformation begins as:

$$\begin{aligned}
&\xi_t\frac{\partial E_t}{\partial \xi} + \eta_t\frac{\partial E_t}{\partial \eta} + \zeta_t\frac{\partial E_t}{\partial \zeta} + \frac{\partial E_t}{\partial \tau} + \\
&\xi_x\frac{\partial((E_t+p)u)}{\partial \xi} + \eta_x\frac{\partial((E_t+p)u)}{\partial \eta} + \zeta_x\frac{\partial((E_t+p)u)}{\partial \zeta} + \\
&\xi_y\frac{\partial((E_t+p)v)}{\partial \xi} + \eta_y\frac{\partial((E_t+p)v)}{\partial \eta} + \zeta_y\frac{\partial((E_t+p)v)}{\partial \zeta} + \\
&\xi_z\frac{\partial((E_t+p)w)}{\partial \xi} + \eta_z\frac{\partial((E_t+p)w)}{\partial \eta} + \zeta_z\frac{\partial((E_t+p)w)}{\partial \zeta} = LHS
\end{aligned} \tag{E.44}$$

Rearranging:

$$\begin{aligned}
&\frac{\partial E_t}{\partial \tau} + \\
&\frac{\partial(\xi_t E_t + ((E_t+p)\xi_x u) + ((E_t+p)\xi_y v) + ((E_t+p)\xi_z w))}{\partial \xi} + \\
&\frac{\partial(\eta_t E_t + ((E_t+p)\eta_x u) + ((E_t+p)\eta_y v) + ((E_t+p)\eta_z w))}{\partial \eta} + \\
&\frac{\partial(\zeta_t E_t + ((E_t+p)\zeta_x u) + ((E_t+p)\zeta_y v) + ((E_t+p)\zeta_z w))}{\partial \zeta} = LHS
\end{aligned} \tag{E.45}$$

Further rearranging:

$$\begin{aligned}
&\frac{\partial E_t}{\partial \tau} + \\
&\frac{\partial(\xi_t E_t + (E_t+p)(\xi_x u + \xi_y v + \xi_z w))}{\partial \xi} + \\
&\frac{\partial(\eta_t E_t + (E_t+p)(\eta_x u + \eta_y v + \eta_z w))}{\partial \eta} + \\
&\frac{\partial(\zeta_t E_t + (E_t+p)(\zeta_x u + \zeta_y v + \zeta_z w))}{\partial \zeta} = LHS
\end{aligned} \tag{E.46}$$

Adding and Subtracting like terms to help in reduction:

$$\begin{aligned}
&\frac{\partial E_t}{\partial \tau} + \\
&\frac{\partial(\xi_t E_t + (\xi_t p - \xi_t p) + (E_t + p)(\xi_x u + \xi_y v + \xi_z w))}{\partial \xi} + \\
&\frac{\partial(\eta_t E_t + (\eta_t p - \eta_t p) + (E_t + p)(\eta_x u + \eta_y v + \eta_z w))}{\partial \eta} + \\
&\frac{\partial(\zeta_t E_t + (\zeta_t p - \zeta_t p) + (E_t + p)(\zeta_x u + \zeta_y v + \zeta_z w))}{\partial \zeta} = LHS
\end{aligned} \tag{E.47}$$

Rearranging terms to help to combine terms defined as contravariant velocities we have:

$$\begin{aligned}
&\frac{\partial E_t}{\partial \tau} + \\
&\frac{\partial((E_t + p)(\xi_t + \xi_x u + \xi_y v + \xi_z w) - \xi_t p)}{\partial \xi} + \\
&\frac{\partial((E_t + p)(\eta_t + \eta_x u + \eta_y v + \eta_z w) - \eta_t p)}{\partial \eta} + \\
&\frac{\partial((E_t + p)(\zeta_t + \zeta_x u + \zeta_y v + \zeta_z w) - \zeta_t p)}{\partial \zeta} = LHS
\end{aligned} \tag{E.48}$$

Final reduction yields:

$$\begin{aligned}
&\frac{\partial E_t}{\partial \tau} + \frac{\partial((E_t + p)U - \xi_t p)}{\partial \xi} + \\
&\frac{\partial((E_t + p)V - \eta_t p)}{\partial \eta} + \frac{\partial((E_t + p)W - \zeta_t p)}{\partial \zeta} = LHS
\end{aligned} \tag{E.49}$$

Continuing on with the right-hand-side, we have:

$$
\begin{aligned}
&RHS(Re_L)= \\
&\xi_x \frac{\partial(u\tau_{xx} + v\tau_{xy} + w\tau_{xz} - q_x)}{\partial\xi} + \eta_x \frac{\partial(u\tau_{xx} + v\tau_{xy} + w\tau_{xz} - q_x)}{\partial\eta} + \\
&\zeta_x \frac{\partial(u\tau_{xx} + v\tau_{xy} + w\tau_{xz} - q_x)}{\partial\zeta} + \xi_y \frac{\partial(u\tau_{xy} + v\tau_{yy} + w\tau_{yz} - q_y)}{\partial\xi} + \\
&\eta_y \frac{\partial(u\tau_{xy} + v\tau_{yy} + w\tau_{yz} - q_y)}{\partial\eta} + \zeta_y \frac{\partial(u\tau_{xy} + v\tau_{yy} + w\tau_{yz} - q_y)}{\partial\zeta} + \\
&\xi_z \frac{\partial(u\tau_{xz} + v\tau_{yz} + w\tau_{zz} - q_z)}{\partial\xi} + \eta_z \frac{\partial(u\tau_{xz} + v\tau_{yz} + w\tau_{zz} - q_z)}{\partial\eta} + \\
&\zeta_z \frac{\partial(u\tau_{xz} + v\tau_{yz} + w\tau_{zz} - q_z)}{\partial\zeta}
\end{aligned}
\tag{E.50}
$$

Combining terms:

$$
\begin{aligned}
&RHS(Re_L)= \\
&\frac{\partial(\xi_x(u\tau_{xx} + v\tau_{xy} + w\tau_{xz} - q_x))}{\partial\xi} + \frac{\partial(\xi_y(u\tau_{xy} + v\tau_{yy} + w\tau_{yz} - q_y))}{\partial\xi} + \\
&\frac{\partial(\xi_z(u\tau_{xz} + v\tau_{yz} + w\tau_{zz} - q_z))}{\partial\xi} + \\
&\frac{\partial(\eta_x(u\tau_{xx} + v\tau_{xy} + w\tau_{xz} - q_x))}{\partial\eta} + \frac{\partial(\eta_y(u\tau_{xy} + v\tau_{yy} + w\tau_{yz} - q_y))}{\partial\eta} + \\
&\frac{\partial(\eta_z(u\tau_{xz} + v\tau_{yz} + w\tau_{zz} - q_z))}{\partial\eta} + \\
&\frac{\partial(\zeta_x(u\tau_{xx} + v\tau_{xy} + w\tau_{xz} - q_x))}{\partial\zeta} + \frac{\partial(\zeta_y(u\tau_{xy} + v\tau_{yy} + w\tau_{yz} - q_y))}{\partial\zeta} + \\
&\frac{\partial(\zeta_z(u\tau_{xz} + v\tau_{yz} + w\tau_{zz} - q_z))}{\partial\zeta}
\end{aligned}
\tag{E.51}
$$

At this point we have already transformed the viscous shear stress terms. The only other terms that contain derivatives are the heat flux terms.

Applying the transformation to the x-direction heat flux term, we get:

$$q_x = -\frac{\mu}{(\gamma-1)M^2{}_\infty Re_L Pr}\left(\frac{\partial\xi}{\partial x}\frac{\partial T}{\partial \xi}+\frac{\partial\eta}{\partial x}\frac{\partial T}{\partial \eta}+\frac{\partial\zeta}{\partial x}\frac{\partial T}{\partial \zeta}\right) \tag{E.52}$$

Reducing to its final form:

$$q_x = -\frac{\mu}{(\gamma-1)M^2{}_\infty Re_L Pr}\left(\xi_x\frac{\partial T}{\partial \xi}+\eta_x\frac{\partial T}{\partial \eta}+\zeta_x\frac{\partial T}{\partial \zeta}\right) \tag{E.53}$$

Similarly, for the y and z directions respectively are:

$$q_y = -\frac{\mu}{(\gamma-1)M^2{}_\infty Re_L Pr}\left(\xi_y\frac{\partial T}{\partial \xi}+\eta_y\frac{\partial T}{\partial \eta}+\zeta_y\frac{\partial T}{\partial \zeta}\right) \tag{E.54}$$

$$q_z = -\frac{\mu}{(\gamma-1)M^2{}_\infty Re_L Pr}\left(\xi_z\frac{\partial T}{\partial \xi}+\eta_z\frac{\partial T}{\partial \eta}+\zeta_z\frac{\partial T}{\partial \zeta}\right) \tag{E.55}$$

Finally we can put equations (E.16), (E.22), (E.41), (E.42), (E.49), and (E.51) back into vector form.

$$\frac{\partial\bar{Q}}{\partial\tau}+\frac{\partial\bar{E}}{\partial\xi}+\frac{\partial\bar{F}}{\partial\eta}+\frac{\partial\bar{G}}{\partial\zeta}=\frac{1}{Re_L}\left(\frac{\partial\bar{E}_v}{\partial\xi}+\frac{\partial\bar{F}_v}{\partial\eta}+\frac{\partial\bar{G}_v}{\partial\zeta}\right) \tag{E.56}$$

Where

$$\bar{Q} = \frac{1}{J}\begin{bmatrix} \rho \\ \rho u \\ \rho v \\ \rho w \\ E_t \end{bmatrix} \quad \bar{E} = \frac{1}{J}\begin{bmatrix} \rho u \\ \rho u U + \xi_x p \\ \rho v U + \xi_y p \\ \rho w U + \xi_z p \\ (E_t + p)U - \xi_t p \end{bmatrix}$$

$$\bar{F} = \frac{1}{J}\begin{bmatrix} \rho V \\ \rho u V + \eta_x p \\ \rho v V + \eta_y p \\ \rho w V + \eta_z p \\ (E_t + p)V - \eta_t p \end{bmatrix} \quad \bar{G} = \frac{1}{J}\begin{bmatrix} \rho W \\ \rho u W + \zeta_x p \\ \rho v W + \zeta_y p \\ \rho w W + \zeta_z p \\ (E_t + p)W - \zeta_t p \end{bmatrix} \tag{E.57}$$

The viscous flux terms $\overline{E_v}, \overline{F_v}, \overline{G_v}$ are:

$$\begin{aligned} \overline{E_v} &= \frac{1}{J}(\xi_x E_v + \xi_y F_v + \xi_z G_v) \\ \overline{F_v} &= \frac{1}{J}(\eta_x E_v + \eta_y F_v + \eta_z G_v) \\ \overline{G_v} &= \frac{1}{J}(\zeta_x E_v + \zeta_y F_v + \zeta_z G_v) \end{aligned} \tag{E.58}$$

Here, both sides of the equation (E.54) have been divided by the Jacobian.

APPENDIX F

Derivation of the Thin Layer Approximation

Let us first begin with equation (E.22), the x-direction momentum equation. Written again:

$$\frac{\partial(\rho u)}{\partial\tau}+\frac{\partial(\rho uU+\xi_x p)}{\partial\xi}+\frac{\partial(\rho uV+\eta_x p)}{\partial\eta}+\frac{\partial(\rho uW+\zeta_x p)}{\partial\zeta}=$$
$$\frac{1}{Re_L}\frac{\partial(\xi_x\tau_{xx}+\xi_y\tau_{xy}+\xi_z\tau_{xz})}{\partial\xi}+$$
$$\frac{1}{Re_L}\frac{\partial(\eta_x\tau_{xx}+\eta_y\tau_{xy}+\eta_z\tau_{xz})}{\partial\xi}+ \tag{F.1}$$
$$\frac{1}{Re_L}\frac{\partial(\zeta_x\tau_{xx}+\zeta_y\tau_{xy}+\zeta_z\tau_{xz})}{\partial\zeta}$$

Lets only consider the right-hand-side of this equation, the viscous flux terms:

$$RHS=\frac{1}{Re_L}\frac{\partial(\xi_x\tau_{xx}+\xi_y\tau_{xy}+\xi_z\tau_{xz})}{\partial\xi}+\frac{1}{Re_L}\frac{\partial(\eta_x\tau_{xx}+\eta_y\tau_{xy}+\eta_z\tau_{xz})}{\partial\xi}+ \tag{F.2}$$
$$\frac{1}{Re_L}\frac{\partial(\zeta_x\tau_{xx}+\zeta_y\tau_{xy}+\zeta_z\tau_{xz})}{\partial\zeta}$$

As stated in chapter two, the thin layer approximation reduces down to terms that contain derivatives only taken with respect to Zeta. Reducing equation (F.2) we have:

$$RHS=\frac{1}{Re_L}\frac{\partial(\zeta_x\tau_{xx}+\zeta_y\tau_{xy}+\zeta_z\tau_{xz})}{\partial\zeta} \tag{F.3}$$

Expanding this out we have:

$$RHS=\frac{1}{Re_L}\partial\Big[\zeta_x\Big(\frac{2}{3}\mu(2(\xi_x u_\xi+\eta_x u_\eta+\zeta_x u_\zeta)-(\xi_y v_\xi+\eta_y v_\eta+\zeta_y v_\zeta)-$$
$$(\xi_z w_\xi+\eta_z w_\eta+\zeta_z w_\zeta))\Big)+ \tag{F.4}$$
$$\zeta_y(\mu(\xi_y u_\xi+\eta_y u_\eta+\zeta_y u_\zeta+\xi_x v_\xi+\eta_x v_\eta+\zeta_x v_\zeta))+$$
$$\zeta_z(\mu(\xi_z u_\xi+\eta_z u_\eta+\zeta_z u_\zeta+\xi_x w_\xi+\eta_x w_\eta+\zeta_x w_\zeta))\Big]/\partial\zeta$$

Further reduction yields:

$$RHS = \frac{1}{Re_L}\partial\left[\zeta_x\left(\frac{2}{3}\mu(2\zeta_x u_\zeta - \zeta_y v_\zeta - \zeta_z w_\zeta)\right) + \zeta_y(\mu(\zeta_y u_\zeta + \zeta_x v_\zeta)) + \right. \tag{F.5}$$

$$\left.\zeta_z(\mu(\zeta_z u_\zeta + \zeta_x w_\zeta))\right]/\partial\zeta$$

Expanding out:

$$RHS = \frac{1}{Re_L}\frac{\partial\left[\frac{4}{3}\zeta_x^2 u_\zeta\mu - \frac{2}{3}\zeta_x\zeta_y v_\zeta\mu - \frac{2}{3}\zeta_x\zeta_z w_\zeta\mu + \zeta_y^2 u_\zeta\mu + \zeta_x\zeta_y v_\zeta\mu + \zeta_z^2 u_\zeta\mu + \zeta_x\zeta_{xz} w_\zeta\mu\right]}{\partial\zeta} \tag{F.6}$$

Rearranging:

$$RHS = \frac{1}{Re_L}\frac{\partial\left[\mu\left(\frac{4}{3}\zeta_x^2 + \zeta_y^2 + \zeta_z^2\right)u_\zeta - \frac{2}{3}\zeta_x\zeta_y v_\zeta\mu - \frac{2}{3}\zeta_x\zeta_z w_\zeta\mu + \zeta_x\zeta_y v_\zeta\mu + \zeta_x\zeta_{xz} w_\zeta\mu\right]}{\partial\zeta} \tag{F.7}$$

Further rearranging:

$$RHS = \frac{1}{Re_L}\frac{\partial\left[\mu(\zeta_x^2 + \zeta_y^2 + \zeta_z^2)u_\zeta + \frac{1}{3}\mu\zeta_x\zeta_y v_\zeta + \frac{1}{3}\mu\zeta_x\zeta_z w_\zeta + \frac{1}{3}\mu\zeta_x^2 u_\zeta\right]}{\partial\zeta} \tag{F.8}$$

Finally we have:

$$RHS = \frac{1}{Re_L}\frac{\partial\left[\mu(\zeta_x^2 + \zeta_y^2 + \zeta_z^2)u_\zeta + \frac{1}{3}\mu\zeta_x(\zeta_x u_\zeta + \zeta_y v_\zeta + \zeta_z w_\zeta)\right]}{\partial\zeta} \tag{F.9}$$

A similar analysis can be done for the y and z components of the momentum equations.

There results respectively are:

$$RHS = \frac{1}{Re_L}\frac{\partial\left[\mu(\zeta_x^2 + \zeta_y^2 + \zeta_z^2)v_\zeta + \frac{1}{3}\mu\zeta_y(\zeta_x u_\zeta + \zeta_y v_\zeta + \zeta_z w_\zeta)\right]}{\partial\zeta} \tag{F.10}$$

$$RHS = \frac{1}{Re_L}\frac{\partial\left[\mu(\zeta_x^2+\zeta_y^2+\zeta_z^2)w_\zeta+\frac{1}{3}\mu\zeta_z(\zeta_x u_\zeta+\zeta_y v_\zeta+\zeta_z w_\zeta)\right]}{\partial\zeta} \tag{F.11}$$

Lastly, we will reduce the energy equation. Rewriting equation (E.49):

$$\begin{aligned}
&RHS(Re_L)= \\
&\frac{\partial(\xi_x(u\tau_{xx}+v\tau_{xy}+w\tau_{xz}-q_x))}{\partial\xi}+\frac{\partial(\xi_y(u\tau_{xy}+v\tau_{yy}+w\tau_{yz}-q_y))}{\partial\xi}+ \\
&\frac{\partial(\xi_z(u\tau_{xz}+v\tau_{yz}+w\tau_{zz}-q_z))}{\partial\xi}+ \\
&\frac{\partial(\eta_x(u\tau_{xx}+v\tau_{xy}+w\tau_{xz}-q_x))}{\partial\eta}+\frac{\partial(\eta_y(u\tau_{xy}+v\tau_{yy}+w\tau_{yz}-q_y))}{\partial\eta}+ \\
&\frac{\partial(\eta_z(u\tau_{xz}+v\tau_{yz}+w\tau_{zz}-q_z))}{\partial\eta}+ \\
&\frac{\partial(\zeta_x(u\tau_{xx}+v\tau_{xy}+w\tau_{xz}-q_x))}{\partial\zeta}+\frac{\partial(\zeta_y(u\tau_{xy}+v\tau_{yy}+w\tau_{yz}-q_y))}{\partial\zeta}+ \\
&\frac{\partial(\zeta_z(u\tau_{xz}+v\tau_{yz}+w\tau_{zz}-q_z))}{\partial\zeta}
\end{aligned} \tag{F.12}$$

Reducing yields:

$$\begin{aligned}
&RHS(Re_L)= \\
&\frac{\partial(\zeta_x(u\tau_{xx}+v\tau_{xy}+w\tau_{xz}-q_x))}{\partial\zeta}+\frac{\partial(\zeta_y(u\tau_{xy}+v\tau_{yy}+w\tau_{yz}-q_y))}{\partial\zeta}+ \\
&\frac{\partial(\zeta_z(u\tau_{xz}+v\tau_{yz}+w\tau_{zz}-q_z))}{\partial\zeta}
\end{aligned} \tag{F.13}$$

Let us first reduce each of the shear stress terms and the heat flux terms.

$$\tau_{xx} = \frac{2}{3}\mu\left(2\xi_x\frac{\partial u}{\partial \xi}-\xi_y\frac{\partial v}{\partial \xi}-\xi_z\frac{\partial w}{\partial \xi}\right)+ \\ \frac{2}{3}\mu\left(2\eta_x\frac{\partial u}{\partial \eta}-\eta_y\frac{\partial v}{\partial \eta}-\eta_z\frac{\partial w}{\partial \eta}\right)+ \\ \frac{2}{3}\mu\left(2\zeta_x\frac{\partial u}{\partial \zeta}-\zeta_y\frac{\partial v}{\partial \zeta}-\zeta_z\frac{\partial w}{\partial \zeta}\right) \tag{F.14}$$

Reducing:

$$\tau_{xx} = \frac{2}{3}\mu\left(2\zeta_x\frac{\partial u}{\partial \zeta}-\zeta_y\frac{\partial v}{\partial \zeta}-\zeta_z\frac{\partial w}{\partial \zeta}\right) \tag{F.15}$$

Similarly:

$$\tau_{yy} = \frac{2}{3}\mu\left(2\zeta_y\frac{\partial v}{\partial \zeta}-\zeta_x\frac{\partial u}{\partial \zeta}-\zeta_z\frac{\partial w}{\partial \zeta}\right) \tag{F.16}$$

$$\tau_{zz} = \frac{2}{3}\mu\left(2\zeta_z\frac{\partial w}{\partial \zeta}-\zeta_x\frac{\partial u}{\partial \zeta}-\zeta_y\frac{\partial v}{\partial \zeta}\right) \tag{F.17}$$

$$\tau_{xy} = \mu\left(\zeta_y\frac{\partial u}{\partial \zeta}+\zeta_x\frac{\partial v}{\partial \zeta}\right) \tag{F.18}$$

$$\tau_{xz} = \mu\left(\zeta_x\frac{\partial w}{\partial \zeta}+\zeta_z\frac{\partial u}{\partial \zeta}\right) \tag{F.19}$$

$$\tau_{yz} = \mu\left(\zeta_z\frac{\partial v}{\partial \zeta}+\zeta_y\frac{\partial w}{\partial \zeta}\right) \tag{F.20}$$

The heat flux terms can be reduced to the following:

$$q_x = -\frac{\mu}{(\gamma-1)M^2_{\infty}Re_L Pr}\left(\zeta_x\frac{\partial T}{\partial \zeta}\right) \tag{F.21}$$

Similarly for the y and z directions:

$$q_y = -\frac{\mu}{(\gamma - 1)M^2{}_\infty Re_L Pr}\left(\zeta_y \frac{\partial T}{\partial \zeta}\right) \tag{F.22}$$

$$q_z = -\frac{\mu}{(\gamma - 1)M^2{}_\infty Re_L Pr}\left(\zeta_z \frac{\partial T}{\partial \zeta}\right) \tag{F.23}$$

Substituting the shear stress and heat flux terms into equation (F.13), we have:

$$\begin{aligned} &RHS(Re_L)= \\ &\frac{\partial\left(\zeta_x\left(u\frac{2}{3}\mu\left(2\zeta_x\frac{\partial u}{\partial \zeta}-\zeta_y\frac{\partial v}{\partial \zeta}-\zeta_z\frac{\partial w}{\partial \zeta}\right)+v\mu\left(\zeta_y\frac{\partial u}{\partial \zeta}+\zeta_x\frac{\partial v}{\partial \zeta}\right)+w\mu\left(\zeta_x\frac{\partial w}{\partial \zeta}+\zeta_z\frac{\partial u}{\partial \zeta}\right)+\frac{\mu}{(\gamma-1)M^2{}_\infty Re_L Pr}\left(\zeta_x\frac{\partial T}{\partial \zeta}\right)\right)\right)}{\partial \zeta}+ \\ &\frac{\partial\left(\zeta_y\left(u\mu\left(\zeta_y\frac{\partial u}{\partial \zeta}+\zeta_x\frac{\partial v}{\partial \zeta}\right)+v\frac{2}{3}\mu\left(2\zeta_y\frac{\partial v}{\partial \zeta}-\zeta_x\frac{\partial u}{\partial \zeta}-\zeta_z\frac{\partial w}{\partial \zeta}\right)+w\mu\left(\zeta_z\frac{\partial v}{\partial \zeta}+\zeta_y\frac{\partial w}{\partial \zeta}\right)+\frac{\mu}{(\gamma-1)M^2{}_\infty Re_L Pr}\left(\zeta_y\frac{\partial T}{\partial \zeta}\right)\right)\right)}{\partial \zeta}+ \\ &\frac{\partial\left(\zeta_z\left(u\mu\left(\zeta_x\frac{\partial w}{\partial \zeta}+\zeta_z\frac{\partial u}{\partial \zeta}\right)+v\mu\left(\zeta_z\frac{\partial v}{\partial \zeta}+\zeta_y\frac{\partial w}{\partial \zeta}\right)+w\frac{2}{3}\mu\left(2\zeta_z\frac{\partial w}{\partial \zeta}-\zeta_x\frac{\partial u}{\partial \zeta}-\zeta_y\frac{\partial v}{\partial \zeta}\right)+\frac{\mu}{(\gamma-1)M^2{}_\infty Re_L Pr}\left(\zeta_z\frac{\partial T}{\partial \zeta}\right)\right)\right)}{\partial \zeta} \end{aligned} \tag{F.24}$$

Expanding:

$$\begin{aligned} &RHS(Re_L)= \\ &\frac{\partial\left(\frac{4}{3}\mu u\zeta_x^2\frac{\partial u}{\partial \zeta}-\frac{2}{3}\mu u\zeta_x\zeta_y\frac{\partial v}{\partial \zeta}-\frac{2}{3}\mu u\zeta_x\zeta_y\frac{\partial w}{\partial \zeta}+v\mu\zeta_x\zeta_y\frac{\partial u}{\partial \zeta}+v\mu\zeta_x^2\frac{\partial v}{\partial \zeta}+w\mu\zeta_x^2\frac{\partial w}{\partial \zeta}+w\mu\zeta_x\zeta_z\frac{\partial u}{\partial \zeta}+\frac{\mu}{(\gamma-1)M^2{}_\infty Re_L Pr}\zeta_x^2\frac{\partial T}{\partial \zeta}\right)}{\partial \zeta}+ \\ &\frac{\partial\left(u\mu\zeta_y^2\frac{\partial u}{\partial \zeta}+u\mu\zeta_y\zeta_x\frac{\partial v}{\partial \zeta}+\frac{4}{3}\mu v\zeta_y^2\frac{\partial v}{\partial \zeta}-\frac{2}{3}\mu v\zeta_y\zeta_x\frac{\partial u}{\partial \zeta}-\frac{2}{3}\mu v\zeta_y\zeta_z\frac{\partial w}{\partial \zeta}+w\mu\zeta_y\zeta_z\frac{\partial v}{\partial \zeta}+w\mu\zeta_y^2\frac{\partial w}{\partial \zeta}+\frac{\mu}{(\gamma-1)M^2{}_\infty Re_L Pr}\zeta_y^2\frac{\partial T}{\partial \zeta}\right)}{\partial \zeta}+ \\ &\frac{\partial\left(u\mu\zeta_x\zeta_z\frac{\partial w}{\partial \zeta}+u\mu\zeta_z^2\frac{\partial u}{\partial \zeta}+v\mu\zeta_z^2\frac{\partial v}{\partial \zeta}+v\mu\zeta_y\zeta_z\frac{\partial w}{\partial \zeta}+\frac{4}{3}w\mu\zeta_z^2\frac{\partial w}{\partial \zeta}-\frac{2}{3}w\mu\zeta_x\zeta_z\frac{\partial u}{\partial \zeta}-\frac{2}{3}w\mu\zeta_y\zeta_z\frac{\partial v}{\partial \zeta}+\frac{\mu}{(\gamma-1)M^2{}_\infty Re_L Pr}\zeta_z^2\frac{\partial T}{\partial \zeta}\right)}{\partial \zeta} \end{aligned} \tag{F.25}$$

Rearranging:

$$RHS(Re_L)=$$

$$\frac{\partial\left(\zeta_x^2\left[\mu\left(\frac{\partial u^2}{\partial \zeta}+\frac{\partial v^2}{\partial \zeta}+\frac{\partial w^2}{\partial \zeta}\right)+\alpha\frac{\partial T}{\partial \zeta}\right]+\left(\frac{1}{3}\zeta_x^2\mu\frac{\partial u^2}{\partial \zeta}\right)-\frac{2}{3}\mu u\zeta_x\zeta_y\frac{\partial v}{\partial \zeta}-\frac{2}{3}\mu u\zeta_x\zeta_y\frac{\partial w}{\partial \zeta}+v\mu\zeta_x\zeta_y\frac{\partial u}{\partial \zeta}+w\mu\zeta_x\zeta_z\frac{\partial u}{\partial \zeta}\right)}{\partial \zeta}+$$
$$\frac{\partial\left(\zeta_y^2\left[\mu\left(\frac{\partial u^2}{\partial \zeta}+\frac{\partial v^2}{\partial \zeta}+\frac{\partial w^2}{\partial \zeta}\right)+\alpha\frac{\partial T}{\partial \zeta}\right]+\left(\frac{1}{3}\zeta_y^2\mu\frac{\partial v^2}{\partial \zeta}\right)-\frac{2}{3}\mu v\zeta_y\zeta_x\frac{\partial u}{\partial \zeta}-\frac{2}{3}\mu v\zeta_y\zeta_z\frac{\partial w}{\partial \zeta}+u\mu\zeta_y\zeta_x\frac{\partial v}{\partial \zeta}+w\mu\zeta_y\zeta_z\frac{\partial v}{\partial \zeta}\right)}{\partial \zeta}+ \quad (F.26)$$
$$\frac{\partial\left(\zeta_z^2\left[\mu\left(\frac{\partial u^2}{\partial \zeta}+\frac{\partial v^2}{\partial \zeta}+\frac{\partial w^2}{\partial \zeta}\right)+\alpha\frac{\partial T}{\partial \zeta}\right]+\left(\frac{1}{3}\zeta_y^2\mu\frac{\partial w^2}{\partial \zeta}\right)-\frac{2}{3}w\mu\zeta_x\zeta_z\frac{\partial u}{\partial \zeta}-\frac{2}{3}w\mu\zeta_y\zeta_z\frac{\partial v}{\partial \zeta}+u\mu\zeta_x\zeta_z\frac{\partial w}{\partial \zeta}+v\mu\zeta_y\zeta_z\frac{\partial w}{\partial \zeta}\right)}{\partial \zeta}$$

where α is:

$$\alpha=\frac{\mu}{(\gamma-1)M^2{}_\infty Re_L Pr} \quad (F.27)$$

Reducing even further we finally, with further reduction, we have:

$$RHS(Re_L)=\frac{\partial\left\{(\zeta_x^2+\zeta_y^2+\zeta_z^2)\left[\mu\left(\frac{\partial u^2}{\partial \zeta}+\frac{\partial v^2}{\partial \zeta}+\frac{\partial w^2}{\partial \zeta}\right)+\alpha\frac{\partial T}{\partial \zeta}\right]+\frac{1}{3}\mu\left(\zeta_x\frac{\partial u}{\partial \zeta}+\zeta_y\frac{\partial v}{\partial \zeta}+\zeta_z\frac{\partial w}{\partial \zeta}\right)(\zeta_x u+\zeta_y v+\zeta_z w)\right\}}{\partial \zeta} \quad (F.28)$$

We can now put equations (F.9), (F.10), (F.11), and (F.28) into vector form. One will notice there are no viscous contributions from the continuity equation, and therefore the first element of the viscous flux vector will be zero. We can now show the thin layer viscous flux vector S as:

$$\bar{S}=\frac{1}{J}\begin{bmatrix} 0 \\ \mu(\zeta_x^2+\zeta_y^2+\zeta_z^2)u_\zeta+\frac{1}{3}\mu\zeta_x(\zeta_x u_\zeta+\zeta_y v_\zeta+\zeta_z w_\zeta) \\ \mu(\zeta_x^2+\zeta_y^2+\zeta_z^2)v_\zeta+\frac{1}{3}\mu\zeta_y(\zeta_x u_\zeta+\zeta_y v_\zeta+\zeta_z w_\zeta) \\ \mu(\zeta_x^2+\zeta_y^2+\zeta_z^2)w_\zeta+\frac{1}{3}\mu\zeta_z(\zeta_x u_\zeta+\zeta_y v_\zeta+\zeta_z w_\zeta) \\ (\zeta_x^2+\zeta_y^2+\zeta_z^2)\left[\mu\left(\frac{\partial u^2}{\partial \zeta}+\frac{\partial v^2}{\partial \zeta}+\frac{\partial w^2}{\partial \zeta}\right)+\alpha\frac{\partial T}{\partial \zeta}\right]+\frac{1}{3}\mu\left(\zeta_x\frac{\partial u}{\partial \zeta}+\zeta_y\frac{\partial v}{\partial \zeta}+\zeta_z\frac{\partial w}{\partial \zeta}\right)(\zeta_x u+\zeta_y v+\zeta_z w) \end{bmatrix} \quad (F.29)$$